Structural Chromosomal Rearrangements Require Nucleotide-Level Resolution: Lessons from Next-Generation Sequencing in Prenatal Diagnosis

Zehra Ordulu,[1,2] Tammy Kammin,[1] Harrison Brand,[3,4,5] Vamsee Pillalamarri,[3] Claire E. Redin,[2,3,4,5] Ryan L. Collins,[3] Ian Blumenthal,[3] Carrie Hanscom,[3] Shahrin Pereira,[1] India Bradley,[6] Barbara F. Crandall,[6] Pamela Gerrol,[1] Mark A. Hayden,[1] Naveed Hussain,[7] Bibi Kanengisser-Pines,[8] Sibel Kantarci,[9] Brynn Levy,[10] Michael J. Macera,[11] Fabiola Quintero-Rivera,[9] Erica Spiegel,[12] Blair Stevens,[13] Janet E. Ulm,[14] Dorothy Warburton,[15,16] Louise E. Wilkins-Haug,[1,2] Naomi Yachelevich,[17] James F. Gusella,[3,4,5,18] Michael E. Talkowski,[2,3,4,5,19] and Cynthia C. Morton[1,2,5,20,21,*]

In this exciting era of "next-gen cytogenetics," integrating genomic sequencing into the prenatal diagnostic setting is possible within an actionable time frame and can provide precise delineation of balanced chromosomal rearrangements at the nucleotide level. Given the increased risk of congenital abnormalities in newborns with de novo balanced chromosomal rearrangements, comprehensive interpretation of breakpoints could substantially improve prediction of phenotypic outcomes and support perinatal medical care. Herein, we present and evaluate sequencing results of balanced chromosomal rearrangements in ten prenatal subjects with respect to the location of regulatory chromatin domains (topologically associated domains [TADs]). The genomic material from all subjects was interpreted to be "normal" by microarray analyses, and their rearrangements would not have been detected by cell-free DNA (cfDNA) screening. The findings of our systematic approach correlate with phenotypes of both pregnancies with untoward outcomes (5/10) and with healthy newborns (3/10). Two pregnancies, one with a chromosomal aberration predicted to be of unknown clinical significance and another one predicted to be likely benign, were terminated prior to phenotype-genotype correlation (2/10). We demonstrate that the clinical interpretation of structural rearrangements should not be limited to interruption, deletion, or duplication of specific genes and should also incorporate regulatory domains of the human genome with critical ramifications for the control of gene expression. As detailed in this study, our molecular approach to both detecting and interpreting the breakpoints of structural rearrangements yields unparalleled information in comparison to other commonly used first-tier diagnostic methods, such as non-invasive cfDNA screening and microarray analysis, to provide improved genetic counseling for phenotypic outcome in the prenatal setting.

Introduction

Fetal material obtained through invasive methods can be assessed routinely with different techniques, including karyotyping, fluorescence in situ hybridization, and chromosomal microarray analysis (CMA).[1–3] Although karyotyping remains the principal cytogenetic tool in prenatal diagnosis, CMA has the advantage of higher resolution and is the preferred method in a fetus with one or more major structural abnormalities identified by ultrasonography.[1] However, unlike karyotyping, CMA cannot detect balanced chromosomal rearrangements, such as translocations, inversions, and insertions.

The risk of congenital abnormalities is two to three times higher in newborns with apparently balanced de novo chromosomal rearrangements (6.1% for translocations and 9.4% for inversions) than in a population of pregnancies tested by amniocentesis.[4] The cause of the increase in abnormal phenotypes in such cases can be a submicroscopic deletion, duplication, disruption, dysregulation, or fusion of a gene(s) located at or near the breakpoints. Studies using CMA have demonstrated the presence of a cryptic imbalance in 40%–50% of subjects with an abnormal

[1]Department of Obstetrics, Gynecology, and Reproductive Biology, Brigham and Women's Hospital, Boston, MA 02115, USA; [2]Harvard Medical School, Boston, MA 02115, USA; [3]Center for Human Genetic Research, Massachusetts General Hospital, Boston, MA 02114, USA; [4]Department of Neurology, Massachusetts General Hospital and Harvard Medical School, Boston, MA 02114, USA; [5]Program in Medical and Population Genetics, Broad Institute of MIT and Harvard, Boston, MA 02142, USA; [6]Department of Psychiatry, Prenatal Diagnosis Center, David Geffen School of Medicine, University of California, Los Angeles, Medical Plaza, Los Angeles, CA 90095, USA; [7]Department of Pediatrics, Connecticut Children's Medical Center, University of Connecticut, Farmington, CT 06030, USA; [8]Department of Obstetrics and Gynecology, Kaplan Medical Center, Rehovot 76100, Israel; [9]Department of Pathology and Laboratory Medicine, UCLA Clinical Genomics Center, David Geffen School of Medicine, University of California, Los Angeles, Los Angeles, CA 90095, USA; [10]Department of Pathology and Cell Biology, College of Physicians and Surgeons, Columbia University, New York, NY 10032, USA; [11]New York Presbyterian Hospital, Columbia University Medical Center, New York, NY 10032, USA; [12]Department of Maternal Fetal Medicine, Columbia University Medical Center, New York, NY 10032, USA; [13]Department of Obstetrics, Gynecology, and Reproductive Sciences, University of Texas Medical School at Houston, Houston, TX 77030, USA; [14]Regional Obstetrical Consultants, Chattanooga, TN 37403, USA; [15]Department of Genetics and Development, Columbia University, New York, NY 10032, USA; [16]Department of Pediatrics, Columbia University, New York, NY 10032, USA; [17]Department of Pediatrics, Clinical Genetics Services, New York University School of Medicine, New York, NY 10003, USA; [18]Department of Genetics, Harvard Medical School, Boson, MA 02115, USA; [19]Departments of Psychiatry and Pathology, Massachusetts General Hospital, Boston, MA 02114, USA; [20]Department of Pathology, Brigham and Women's Hospital and Harvard Medical School, Boston, MA 02115, USA; [21]Division of Evolution and Genomic Science, School of Biological Sciences, University of Manchester, Manchester Academic Health Science Center, Manchester 03101, UK

*Correspondence: cmorton@partners.org

http://dx.doi.org/10.1016/j.ajhg.2016.08.022.

Table 1. Pathological Rewiring of Genetic Regulatory Interactions

Genomic Locus on 2q36.1	TAD and TBR Nucleotides (hESC, GRCh37/hg19)[18] (Size)	Structural Rearrangement (Associated Phenotype)
WNT6-IHH-DES	TBR: 219,731,756–219,851,756 (120 kb), TAD: 219,851,756–220,251,756 (400 kb), TBR: 220,251,756–220,411,756 (160 kb)	inversion or duplication altering the 160 kb TBR and bringing the centromeric portion of the *EPHA4*-containing TAD into proximity with *WNT6* (F-syndrome [MIM: 102510])
		duplication or deletion altering the 160 kb TBR and bringing *IHH* into proximity with the centromeric portion of the *EPHA4*-containing TAD (polydactyly)
EPHA4	TAD: 220,411,756–222,891,756 (2.48 Mb)	deletion involving the TBR at 222,891,756 (brachydactyly)
PAX3	TAD: 222,891,756–223,491,756 (600 kb)	

This table shows the pathological rewiring of genetic regulatory interactions of enhancer *EPHA4* through different structural rearrangements altering the TAD boundaries (data presented herein are modified from Lupiãnez et al.[20]). Abbreviations are as follows: hESC, human embryonic stem cell; TAD, topologically associated domain; and TBR, topological boundary region.

phenotype and an apparently balanced chromosomal rearrangement.[5–12] Massively parallel sequencing technologies can provide timely localization of chromosomal breakpoints with nucleotide-level precision in all apparently balanced rearrangements, along with information on the gain or loss of genomic material,[13,14] which could substantially improve the prediction of phenotypic outcomes and support perinatal medical care.

Outcomes of structural rearrangements changing the copy number of a gene or directly disrupting a gene can be predicted from dosage effects. However, if a balanced rearrangement occurs in a non-coding region or the regulatory effect of the rearrangement is more pertinent to an abnormal phenotype than the directly affected gene, predicting pathogenic consequences can become challenging and even erroneous when only the gene(s) with copy-number changes or disrupted gene(s) are evaluated. This is particularly important in prenatal diagnosis, because for many key developmental genes, *cis*-regulatory elements can extend beyond the transcription unit with an estimated median regulator-target gene distance of 120 kb,[15] which can range up to 1.5 Mb.[16,17]

Topologically associated domains (TADs) have been elucidated as key elements of mammalian regulatory organization.[18,19] TADs are highly conserved megabase-sized genomic segments that partition the genome into large units with frequent intra-domain interactions. They are separated by topological boundary regions (TBRs), which represent "genomic insulators" by blocking the interactions between adjacent TADs. Disruption of TBRs by structural rearrangements has been demonstrated to cause rewiring of genomic regulators in the *WNT6-IHH-EPHA4-PAX3* locus (MIM: 604663, 600726, 602188, and 606597) and result in human limb malformations, as described by Lupiãnez et al. (Table 1 and Figure 1).[20] In this context, the developmental genes with historically well-known long-range regulation can be re-evaluated in relation to their TAD and TBR annotations (Table 2 and Figure 1). For example, disruption of *PAX6* (MIM: 607108) and regulatory elements located in the same TAD as *PAX6* (up to 150 kb downstream) results in isolated aniridia,[21] whereas haploinsufficiency of *WT1* (MIM: 194070), which is located in the TAD adjacent to *PAX6*, causes genitourinary anomalies without aniridia.[23] Deletions of the contiguous locus containing both *PAX6* and *WT1*, including the TBR between their two adjacent TADs, result in the autosomal-dominant WAGR syndrome (MIM: 194072) with both aniridia and genitourinary anomalies, supporting the "genomic insulator" role of TBRs. In addition, the size of an individual TAD can be relevant to the extent of long-range regulation. *TWIST1* (MIM: 601622) is known to have long-range regulation up to 260 kb downstream, which is located within the same 440 kb TAD as *TWIST1*. Monoallelic disruption of both *TWIST1* and its downstream regulatory region results in Saethre-Chotzen syndrome (MIM: 101400).[24] *SOX9* (MIM: 608160) is reported to have long-range regulation up to 1.5 Mb upstream, which is located within the same 1.88 Mb TAD as *SOX9*. Monoallelic disruption of both *SOX9* and its regulatory region is associated with campomelic dysplasia (MIM: 114290) and Pierre Robin sequence (MIM: 261800).[25,28,29] There might also be phenotype-specific regulators within the same TAD for a developmental gene depending on their distance from the gene of interest. Monoallelic disruption of regulatory elements located within the same 1.6 Mb TAD as *SHH* (MIM: 600725) can result in type 3 holoprosencephaly (MIM: 142945) or preaxial polydactyly (MIM: 174500), depending on the location (265 kb upstream or 1 Mb upstream of *SHH*, respectively).[26] Lastly, in addition to the genes showing a phenotype with monoallelic disruption, regulatory regions of developmental genes located on the X chromosome or imprinted genes should also be carefully analyzed, given that disruption of a single allele through balanced rearrangements could result in an abnormal phenotype in such cases. For instance, *POU3F4* (MIM: 300039) is an X-linked recessively inherited gene with long-range regulation up to 900 kb upstream[27] in a 3.04 Mb TAD, and disruption of a single allele of *POU3F4* or its regulatory region results in deafness in males. Overall, advances in the understanding of chromatin organization of the human genome, along with

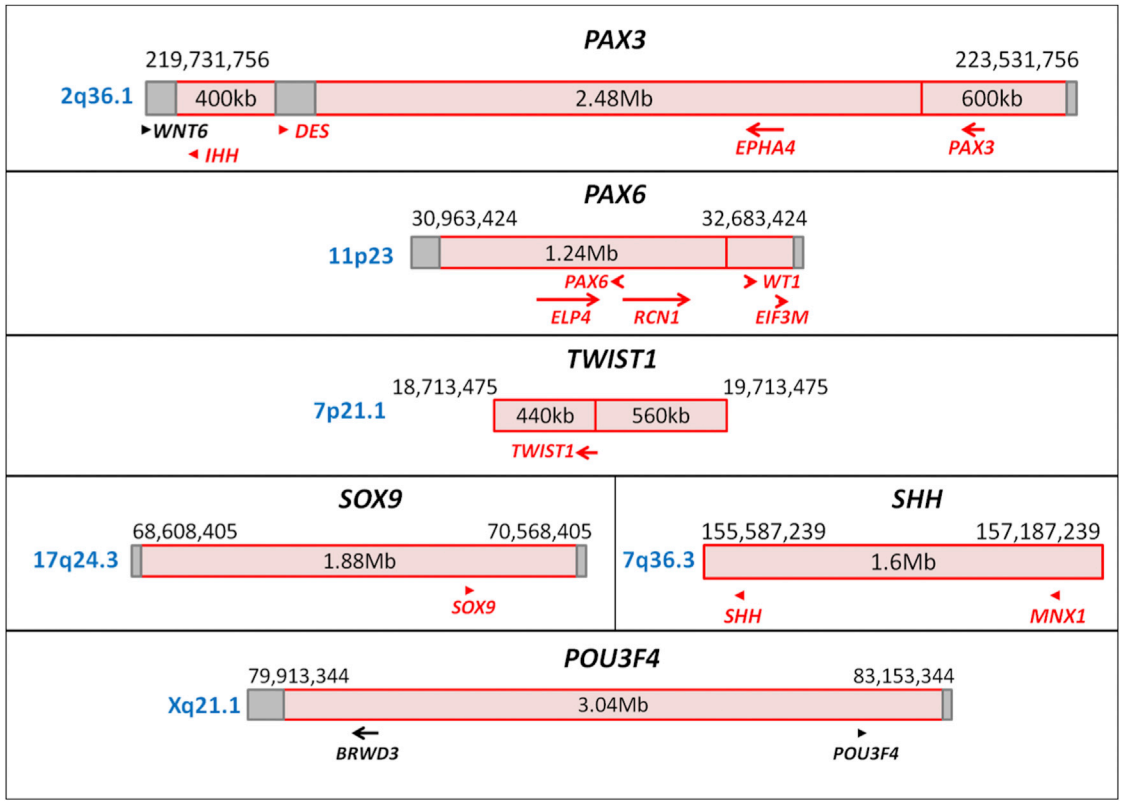

Figure 1. Developmental Genes with Well-Known Long-Range Regulations
Schematic diagrams of representative developmental genes with well-known long-range regulations in relation to their TAD (red box) and TBR (dark-red vertical line if 0 bp or gray box if greater than 0 bp) annotations (genes in red: haploinsufficiency index < 10%).

the evolving databases of phenotypes associated with structural variation, could provide a conceptual framework for the interpretation of balanced-rearrangement breakpoints and their potential *cis*-regulatory effects.

Identifying breakpoints of balanced chromosomal rearrangements has been the foundation of the Developmental Genome Anatomy Project (DGAP), which has sequenced more than 200 subjects. As an extension of these efforts, in this study, we sequenced ten prenatal subjects with balanced chromosomal rearrangements by using customized large-insert libraries and used publicly available databases to interpret the breakpoints on the basis of convergent genomic evidence in light of previously annotated TADs and TBRs in human embryonic stem cells.[29]

Material and Methods

Subjects

Ten subjects were enrolled after proper informed consent was acquired in accordance with an institutional-review-board protocol approved by Partners HealthCare System in Boston. These ten subjects represent the total of a consecutive series of DGAP prenatal referrals to date, and prior to enrollment, all had balanced chromosomal rearrangements according to karyotyping with normal CMA results. Two subjects (DGAP239 and DGAP259) have been reported in part previously.[30,31]

Sequencing and Bioinformatic Analysis

Genomic DNA was extracted from amniocytes or chorionic villi with a Gentra Puregene Cell Kit (QIAGEN). Large-insert structural-variation sequencing was performed as previously described.[12,26] In brief, after the production of large-insert libraries (target size of 2–3.5 kb) and quality control, massively parallel paired-end sequencing of 25 or 50 cycles was performed with an Illumina HiSeq 2000 or 2500. Reads were processed with our customized structural-variant sequencing pipelines, which include alignment, clustering of anomalous read pairs, extensive cluster filtering, and variant screening against known structural variants.[32–35] Genome-wide physical coverage of inserts ranged from 35× to 68×, and DNA input ranged from 900 ng to 5 μg. For all subjects with sufficient material, DNA was amplified by PCR with primers based on sequence reads supporting the rearrangement junction for confirmation of breakpoints.

Analysis of Convergent Genomic Evidence

In addition to genes located directly at breakpoints, phenotypic associations were evaluated in relation to previously annotated TADs and TBRs in human embryonic stem cells[18] for positional effects on protein-coding genes through disruption of potential regulatory elements. DECIPHER was utilized for predicting the probability of haploinsufficiency, which was determined on the basis of genes known to produce a phenotype through haploinsufficiency and genes disrupted by unambiguous loss-of-function variants in at least two apparently healthy individuals. Low haploinsufficiency indices (<10%) indicate a high predicted probability that a gene will exhibit haploinsufficiency (i.e., disruption

Table 2. TADs and TBRs of Genes with Historically Well-Known Long-Range *cis*-Regulation Associated with a Phenotype

Locus (Chromosome Band)	TAD and TBR Nucleotides (hESC, GRCh37/hg19)[18] (Size)	Genetic Alterations	Phenotype
PAX6-WT1 (11p23)	TBR: 30,963,424–31,083,424 (120 kb), TAD: 31,083,424–32,323,424 (1.24 Mb), TAD: 32,323,424–32,643,424 (320 kb), TBR: 32,643,424–32,683,424 (40 kb),	disruption of regulatory elements up to 150 kb downstream of *PAX6*	aniridia[21]
		deletions involving *PAX6* and *WT1*, which includes the TBR between the TADs of these genes	WAGR syndrome[22]
		haploinsufficiency of *WT1*	syndromes involving genitourinary anomalies without aniridia[23]
TWIST1 (7p21.1)	TAD: 18,713,475–19,153,475 (440 kb), TAD: 19,153,475–19,713,475 (560 kb)	disruption of regulatory elements up to 260 kb downstream of *TWIST1*	Saethre-Chotzen syndrome[24]
SOX9 (17q24.3)	TAD: 68,648,405–70,528,405 (1.88 Mb)	disruption of regulatory elements up to 1.5 Mb upstream of *SOX9*	Pierre Robin sequence[25]
SHH (7q36.3)	TAD: 155,587,239–157,187,239 (1.6 Mb)	disruption of regulatory elements up to 265 kb upstream of *SHH*	HPE3[26]
		disruption of regulatory elements up to 1 Mb upstream of *SHH*	preaxial polydactyly[26]
POU3F4 (Xq21.1)	TAD: 80,073,344–83,113,344 (3.04 Mb)	disruption of regulatory elements up to 900 kb upstream of *POU3F4*	X-linked deafness[27]

Abbreviations are as follows: hESC, human embryonic stem cell; HPE3, holoprosencephaly type 3; TAD, topologically associated domain; TBR, topological boundary region; and WAGR, Wilms tumor, aniridia, genitourinary anomalies, and mental retardation.

of one allele might be pathogenic, also referred to as monoallelic).[36] Within the analyzed intervals, disrupted genes, genes with a haploinsufficiency index < 10%, hemizygous or imprinted genes, and genes associated with a phenotype were evaluated in detail for each subject in relation to the disrupted TADs and TBRs. Abnormal phenotypic associations of disrupted or dysregulated regions were reviewed in the scientific literature, OMIM,[37] OMIM Gene Map and Morbid Map,[37] DECIPHER,[38] and the Developmental Disorders Genotype-to-Phenotype (DDG2P) database.[39]

Expression Studies

qRT-PCR was performed with RNA extracted from cultured prenatal cells of the available subjects (amniocytes from DGAP247 and chorionic villi from DGAP248 and DGAP288) and control samples (amniocytes or chorionic villi with a normal karyotype referred for advanced maternal age) or cord blood (DGAP247 and DGAP288). qRT-PCR was performed according to standard conditions of the CFX Real-Time PCR Detection System (Bio-Rad), and transcription levels were quantified with the ΔΔCT method.[30]

Results

Prior to enrollment, karyotyping was performed for all pregnancies because they were considered to be high risk (e.g., advanced maternal age, abnormal first-trimester serum screening, and/or ultrasound abnormality) with normal CMA results during clinical assessment (see Supplemental Note). Among the ten subjects analyzed, four had reciprocal translocations, five had inversions, and one had a complex rearrangement according to karyotyping. Sequencing revised the initial karyotype by providing nucleotide-level resolution to the initially described chromosome bands with a size ranging from 2.8 to 53.6 Mb, encompassing 63–1,032 genes and 16–358 phenotype-associated loci for each rearrangement (Table 3 and Table S1).[40] In addition to refining breakpoints, including those in a subject with a very complex karyotype (DGAP259), sequencing revealed cryptic rearrangements unapparent by karyotyping in four subjects (DGAP258, DGAP268, DGAP290, and DGAP295). All rearrangements were located within a TAD, except for one that was located in a TBR at Xq28 (DGAP285) (Figures 2, 3, and 4; Tables 4, 5, and 6; and Table S2). Five subjects had abnormal clinical outcomes, three continue to be healthy, and two were terminated prior to detection of any potential abnormal findings (Table 7).

DGAP239

DGAP239[30] (46,XY,t(6;8)(q13;q13)dn.arr(1-22)x2,(XY)x1.seq[GRCh37/hg19] t(6;8)(q13;q12.2)dn) had multisystemic abnormalities detected by imaging studies starting in the second trimester and was diagnosed clinically with CHARGE syndrome (MIM: 214800) only after birth. Sequencing the prenatal DNA sample identified translocation breakpoints (designated as t(6;8)(q13;q13) by karyotyping) disrupting *CHD7* (MIM: 608892) at 8q12.2 and *LMBRD1* (MIM: 612625) at 6q13 (Figure 2A and Table 4). Whereas biallelic losses of *LMBRD1* are associated with methylmalonic aciduria and homocystinuria, cblF type (MIM: 277380) (no phenotypic overlap with DGAP239),[42] monoallelic loss of *CHD7* is well known to be associated with CHARGE syndrome (it is mutated in more than 90% of subjects), correlating with the low haploinsufficiency index of *CHD7* and the clinical outcome of DGAP239 (see Supplemental Note and Tables S3 and S4).[43]

Table 3. Genomic Localization of the Disrupted Chromosome Bands in Comparison to Karyotypically Reported Bands

Subject	Next-Gen Cytogenetic Nomenclature[40] (Short System)	G-Band	Next-Gen Band	Revised Band Range: Nucleotides (Distance)	Genes[a]	Phenotype-Associated Loci[b]
DGAP239	46,XY,t(6;8)(q13;q13)dn.arr(1-22)x2,(XY)x1. seq[GRCh37/hg19] t(6;8)(q13;q12.2)dn	6q13	6q13	6q13: 70,000,001–75,900,000 (5.9 Mb)	63	16
		8q13	8q12.2	8q12q21: 55,500,001–93,300,000 (37.8 Mb)	334	41
DGAP247	46,XY,inv(8)(q13q24.1)dn.arr(1-22)x2,(XY)x1. seq[GRCh37/hg19] inv(8)(q11.21q24.23)dn	8q13	8q11.21	8q11q21: 45,600,001–93,300,000 (47.7 Mb)	406	47
		8q24.1	8q24.23	8q24: 117,700,001–146,364,022 (28.7 Mb)	306	47
DGAP248	46,XY,t(2;13)(p13;q14)dn.arr(1-22)x2,(XY)x1. seq[GRCh37/hg19] t(2;13)(p12;q13.2)dn	2p13	2p12	2p14p12: 64,100,001–83,300,000 (19.2 Mb)	225	32
		13q14	13q13.2	13q13q21: 32,200,001–73,300,000 (41.1 Mb)	375	47
DGAP258	46,XY,inv(6)(p23q13)dn.arr(1-22)x2,(XY)x1. seq[GRCh37/hg19] inv(6)(p25.3q16.1)dn[c]	6p23	6p25.3	6p25p22: 1–30,400,000 (30.4 Mb)	679	74
		6q13	6q16.1	6q11q16: 61,000,001–105,500,000 (44.5 Mb)	293	44
DGAP259	46,XX,t(3;18;5;7)(p25;p11.2;q13.3;q32),t(9;18)(p22;q21)dn.arr(1-22,X)x2. seq[GRCh37/hg19](3,5,7,9,18)cx,der(3)t(3;7)(p24.3;q36.3)dn,der(5)t(5;7)(q14.3;q35)t(3;7)(p24.3;q36.3) t(3;18)(p26.3;p11.31)dn,der(7)t(5;7)dn, der(9)t(9;18)(p23;q21.3)dn, der(18)t(3;18)inv(18)(p11.31q21.3)t(9;18)dn	3p25	3p26.3 3p24.3	3p26p24:1–30,900,000 (30.9 Mb)	277	49
		5q13.3	5q14.3	5q12q14: 58,900,001–92,300,000 (33.4 Mb)	323	358
		7q32	7q35 7q36.3	7q31q36: 107,400,001–159,138,663 (51.8 Mb)	693	80
		9p22	9p23	9p23p21: 9,000,001–33,200,000 (24.2 Mb)	181	33
		18p11.2	18p11.31	18p11: 1–17,200,000 (17.2 Mb)	192	29
		18q21	18q21.3	18q21: 43,500,001–61,600,000 (18.1 Mb)	172	33
DGAP268	46,XY,inv(10)(p13q24)dn.arr(1-22)x2,(XY)x1. seq[GRCh37/hg19]inv(10)(p12.2p12.31)(p12.2q23.32)dn	10p13	10p12.31 10p12.2	10p14p12: 6,600,001–29,600,000 (23 Mb)	233	26
		10q24	10q23.32	10q23q25: 82,000,001–119,100,000 (37.1 Mb)	467	84
DGAP285	46,Y,inv(X)(p11.2q28).arr(1-22)x2,(XY)x1. seq[GRCh37/hg19] inv(X)(p11.2q28)	Xp11.2	Xp11.21	Xp11.2: 46,400,001–58,100,000 (11.7 Mb)	274	65
		Xq28	Xq28	Xq28: 147,100,001–155,270,560 (8.2 Mb)	192	63
DGAP288	46,XX,t(6;17)(q13;q21)dn.arr(1-22,X)x2. seq[GRCh37/hg19] t(6;17)(q21;q24.3)dn	6q13	6q21	6q11q21: 61,000,001–114,600,000 (53.6 Mb)	404	57
		17q21	17q24.3	17q11q24: 24,000,001–70,900,000 (46.9 Mb)	1,032	138
DGAP290	46,XY,t(2;7)(q33;q32)dn.arr(1-22)x2,(XY)x1. seq[GRCh37/hg19](2,7)cx, der(2)t(2;7)(q32.3;q33) inv(7)(q33q33)dn,der(7)t(2;7)dn	2q33	2q32.3	2q32q34: 183,000,001–215,300,000 (32.3 Mb)	313	51
		7q32	7q33	7q31q33: 107,400,001–138,200,000 (30.8 Mb)	291	49
DGAP295	46,XY,t(2;11)(p13.1;p15.5)dn.arr(1-22)x2,(XY)x1. seq[GRCh37/hg19](2,11)cx,der(2)inv(11)(p15.5)inv(11)(p15.5) t(2;11)(p13.3;p15.5)dn,der(11)t(2;11)dn	2p13.1	2p13.3	2p13: 68,600,001–75,000,000 (6.4 Mb)	133	32
		11p15.5	11p15.5	11p15.5: 1–2,800,000 (2.8 Mb)	114	31

[a]Number of genes for the presented nucleotide range (NCBI Map Viewer, annotation release 105 [GrCh37.p13]).
[b]OMIM Phenotypic Series-specific entries for the presented nucleotide range (June 9, 2015).
[c]Cryptic paternal inversion is not included.

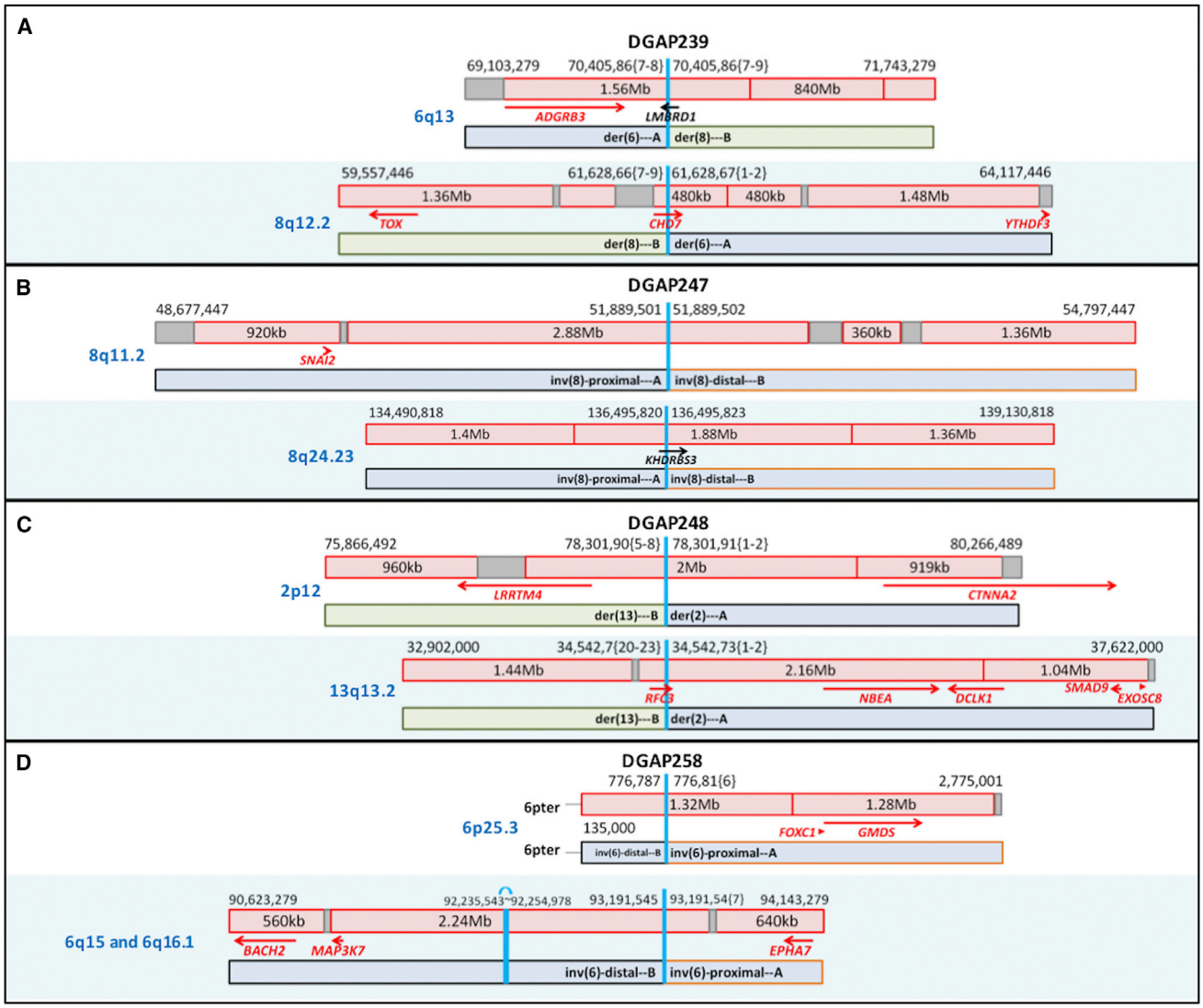

Figure 2. Diagrams of DGAP239, DGAP247, DGAP248, and DGAP258 Rearrangements
Schematic diagrams of the breakpoints of DGAP239 (A), DGAP247 (B), DGAP248 (C), and DGAP258 (D) in relation to their TAD (red box) and TBR (dark-red vertical line if 0 bp or gray box if greater than 0 bp) annotations (genes in red: haploinsufficiency index < 10%).

DGAP247

DGAP247 (46,XY,inv(8)(q13q24.1)dn.arr(1-22)x2,(XY)x1.seq[GRCh37/hg19] inv(8)(q11.21q24.23)dn) had normal prenatal findings without complications during the perinatal period. At 31 months of age, he continues to be healthy. Sequencing of the prenatal DNA sample identified inversion breakpoints (designated as inv(8)(q13q24.1) by karyotyping) within a non-genic region at 8q11.2 and disruption of *KHDRBS3* (MIM: 610421) at 8q24.23 (Figure 2B and Table 4). Although *KHDRBS3* has a borderline haploinsufficiency index and showed decreased RNA expression in the prenatal sample (see Supplemental Note, Figures S1 and S2, and Tables S5 and S6), it is not reported to be associated with a developmental role and/or abnormal phenotype, and no additional genes located in the rearranged TADs have been implicated in a phenotype or developmental role, correlating with the normal clinical phenotype.

DGAP248

DGAP248 (46,XY,t(2;13)(p13;q14)dn.arr(1-22)x2,(XY)x1.seq[GRCh37/hg19] t(2;13)(p12;q13.2)dn) had normal first-trimester screening. At 19.4 weeks, the pregnancy was terminated before the sequencing results were available. Sequencing of the prenatal DNA sample identified translocation breakpoints (designated as t(2;13)(p13;q14) by karyotyping) within a non-genic region at 2p12 and disrupting *RFC3* (MIM: 600405) at 13q13.2 (Figure 1C). The 2p12 breakpoint is located within a TAD that includes *LRRTM4* (MIM: 610870), a gene with a low haploinsufficiency index and no reported abnormal phenotypic association. However, structure and expression profiles of *LRRTM* mRNAs in mice suggest a role in development and maintenance of the vertebrate nervous system.[44] *RFC3* has a low haploinsufficiency index and showed decreased RNA expression in the prenatal sample (Figure S3).[36] In addition, *NBEA* (MIM: 6084889), a candidate autism gene with a low

Table 4. DGAP239, DGAP247, DGAP248 and DGAP258: Significant Protein-Coding Genes Surrounding the Breakpoints according to TADs and Convergent Genomic Evidence

Gene	Nucleotides (GRCh37/hg19)	Description	OMIM[37]	OMIM Morbid[37]	DDG2P[39]	HI (%)[36]	Notes
DGAP239: 6q13 Breakpoints on Rearrangement_A (70,405,86{7-8}) and Rearrangement_B (70,405,86{7-9})							
ADGRB3	69,345,259–70,099,403	adhesion G protein-coupled receptor B3	602684	–	–	3.02	no reported phenotype association; homologous to *ADGRB1*, an angiogenesis inhibitor that is a candidate for involvement in development of glioblastoma[41]
LMBRD1 (disrupted)	70,385,694–70,507,003	LMBR1 domain containing 1	612625	+	+	12.92	biallelic loss of function (autosomal recessive) associated with methylmalonic aciduria and homocystinuria, cblF type[42] (no phenotypic overlap with DGAP239)
DGAP239: 8q12.2 Breakpoints on Rearrangement_A (61,628,67{1-2}) and Rearrangement_B (61,628,66{7-9})							
CHD7 (disrupted)	61,591,337–61,779,465	chromodomain helicase DNA binding protein 7	608892	+	+	2.4	haploinsufficiency (autosomal dominant, monoallelic) reported to be associated with CHARGE syndrome, such that mutations in >90% of subjects meet diagnostic criteria of CHARGE syndrome[43] (consistent with the clinical diagnosis of CHARGE syndrome during the postnatal period of DGAP239)
DGAP247: 8q11.2 Breakpoints on Rearrangement_A (51,889,501) and Rearrangement_B (51,889,502)							
No significant gene within the same TAD as the breakpoints							
DGAP247: 8q24.23 Breakpoints on Rearrangement_A (136,495,820) and Rearrangement_B (136,495,823)							
KHDRBS3	136,469,700–136,668,965	KH domain containing, RNA binding, signal transduction associated 3	610421	–	–	10.52	no reported phenotype association
DGAP248: 2p12 Breakpoints on Rearrangement_A (78,301,91{1-2}) and Rearrangement_B (78,301,90{8-5})							
LRRTM4	76,974,845–77,820,445	leucine rich repeat transmembrane neuronal 4	610870	–	–	7.26	no reported phenotype association; structure and expression profile of *LRRTM* mRNAs in mice suggest role in development and maintenance of the vertebrate nervous system[44]
DGAP248: 13q13.2 breakpoints on Rearrangement_A (34,542,73{2-1}) and Rearrangement_B (34,542,7{20-23})							
RFC3 (disrupted)	34,392,186–34,540,695	replication factor C subunit 3	600405	–	–	4.93	no reported phenotype association
NBEA	35,516,424–36,247,159	neurobeachin	6084889	–	–	6.83	disrupted in a subject with a de novo translocation and idiopathic autism,[45] and haploinsufficiency causes autism-like behaviors in animal models[46,47]
DGAP258: 6p25.3 Breakpoints on Rearrangement_A (776,81{6}) and Rearrangement_B (776,787)							
No significant gene within the same TAD as the breakpoints							
DGAP258: 6q16.1 Breakpoints on Rearrangement_A (93,191,54{7}) and Rearrangement_B (93,191,545)							
MAP3K7	91,223,292–91,296,764	mitogen-activated protein kinase kinase kinase 7	602614	–	–	2.75	no reported phenotype association

Abbreviations are as follows: DDG2P, Developmental Disorders Genotype-to-Phenotype database; and HI, haploinsufficiency index.

haploinsufficiency score,[45,46] is located within the same 2.16 Mb TAD and 973 kb downstream of the breakpoints (Figure 2C and Table 4). Given the presence of two genes with low haploinsufficiency indices—one associated with a phenotype and located within the 13q13.2 rearrangement TAD (*NBEA*) and the other implicated in nervous

system development and located within the 2p12 rearrangement TAD (*LRRTM4*)—but the lack of strong evidence for a phenotypic correlation, these results are interpreted as "unknown clinical significance. Clinical follow-up was not possible because the pregnancy was terminated (see Supplemental Note and Tables S7 and S8). Of note, the pregnancy was terminated prior to communication of the sequencing results on the basis of an informed decision after karyotyping, CMA, and genetic counseling.

DGAP258

DGAP258 (46,XY,inv(6)(p23q13)dn.arr(1-22)x2,(XY)x1.seq[GRCh37/hg19] inv(6)(p25.3q16.1)dn(q15q15)pat or 46,XY,inv(6)(p23q13)dn.arr(1-22)x2,(XY)x1.seq[GRCh37/hg19] inv(6)(p25.3q16.1)dn,inv(6)(q15q15)pat) was a monozygotic twin pregnancy, and amniocentesis was performed as a result of abnormal first-trimester serum screening. Other than minor complications due to a twin pregnancy, there were no abnormal clinical findings during the perinatal period. At 2.5 years of age, the twins continue to be healthy. Sequencing of the prenatal DNA sample identified inversion breakpoints (designated as inv(6)(p23q13) by karyotyping) within non-genic regions at both 6p25.3 and 6q16.1. In addition, a paternally inherited cryptic non-genic rearrangement at 6q15 was detected (Figure 2D and Table 4). Because of the length of the sequencing reads, it was not possible to determine whether both of the breakpoints on 6q reside in the same paternally inherited chromosome; however, given their relative proximity and localization within the same 2.21 Mb TAD, this is a likely possibility. Analysis of protein-coding genes localized in the same TAD as the breakpoints did not reveal any additional genes associated with an abnormal phenotype or a developmental role, correlating with the normal clinical phenotype of DGAP258 (see Supplemental Note and Tables S9 and S10).

DGAP259

DGAP259[31] (46,XX,t(3;18;5;7)(p25;p11.2;q13.3;q32),t(9;18)(p22;q21)dn.arr(1-22,X)x2.seq[GRCh37/hg19](3,5,7,9,18)cx,der(3)t(3;7)(p24.3;q36.3)dn,der(5)t(5;7)(q14.3;q35)t(3;7)(p24.3;q36.3)t(3;18)(p26.3;p11.31)dn,der(7)t(5;7)dn,der(9)t(9;18)(p23;q21.3)dn,der(18)t(3;18)inv(18)(p11.31q21.3)t(9;18)dn) had abnormal prenatal findings of bilateral ventriculomegaly and colpocephaly with partial agenesis of the corpus callosum and a complex amniotic fluid karyotype designated as 46,XX,t(3;18;5;7)(p25;p11.2;q13.3;q32),t(9;18)(p22;q21)dn. The pregnancy was terminated at 22 weeks as a result of the abnormal findings. Sequencing of the prenatal DNA sample identified nine rearrangement sequences located at 3p26.3, 3p24.3, 5q14.3, 7q35, 7q36.3, 9p23, 18p11.31, and 18q21.3 with small deletions and duplications less than 1 kb (Figure 3 and Table 5). Among six disrupted protein-coding genes, *TBC1D5* (MIM: 615740) and *CNTNAP2* (MIM: 604569) reside in the vicinity of well-known genome-organizer- and chromatin-regulator-encoding regions—*SATB1* (MIM: 602075)[50] and *EZH2* (MIM: 601573)[61] at 3p24.3 and 7q35, respectively—which might be relevant to the complex chromosomal aberration of DGAP259 (all four of these genes are predicted to have low haploinsufficiency indices). Breakpoints at 7q36.3 disrupt the regulatory region of *SHH*, which has a low haploinsufficiency index. Monoallelic disruption of this *SHH* regulatory region is associated with holoprosencephaly,[26] which is consistent with the cerebral malformation phenotype of DGAP259. Breakpoints at 5q14.3 are located within the same TAD as *MEF2C* (MIM: 600662), another gene that has a low haploinsufficiency index and is associated with cerebral malformation and hypoplastic corpus callosum,[47,54] as observed in DGAP259 (see Supplemental Note and Tables S11–S18).

DGAP268

DGAP268 (46,XY,inv(10)(p13q24)dn.arr(1-22)x2,(XY)x1.seq[GRCh37/hg19] inv(10)(p12.2p12.31)(p12.2q23.32)dn) had abnormal nuchal translucency detected in the first trimester, and there were no complications during the perinatal period. At 1 year of age, he continues to be healthy. Sequencing of the prenatal DNA sample identified a complex inversion with breakpoints (designated as inv(10)(p13q24) by karyotyping) within non-genic regions at 10p12.31 and 10p12.2 and disruption *CPEB3* (MIM: 610606) at 10q23.32 (Figure 4A and Table 6). *CPEB3* does not have a low haploinsufficiency index and does not have any abnormal phenotypic association. Analysis of protein-coding genes localized in the same TAD as the breakpoints also did not reveal any genes associated with an abnormal phenotype, correlating with the normal clinical phenotype of DGAP268 (see Supplemental Note and Tables S19–S21).

DGAP285

DGAP285 (46,Y,inv(X)(p11.2q28).arr(1-22)x2,(XY)x1.seq[GRCh37/hg19] inv(X)(p11.21q28)) showed abnormal prenatal imaging findings, including hydrocephalus, starting at 22.5 weeks and fetal demise at 31.4 weeks after decreased fetal movements. Sequencing of the prenatal DNA sample identified inversion breakpoints (designated as inv(X)(p11.2q28) by karyotyping) disrupting *FAM104B* at Xp11.21 and within a non-genic region at Xq28 (Figure 4B and Table 6). Breakpoints at Xq28 disrupt a TBR, which could result in genomic rewiring of the surrounding TADs and TBRs. *MTM1* (MIM: 300415) is an X-linked recessively inherited gene associated with centronuclear myopathy (MIM: 310400), a prenatal-onset fatal disease with clinical findings including decreased fetal movements, hydrocephalus, and stillbirth.[73–75] *MTM1* is located in a TBR upstream of the TBR at the Xq28 rearrangement, and therefore dysregulation of *MTM1* might contribute to the phenotype of DGAP285 (see Supplemental Note and Tables S22 and S23).

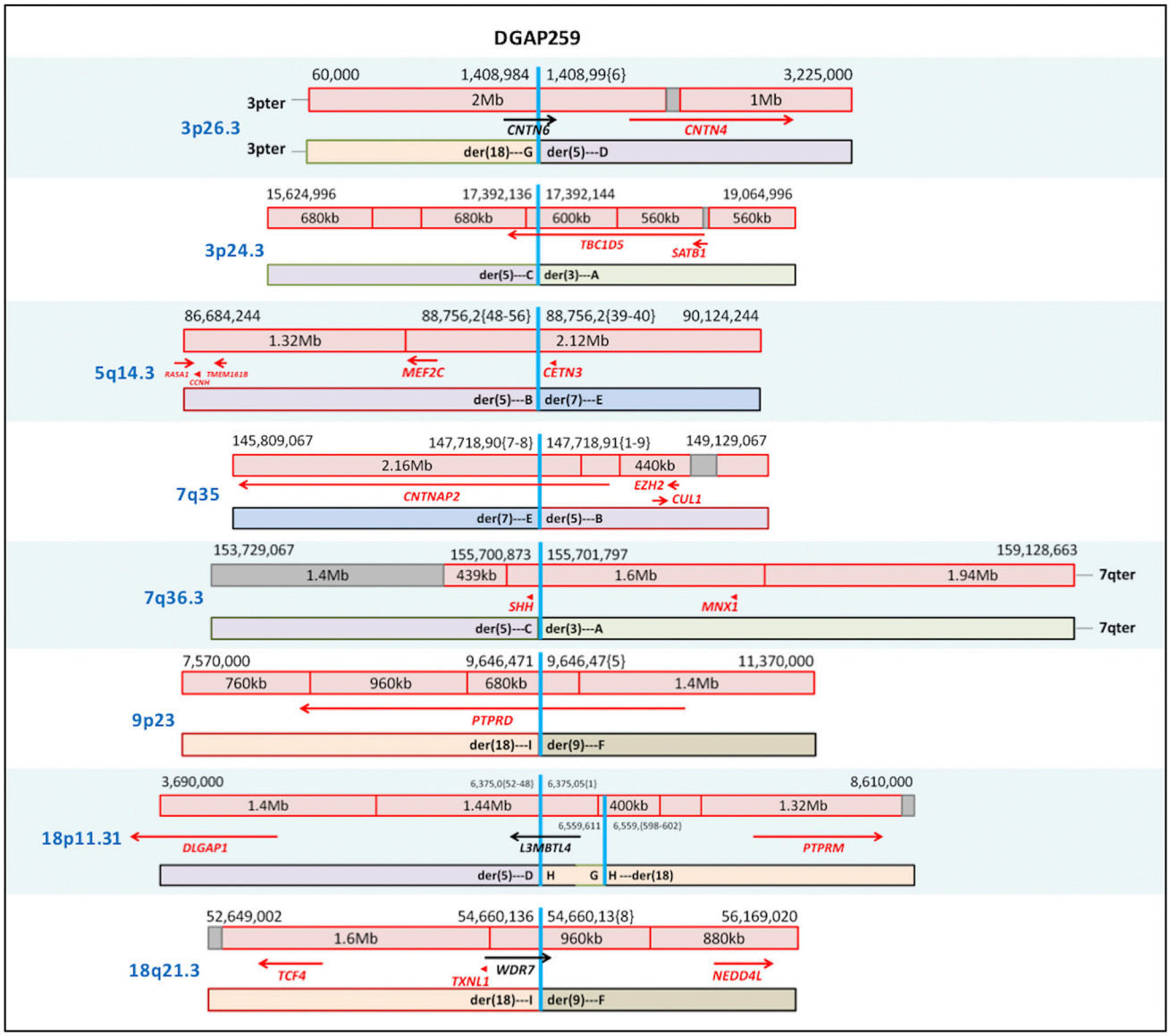

Figure 3. Diagrams of DGAP259 Rearrangements
Schematic diagrams of the breakpoints of DGAP259 in relation to their TAD (red box) and TBR (dark-red vertical line if 0 bp or gray box if greater than 0 bp) annotations (genes in red: haploinsufficiency index < 10%).

DGAP288

DGAP288 (46,XX,t(6;17)(q13;q21)dn.arr(1-22,X)x2.seq [GRCh37/hg19] t(6;17)(q21;q24.3)dn) had cystic hygroma at 11.1 weeks, followed by prenatal imaging findings consistent with Pierre Robin sequence, which were confirmed during the postnatal period. Sequencing of the prenatal DNA sample identified translocation breakpoints (designated as t(6;17)(q13;q21) by karyotyping) within non-genic regions at 6q21 and 17q24.3 (Figure 4C and Table 6). Breakpoints at 17q24.3 were in a 1.88 Mb TAD corresponding to an upstream *cis*-regulatory region of *SOX9* (MIM: 608160), a region known to be associated with Pierre Robin sequence as a result of dysregulation of *SOX9*, an autosomal-dominantly inherited gene with a low haploinsufficiency index.[25,28,29] The prenatal sample showed decreased RNA expression of *SOX9* (Figure 5), correlating with the clinical outcome of DGAP288 (see Supplemental Note and Tables S24 and S25).

DGAP290

DGAP290 (46,XY,t(2;7)(q33;q32)dn.arr(1-22)x2,(XY)x1.seq[GRCh37/hg19](2,7)cx,der(2)t(2;7)(q32.3;q33)inv(7)(q33q33)dn,der(7)t(2;7)dn) was a high-risk pregnancy according to first-trimester screening, which showed normal imaging up to 18 weeks. The parents decided to terminate the pregnancy at 23 weeks because of uncertainty of the clinical significance of the balanced rearrangement. Sequencing of the prenatal DNA sample identified translocation breakpoints (designated as t(2;7)(q33;q32) by karyotyping) disrupting *HECW2* at 2q32.3 and *NUP205*

Table 5. DGAP259: Significant Protein-Coding Genes Surrounding the Breakpoints according to TADs and Convergent Genomic Evidence

Gene	Nucleotides (GRCh37/hg19)	Description	OMIM[37]	OMIM Morbid[37]	DDG2P[39]	HI (%)[36]	Notes
3p26.3 Breakpoints on Rearrangement_D (1,408,99{6}) and Rearrangement_G (1,408,984)							
CNTN6 (disrupted)	1,134,260–1,445,901	contactin 6	607220	–	–	39.69	no reported phenotype association; neural adhesion molecule[48]
CNTN4	2,140,497–3,099,645	contactin 4	607280	–	–	6.9	disrupted in a subject with a 3p deletion syndrome (autosomal-dominant) phenotype[49] (cerebral and renal malformation phenotype of DGAP259)
3p26.3 Breakpoints on Rearrangement_D (1,408,99{6}) and Rearrangement_G (1,408,984)							
TBC1D5 (disrupted)	17,198,654–18,486,309	TBC1 domain family member 5	615740	–	–	5.84	no reported phenotype association
SATB1[a]	18,386,879–18,487,080	SATB homeobox 1	602075	–	–	2.15	global genome organizer[50,51] (complex chromosomal rearrangement of DGAP259); role in neuronal plasticity of cortical neurons and regulation of key neuronal genes[52,53] (cerebral malformation phenotype of DGAP259)
5q14.3 Breakpoints on Rearrangement_B (88,756,2{48-56}) and Rearrangement_E (88,756,2{39-40})							
MEF2C	88,013,975–88,199,922	myocyte enhancer factor 2C	600662	+	+	0.26	haploinsufficiency (autosomal dominant, monoallelic) associated with mental retardation, stereotypic movements, epilepsy, and cerebral malformations (MIM: 613443)[47,54] (cerebral malformation and hypoplastic corpus callosum phenotype of DGAP259); role in synaptic plasticity and hippocampal-dependent learning and memory[55] (9p23 breakpoints of DGAP259 disrupt *PTPRD1* with similar role)
CETN3	89,688,078–89,705,603	centrin 3	602907	–	–	5.94	present in centrosomes and important role in early cleavage of frog embryos[56] (complex chromosomal rearrangement of DGAP259)
7q35 Breakpoints on Rearrangement_B (147,718,91{1-9}) and Rearrangement_E (147,718,90{7-8})							
CNTNAP2 (disrupted)	145,813,453–148,118,090	contactin associated protein-like 2	604569	+	+	4.94	susceptibility to autism type 15;[57] homozygous or compound-heterozygous mutations cause Pitt-Hopkins-like syndrome 1 (MIM: 610042)[58] (cerebral malformation phenotype of DGAP259; 18q21 breakpoints are one TAD downstream of *TCF4*, associated with Pitt-Hopkins syndrome)
CUL1[a]	148,395,006–148,498,128	cullin 1	603134	–	–	4.3	regulates the mammalian G1/S transition[59]
EZH2[a]	148,504,475–148,581,413	enhancer of zeste 2 polycomb repressive complex 2 subunit	601573	+	+	3.07	has a critical role during normal and perturbed development of the hematopoietic and central nervous systems,[60] maintains homeotic gene repression, and is thought to control gene expression by regulating chromatin[61] (cerebral malformation and complex chromosomal rearrangement of DGAP259)

(*Continued on next page*)

Table 5. *Continued*

Gene	Nucleotides (GRCh37/hg19)	Description	OMIM[37]	OMIM Morbid[37]	DDG2P[39]	HI (%)[36]	Notes
7q36.3 Breakpoints on Rearrangement_A (155,701,797) and Rearrangement_C (155,700,873)							
SHH	155,592,680–155,604,967	sonic hedgehog	600725	+	+	0.66	haploinsufficiency (autosomal dominant, monoallelic) associated with HPE3,[62] which has a long-range regulation-associated phenotype[63] (cerebral malformation phenotype of DGAP259)
9p23 Breakpoints on Rearrangement_F (9,646,47{5}) and Rearrangement_I (9,646,471)							
PTPRD (disrupted)	8,314,246–10,612,723	protein tyrosine phosphatase, receptor type D	601598	–	–	0.14	homozygous microdeletion causes trigonocephaly, hearing loss, and intellectual disability, which overlap the autosomal-dominant 9p deletion syndrome[64] (cerebral malformation phenotype of DGAP259); role in synaptic plasticity and hippocampal-dependent learning and memory[65] (5q14.3 breakpoints are within the same TAD as *MEF2C* with similar role)
18p11.31 Breakpoints on Rearrangement_D (6,375,05{1}), Rearrangement_G (6,559,611), and Rearrangement_H (6,375,0{52-48} and 6,559,{598-602})							
L3MBTL4 (disrupted)	5,954,705–6,415,236	L(3)Mbt-like 4 (*Drosophila*)	–	–	–	59.07	no reported phenotype association
18q21.3 Breakpoints on Rearrangement_F (54,660,13{8}) and Rearrangement_I (54,660,136)							
TCF4[a]	52,889,562–53,332,018	transcription factor 4	602272	+	+	0.38	haploinsufficiency (autosomal dominant, monoallelic) is associated with Pitt-Hopkins syndrome[66] (cerebral malformation phenotype of DGAP259, 7q35 breakpoints disrupt *CNTNAP2*, related to Pitt-Hopkins-like syndrome[58])
WDR7 (disrupted)	54,318,574–54,698,828	WD repeat domain 7	613473	–	–	14.85	no reported phenotype association; localized to synaptic vesicles in rat and mouse brain[67]
NEDD4L[a]	55,711,599–56,068,772	neural precursor cell expressed, developmentally down-regulated 4-like, E3 ubiquitin protein ligase	606384	–	–	8.66	regulator of renal sodium channels; involved in induction of mesoendodermal fates in mouse embryonic stem cells[68] (renal malformation phenotype of DGAP259)

Abbreviations are as follows: DDG2P, Developmental Disorders Genotype-to-Phenotype database; HI, haploinsufficiency index; and HPD3, holoprosencephaly type 3.
[a]Although not located within the same hESC TAD[18] as the breakpoint, these genes might be relevant to the phenotype of DGAP259 given the complexity of the rearrangement.

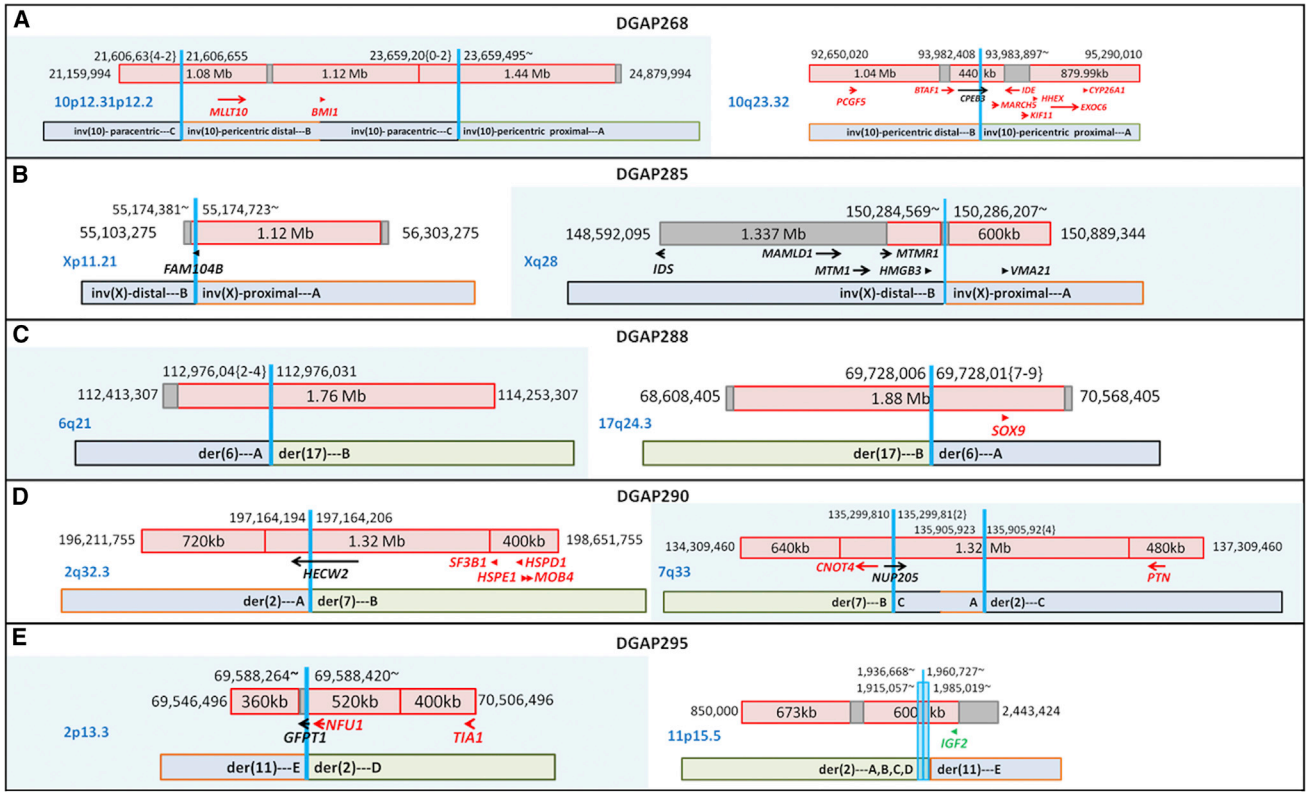

Figure 4. Diagrams of DGAP268, DGAP285, DGAP288, DGAP290, and DGAP290 Rearrangements
Schematic diagrams of the breakpoints of DGAP268 (A), DGAP285 (B), DGAP288 (C), DGAP290 (D), and DGAP290 (E) in relation to their TAD (red box) and TBR (dark-red vertical line if 0 bp or gray box if greater than 0 bp) annotations (genes in red: haploinsufficiency index < 10%; green: imprinted).

(MIM: 614352) at 7q33 and an additional non-genic disruption at 7q33 (Figure 4D and Table 6). Neither disrupted gene had a low haploinsufficiency index, and analysis of protein-coding genes in the same TAD as the breakpoints did not reveal any genes associated with an abnormal phenotype. These results are interpreted as "unknown clinical significance, likely to be benign"; however, clinical correlation was not possible because the pregnancy was terminated (see Supplemental Note and Tables S26 and S27).

DGAP295

DGAP295 (46,XY,t(2;11)(p13.1;p15.5)dn.arr(1-22)x2,(XY)x1.seq[GRCh37/hg19](2,11)cx,der(2)inv(11)(p15.5)inv(11)(p15.5)t(2;11)(p13.3;p15.5)dn,der(11)t(2;11)dn) had abnormal first-trimester screening, which showed an abnormal prenatal imaging finding of growth restriction starting from 19 weeks, and weighed 450 g upon delivery at 31 weeks. Sequencing of the prenatal DNA sample identified translocation breakpoints (designated as t(2;11)(p13.1;p15.5) by karyotyping) disrupting *GFPT1* (MIM: 138292) at 2p13.3 and multiple non-genic regions at 11p15.5 within a 70 kb distribution (Figure 4E and Table 6). The complex breakpoints at 11p15.5 are within the same 600 kb TAD as *IGF2* (MIM: 147470), an imprinted region known to be associated with growth restriction with distinctive facies (GRDF [MIM: 616489])[71] and Silver-Russell syndrome (MIM: 180860),[72] consistent with the growth restricted phenotype of DGAP295 (see Supplemental Note and Tables S28 and S29).

Discussion

We report whole-genome sequencing of ten prenatal subjects with balanced chromosomal rearrangements with "normal" CMA results and their phenotypic interpretation through publicly available resources. Each subject has contributed uniquely to our experience in the evolution of this approach to a new standard of care in prenatal diagnosis by providing further insight into prognosis through incorporation of an understanding of the regulatory genome (Table 7).

In the evaluation of the pathogenic outcomes of balanced rearrangements, disruption or dysregulation of a single allele is of particular significance when it involves a region known to be hemizygous for X-linked traits, haploinsufficient (autosomal dominant), or imprinted and associated with an abnormal phenotype. Next-generation sequencing can identify the disrupted regions at the nucleotide level; however, predicting the dysregulation of the genes in the vicinity of the breakpoints is more challenging. Advances in the understanding of large-scale regulatory chromatin

Table 6. DGAP268, DGAP285, DGAP288, DGAP290, and DGAP295: Significant Protein-Coding Genes Surrounding the Breakpoints according to TADs and Convergent Genomic Evidence

Gene	Nucleotides (GRCh37/hg19)	Description	OMIM[37]	OMIM Morbid[37]	DDG2P[39]	HI (%)[36]	Notes
DGAP268: 10p12.31 Breakpoints on Rearrangement_B (21,606,655) and Rearrangement_C (21,606,63{4-2})							
No significant gene within the same TAD as the breakpoints							
DGAP268: 10p12.2 Breakpoints on Rearrangement_A (23,659,495~) and Rearrangement_C (23,659,20{0-2})							
No significant gene within the same TAD as the breakpoints							
DGAP268: 10q23.32 Breakpoints on Rearrangement_A (93,983,897~) and Rearrangement_B (93,982,408)							
CPEB3 (disrupted)	93,806,449–94,050,844	cytoplasmic polyadenylation element binding protein 3	610606	–	–	12.96	no reported phenotype association
DGAP285: Xp11.21 Breakpoints on Rearrangement_A (55,174,723~) and Rearrangement_B (55,174,381~)							
FAM104B (disrupted)	55,169,535–55,187,743	family with sequence similarity 104 member B	–	–	–	93.08	no reported phenotype association
DGAP285: Xq28 Breakpoints on Rearrangement_A (150,286,207~) and Rearrangement_B (150,284,569~)							
MTM1	149,737,069–149,841,795	myotubularin 1	300415	+	+	12.54	hemizygous loss of function (X-linked recessive) associated with X-linked myotubular myopathy[69] (overlapping the phenotype of DGAP285)
DGAP288: 6q21 Breakpoints on Rearrangement_A (112,976,04{2-4}) and Rearrangement_B (112,976,031)							
No significant gene within the same TAD as the breakpoints							
DGAP288: 17q24.3 Breakpoints on Rearrangement_A (69,728,01{7-9}) and Rearrangement_B (69,728,006)							
SOX9	70,117,161–70,122,561	SRY-box 9	608160	+	+	0.56	haploinsufficient (autosomal dominant, monoallelic) long-range *cis*-regulation associated with Pierre Robin sequence[28] (overlapping the phenotype of DGAP288)
DGAP290: 2q32.3 Breakpoints on Rearrangement_A (197,164,194) and Rearrangement_B (197,164,206)							
HECW2 (disrupted)	197,059,094–197,458,416	HECT, C2, and WW domain containing E3 ubiquitin protein ligase 2	–	–	–	18.5	no reported phenotype association
DGAP290: 7q33 Breakpoints on Rearrangement_A (135,905,923), Rearrangement_B (135,299,810), and Rearrangement_C (135,299,81{2} and 135,905,92{4})							
NUP205 (disrupted)	135,242,667–135,333,505	nucleoporin 205	614352	–	–	11.41	no reported phenotype association

(*Continued on next page*)

Table 6. *Continued*

Gene	Nucleotides (GRCh37/hg19)	Description	OMIM[37]	OMIM Morbid[37]	DDG2P[39]	HI (%)[36]	Notes
DGAP295: 2p13.3 Breakpoints on Rearrangement_D (69,588,420~) and Rearrangement_E (69,588,264~)							
GFPT1 (disrupted)	69,546,905–69,614,382	glutamine-fructose-6-phosphate transaminase 1	138292	+	–	22.36	biallelic loss of function (autosomal recessive) associated with congenital myasthenia type 12[70] (no overlap with the phenotype of DGAP295)
DGAP295: 11p15.5 Breakpoints on Rearrangement_A (1,915,057~ and 1,936,993~), Rearrangement_B (1,960,727~ and 1,936,668~), Rearrangement_C (1,915,843~ and 1,961,361~), Rearrangement_D (1,984,895~), and Rearrangement_E (1,985,019~)							
IGF2	2,150,342–2,170,833	insulin-like growth factor 2	147470	+	+	79.01	imprinted loss of function (epimutation) associated with GRDF[71] and Silver-Russell syndrome[72] (overlapping the phenotype of DGAP295)

Abbreviations are as follows: DDG2P, Developmental Disorders Genotype-to-Phenotype database; GRDF, growth restriction with distinctive facies; and HI, haploinsufficiency index.

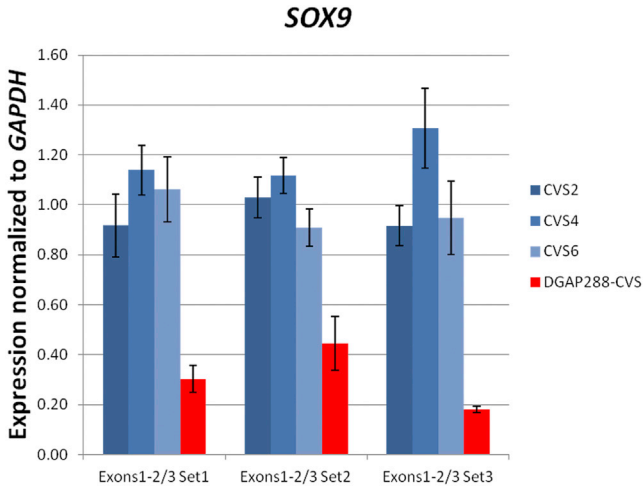

Figure 5. *SOX9* Expression of DGAP288
Decreased expression of *SOX9* in the chorionic villus sample (CVS) of DGAP288 in comparison to three CVS controls (three different primer sets were used for the expression assessment of exons 1 and 2 out of 3, normalized to *GAPDH*). Error bars represent the SE of the normalized ratios.

domains (TADs) contribute to overcoming this obstacle. A recent study analyzing the *WNT6-IHH-EPHA4-PAX3* locus and three related congenital genetic disorders has provided multiple layers of evidence for the significance of these megabase-sized regulatory domains and their contribution to abnormal phenotypes through genomic rewiring of the regulatory boundaries resulting from structural rearrangements.[20] It is well established that the *cis*-regulatory elements for many key developmental genes can extend beyond the transcription unit in the range of 120 kb to 1.5 Mb,[15–17,76,77] which could be explained by these regulatory associations. Therefore, we analyzed the aforementioned characteristics (hemizygosity, haploinsufficiency, and imprinting) of the disrupted genes at the breakpoints, as well as the protein-coding genes located in the regulatory domains and boundaries (TADs and TBRs, respectively) associated with the breakpoints to identify the dysregulated regions. Then, we evaluated the phenotypic and developmental significance of these genes of interest. None of the three subjects with normal outcomes (DGAP247, DGAP258, and DGAP268) had disrupted genes or were predicted to have dysregulated genes involved with an abnormal phenotype. Among five subjects with abnormal outcomes, one (DGAP239) had a disrupted syndromic gene with a low haploinsufficiency index, one (DGAP285) had a disrupted TBR and was predicted to have a dysregulated X-linked recessively inherited syndromic gene, one (DGAP288) had a dysregulated gene involved with an abnormal phenotype, one (DGAP295) was predicted to have a dysregulated imprinted gene involved with a syndrome, and lastly, in one chromothripsis-affected subject (DGAP259), multiple genes associated with CNS malformations and genomic organization were disrupted and predicted to be dysregulated. All showed abnormal phenotypes overlapping the

Table 7. Lessons Learned: Next-Generation Sequencing of Ten Prenatal Subjects

Subject	Gene(s) of Interest according to Sequencing Results	Interpretation of the Sequencing Results	Clinical Significance	Clinical Outcome
DGAP239	*CHD7* (disrupted), *LMBRD1* (disrupted)	disruption of an autosomal-dominant gene with a low haploinsufficiency index and associated with CHARGE syndrome (pathogenic) and an autosomal-recessive gene (non-contributory)	pathogenic	CHARGE syndrome
DGAP247	*KHDRBS3* (disrupted)	disruption of a single gene without pathogenicity	unknown, likely to be benign	healthy newborn
DGAP248	*LRRTM4*, *RFC3* (disrupted), *NBEA*	disruption of a gene with a low haploinsufficiency index but no reported pathogenicity; potential dysregulation of an additional gene with a low haploinsufficiency index and reported to be associated with autism-like behaviors in animal models and disrupted in a subject with idiopathic autism[45,46]	unknown	termination prior to communication of sequencing results
DGAP258	–	non-genic breakpoints with cryptic paternal inversion not at the karyotypically detected breakpoint	unknown, likely to be benign	healthy newborns
DGAP259	*CNTN6* (disrupted), *CNTN4*, *TBC1D5* (disrupted), *SATB1*, *MEF2C*, *CETN3*, *CNTNAP2* (disrupted), *CUL1*, *EZH2*, *SHH*, *PTPRD* (disrupted), *L3MBTL4* (disrupted), *TCF4*, *WDR7* (disrupted), *NEDD4L*	complex rearrangement with potential dysregulation of genes with a low haploinsufficiency index and associated with malformation in the CNS and chromatin organization	pathogenic	termination due to multiple abnormal prenatal findings (bilateral ventriculomegaly and colpocephaly with partial agenesis of the corpus callosum)
DGAP268	*CPEB3* (disrupted)	disruption of a single gene without known pathogenicity and a cryptic inversion at non-genic breakpoints	unknown, likely to be benign	healthy newborn
DGAP285	*FAM104B* (disrupted), *MTM1*	disruption of a single gene without known pathogenicity; disruption of a TBR with potential dysregulation of a gene associated with X-linked myotubular myopathy, a prenatal-onset fatal disease	unknown, likely to be pathogenic	intrauterine fetal demise (overlapping findings with X-linked myotubular myopathy include decreased fetal movements, hydrocephalus, and stillbirth)
DGAP288	*SOX9*	non-genic breakpoints with dysregulation of a gene with a low haploinsufficiency index and known to be associated with Pierre Robin sequence	pathogenic	Pierre Robin sequence
DGAP290	*HECW2* (disrupted), *NUP205* (disrupted)	disruption of two genes without known pathogenicity; non-genic cryptic inversion in one of the breakpoints	unknown, likely to be benign	termination after communication of sequencing results
DGAP295	*GFPT1* (disrupted), *IGF2*	complex rearrangement with potential dysregulation of an imprinted gene associated with Silver-Russell syndrome (pathogenic) and a recessively inherited syndromic gene (noncontributory)	pathogenic	small birth weight and failure to thrive (findings consistent with Silver-Russell syndrome)

predicted outcomes of the sequencing results. Of note, two of the five subjects with abnormal phenotypes (DGAP239 and DGAP295) had additional disrupted genes involved in autosomal-recessive syndromes and did not show any clinical features associated with these syndromes. However, in such cases, a potential "carrier" status for the relevant syndromes might be considered in future genetic counseling of the newborn if the outcome is otherwise normal. Among the two terminated pregnancies without any abnormal phenotypes prior to termination, one subject (DGAP248) is interpreted as having a rearrangement predicted to be of unknown clinical significance, and the other (DGAP290) is interpreted has having a rearrangement predicted to be likely benign.

Although karyotyping remains the standard of care for prenatal diagnosis, advances in genomic technologies are rapidly transitioning into clinical practice. Non-invasive cfDNA screening and CMA in invasive testing are increasingly popular methods in the field of prenatal genetics.[78–80] Non-invasive prenatal testing of cfDNA offers tremendous potential as a screening tool, particularly for fetal aneuploidies. Although this next-generation-sequencing-based approach has been shown to reliably demonstrate copy-number variations greater than 5 Mb,[81] it currently remains a screening method.[2,3] Current guidelines recommend offering CMA to any woman choosing to undergo prenatal invasive diagnostic testing and recommend CMA as the primary test (replacing conventional

karyotype) if the prenatal diagnostic test is performed for an indication of a structural abnormality detected by prenatal imaging studies.[33] Nonetheless, CMA cannot assess balanced rearrangements and, if performed alone in the present study, would have "missed" all five prenatal subjects with abnormal outcomes (each of whom had abnormal prenatal imaging findings), including a subject with complex chromothripsis (DGAP259).

Karyotyping remains superior to CMA for the detection of balanced rearrangements, despite its megabase-sized resolution. Next-generation sequencing using large-insert libraries provides precise delineation of the breakpoints of structural rearrangements while detecting additional high-resolution cryptic rearrangements, as well as copy-number alterations that could potentially be detected by CMA and not karyotyping. Although cfDNA screening is also a sequence-based approach, given the fragmented nature of cell-free DNA, it would be cumbersome to analyze truly balanced rearrangements with the current cfDNA technology. Another sequence-based approach in the field of prenatal genetics is whole-exome sequencing.[82,83] Although this method provides higher nucleotide-level coverage and therefore can more reliably detect nucleotide-level mutations in the exome than our large-insert library method, given the presence of non-genic breakpoints in structural rearrangements, a whole-genome paired-end sequencing approach using large-insert libraries, as presented herein, would be most useful in detecting structural rearrangements. Currently, we would recommend using this method in subjects with a normal CMA and a karyotype with a balanced rearrangement (the order of CMA and karyotyping depends on the clinical scenario). In subjects with an abnormal CMA and/or a karyotype without a balanced rearrangement that fails to explain an abnormal phenotype, our method could still be valuable for identifying cryptic rearrangements in the appropriate clinical setting. We believe next-generation sequencing technologies will eventually be proposed as a first-line diagnostic method because they can provide details on structural rearrangements that cannot be detected by either karyotyping or CMA.

As with other genomic testing methods, whole-genome sequencing also raises the issue of variants of unknown clinical significance. The topic of "unknown clinical significance" is not a new problem for the field of prenatal diagnosis, whether it be a subtle imaging finding such as mildly enlarged ventricles or the detection of a balanced chromosomal rearrangement by karyotyping. Sequencing provides additional understanding of the breakpoints involved in a balanced chromosomal rearrangement. Although this information could fundamentally influence genetic counseling, clinical management, and decision making, it could also bring additional pressure to managing unknown findings on the basis of current genomic evidence. Eventually, evolving annotation of the human genome—including the discovery of disease-associated genes or other predictors of regulatory effect, such as pathogenic increases in gene expression—along with guidelines from expert committees, could close these gaps of interpretation, as has been the case with improved clinical reporting of CMA results over the past decade.[84]

In conclusion, detecting balanced chromosomal rearrangements with whole-genome sequencing provides nucleotide-level precision incomparable to currently employed prenatal genetic-testing methods, thus enabling the regulatory genome to be evaluated in such a way that could prove invaluable in clinical interpretation.

Supplemental Data

Supplemental Data include a Supplemental Note, 3 figures, and 29 tables and can be found with this article online at http://dx.doi.org/10.1016/j.ajhg.2016.08.022.

Acknowledgments

We are grateful to the families of the subjects for their participation. We thank Christina Jabbour, Amelia Lindgren, Samantha Schilit, and Drs. Ozden Altiok Clark and Frederick Bieber for their contributions. We dedicate this article in loving memory of Dorothy Warburton, a co-author on this study and the author of an article also published in *The Journal*,[4] which has served as a foundation for the Developmental Genome Anatomy Project. This study was funded by the NIH (GM061354 to C.C.M., M.E.T., and J.F.G.; HD081256 and March of Dimes 6-FY15-255 to M.E.T.).

Received: June 19, 2016
Accepted: August 26, 2016
Published: October 13, 2016

Web Resources

DECIPHER, https://decipher.sanger.ac.uk/
DGAP, http://www.bwhpathology.org/dgap/
OMIM, http://www.omim.org

References

1. American College of Obstetricians and Gynecologists Committee on Genetics (2013). Committee Opinion No. 581: the use of chromosomal microarray analysis in prenatal diagnosis. Obstet. Gynecol. *122*, 1374–1377.
2. (2016). Practice Bulletin No. 162 Summary: Prenatal Diagnostic Testing for Genetic Disorders. Obstet. Gynecol. 127, 976–978.
3. (2016). Practice Bulletin No. 163: Screening for Fetal Aneuploidy. Obstet. Gynecol. 127, e123–e137.
4. Warburton, D. (1991). De novo balanced chromosome rearrangements and extra marker chromosomes identified at prenatal diagnosis: clinical significance and distribution of breakpoints. Am. J. Hum. Genet. *49*, 995–1013.
5. Gribble, S.M., Prigmore, E., Burford, D.C., Porter, K.M., Ng, B.L., Douglas, E.J., Fiegler, H., Carr, P., Kalaitzopoulos, D., Clegg, S., et al. (2005). The complex nature of constitutional de novo apparently balanced translocations in patients presenting with abnormal phenotypes. J. Med. Genet. *42*, 8–16.
6. De Gregori, M., Ciccone, R., Magini, P., Pramparo, T., Gimelli, S., Messa, J., Novara, F., Vetro, A., Rossi, E., Maraschio, P., et al.

(2007). Cryptic deletions are a common finding in "balanced" reciprocal and complex chromosome rearrangements: a study of 59 patients. J. Med. Genet. *44*, 750–762.
7. Sismani, C., Kitsiou-Tzeli, S., Ioannides, M., Christodoulou, C., Anastasiadou, V., Stylianidou, G., Papadopoulou, E., Kanavakis, E., Kosmaidou-Aravidou, Z., and Patsalis, P.C. (2008). Cryptic genomic imbalances in patients with de novo or familial apparently balanced translocations and abnormal phenotype. Mol. Cytogenet. *1*, 15.
8. Baptista, J., Mercer, C., Prigmore, E., Gribble, S.M., Carter, N.P., Maloney, V., Thomas, N.S., Jacobs, P.A., and Crolla, J.A. (2008). Breakpoint mapping and array CGH in translocations: comparison of a phenotypically normal and an abnormal cohort. Am. J. Hum. Genet. *82*, 927–936.
9. Higgins, A.W., Alkuraya, F.S., Bosco, A.F., Brown, K.K., Bruns, G.A., Donovan, D.J., Eisenman, R., Fan, Y., Farra, C.G., Ferguson, H.L., et al. (2008). Characterization of apparently balanced chromosomal rearrangements from the developmental genome anatomy project. Am. J. Hum. Genet. *82*, 712–722.
10. Schluth-Bolard, C., Delobel, B., Sanlaville, D., Boute, O., Cuisset, J.M., Sukno, S., Labalme, A., Duban-Bedu, B., Plessis, G., Jaillard, S., et al. (2009). Cryptic genomic imbalances in de novo and inherited apparently balanced chromosomal rearrangements: array CGH study of 47 unrelated cases. Eur. J. Med. Genet. *52*, 291–296.
11. Gijsbers, A.C., Bosch, C.A., Dauwerse, J.G., Giromus, O., Hansson, K., Hilhorst-Hofstee, Y., Kriek, M., van Haeringen, A., Bijlsma, E.K., Bakker, E., et al. (2010). Additional cryptic CNVs in mentally retarded patients with apparently balanced karyotypes. Eur. J. Med. Genet. *53*, 227–233.
12. Feenstra, I., Hanemaaijer, N., Sikkema-Raddatz, B., Yntema, H., Dijkhuizen, T., Lugtenberg, D., Verheij, J., Green, A., Hordijk, R., Reardon, W., et al. (2011). Balanced into array: genome-wide array analysis in 54 patients with an apparently balanced de novo chromosome rearrangement and a meta-analysis. Eur. J. Hum. Genet. *19*, 1152–1160.
13. Korbel, J.O., Urban, A.E., Affourtit, J.P., Godwin, B., Grubert, F., Simons, J.F., Kim, P.M., Palejev, D., Carriero, N.J., Du, L., et al. (2007). Paired-end mapping reveals extensive structural variation in the human genome. Science *318*, 420–426.
14. Talkowski, M.E., Ernst, C., Heilbut, A., Chiang, C., Hanscom, C., Lindgren, A., Kirby, A., Liu, S., Muddukrishna, B., Ohsumi, T.K., et al. (2011). Next-generation sequencing strategies enable routine detection of balanced chromosome rearrangements for clinical diagnostics and genetic research. Am. J. Hum. Genet. *88*, 469–481.
15. Sanyal, A., Lajoie, B.R., Jain, G., and Dekker, J. (2012). The long-range interaction landscape of gene promoters. Nature *489*, 109–113.
16. Bhatia, S., and Kleinjan, D.A. (2014). Disruption of long-range gene regulation in human genetic disease: a kaleidoscope of general principles, diverse mechanisms and unique phenotypic consequences. Hum. Genet. *133*, 815–845.
17. Kleinjan, D.A., and van Heyningen, V. (2005). Long-range control of gene expression: emerging mechanisms and disruption in disease. Am. J. Hum. Genet. *76*, 8–32.
18. Dixon, J.R., Selvaraj, S., Yue, F., Kim, A., Li, Y., Shen, Y., Hu, M., Liu, J.S., and Ren, B. (2012). Topological domains in mammalian genomes identified by analysis of chromatin interactions. Nature *485*, 376–380.
19. Sexton, T., and Cavalli, G. (2015). The role of chromosome domains in shaping the functional genome. Cell *160*, 1049–1059.
20. Lupiáñez, D.G., Kraft, K., Heinrich, V., Krawitz, P., Brancati, F., Klopocki, E., Horn, D., Kayserili, H., Opitz, J.M., Laxova, R., et al. (2015). Disruptions of topological chromatin domains cause pathogenic rewiring of gene-enhancer interactions. Cell *161*, 1012–1025.
21. Bhatia, S., Bengani, H., Fish, M., Brown, A., Divizia, M.T., de Marco, R., Damante, G., Grainger, R., van Heyningen, V., and Kleinjan, D.A. (2013). Disruption of autoregulatory feedback by a mutation in a remote, ultraconserved PAX6 enhancer causes aniridia. Am. J. Hum. Genet. *93*, 1126–1134.
22. Yamamoto, T., Togawa, M., Shimada, S., Sangu, N., Shimojima, K., and Okamoto, N. (2014). Narrowing of the responsible region for severe developmental delay and autistic behaviors in WAGR syndrome down to 1.6cMb including PAX6, WT1, and PRRG4. Am. J. Med. Genet. A. *164A*, 634–638.
23. Lehnhardt, A., Karnatz, C., Ahlenstiel-Grunow, T., Benz, K., Benz, M.R., Budde, K., Büscher, A.K., Fehr, T., Feldkötter, M., Graf, N., et al. (2015). Clinical and molecular characterization of patients with heterozygous mutations in wilms tumor suppressor gene 1. Clin. J. Am. Soc. Nephrol. *10*, 825–831.
24. Cai, J., Goodman, B.K., Patel, A.S., Mulliken, J.B., Van Maldergem, L., Hoganson, G.E., Paznekas, W.A., Ben-Neriah, Z., Sheffer, R., Cunningham, M.L., et al. (2003). Increased risk for developmental delay in Saethre-Chotzen syndrome is associated with TWIST deletions: an improved strategy for TWIST mutation screening. Hum. Genet. *114*, 68–76.
25. Gordon, C.T., Tan, T.Y., Benko, S., Fitzpatrick, D., Lyonnet, S., and Farlie, P.G. (2009). Long-range regulation at the SOX9 locus in development and disease. J. Med. Genet. *46*, 649–656.
26. Fernandez, B.A., Siegel-Bartelt, J., Herbrick, J.A., Teshima, I., and Scherer, S.W. (2005). Holoprosencephaly and cleidocranial dysplasia in a patient due to two position-effect mutations: case report and review of the literature. Clin. Genet. *68*, 349–359.
27. de Kok, Y.J., Vossenaar, E.R., Cremers, C.W., Dahl, N., Laporte, J., Hu, L.J., Lacombe, D., Fischel-Ghodsian, N., Friedman, R.A., Parnes, L.S., et al. (1996). Identification of a hot spot for microdeletions in patients with X-linked deafness type 3 (DFN3) 900 kb proximal to the DFN3 gene POU3F4. Hum. Mol. Genet. *5*, 1229–1235.
28. Benko, S., Fantes, J.A., Amiel, J., Kleinjan, D.J., Thomas, S., Ramsay, J., Jamshidi, N., Essafi, A., Heaney, S., Gordon, C.T., et al. (2009). Highly conserved non-coding elements on either side of SOX9 associated with Pierre Robin sequence. Nat. Genet. *41*, 359–364.
29. Amarillo, I.E., Dipple, K.M., and Quintero-Rivera, F. (2013). Familial microdeletion of 17q24.3 upstream of SOX9 is associated with isolated Pierre Robin sequence due to position effect. Am. J. Med. Genet. A. *161A*, 1167–1172.
30. Talkowski, M.E., Ordulu, Z., Pillalamarri, V., Benson, C.B., Blumenthal, I., Connolly, S., Hanscom, C., Hussain, N., Pereira, S., Picker, J., et al. (2012). Clinical diagnosis by whole-genome sequencing of a prenatal sample. N. Engl. J. Med. *367*, 2226–2232.
31. Macera, M.J., Sobrino, A., Levy, B., Jobanputra, V., Aggarwal, V., Mills, A., Esteves, C., Hanscom, C., Pereira, S., Pillalamarri, V., et al. (2015). Prenatal diagnosis of chromothripsis, with nine breaks characterized by karyotyping, FISH, microarray and whole-genome sequencing. Prenat. Diagn. *35*, 299–301.
32. Mills, R.E., Walter, K., Stewart, C., Handsaker, R.E., Chen, K., Alkan, C., Abyzov, A., Yoon, S.C., Ye, K., Cheetham, R.K., et al.;

1000 Genomes Project (2011). Mapping copy number variation by population-scale genome sequencing. Nature *470*, 59–65.
33. Sudmant, P.H., Rausch, T., Gardner, E.J., Handsaker, R.E., Abyzov, A., Huddleston, J., Zhang, Y., Ye, K., Jun, G., Hsi-Yang Fritz, M., et al.; 1000 Genomes Project Consortium (2015). An integrated map of structural variation in 2,504 human genomes. Nature *526*, 75–81.
34. Brand, H., Collins, R.L., Hanscom, C., Rosenfeld, J.A., Pillalamarri, V., Stone, M.R., Kelley, F., Mason, T., Margolin, L., Eggert, S., et al. (2015). Paired-Duplication Signatures Mark Cryptic Inversions and Other Complex Structural Variation. Am. J. Hum. Genet. *97*, 170–176.
35. Brand, H., Pillalamarri, V., Collins, R.L., Eggert, S., O'Dushlaine, C., Braaten, E.B., Stone, M.R., Chambert, K., Doty, N.D., Hanscom, C., et al. (2014). Cryptic and complex chromosomal aberrations in early-onset neuropsychiatric disorders. Am. J. Hum. Genet. *95*, 454–461.
36. Huang, N., Lee, I., Marcotte, E.M., and Hurles, M.E. (2010). Characterising and predicting haploinsufficiency in the human genome. PLoS Genet. *6*, e1001154.
37. Amberger, J.S., Bocchini, C.A., Schiettecatte, F., Scott, A.F., and Hamosh, A. (2015). OMIM.org: Online Mendelian Inheritance in Man (OMIM®), an online catalog of human genes and genetic disorders. Nucleic Acids Res. *43*, D789–D798.
38. Firth, H.V., Richards, S.M., Bevan, A.P., Clayton, S., Corpas, M., Rajan, D., Van Vooren, S., Moreau, Y., Pettett, R.M., and Carter, N.P. (2009). DECIPHER: Database of Chromosomal Imbalance and Phenotype in Humans Using Ensembl Resources. Am. J. Hum. Genet. *84*, 524–533.
39. Bragin, E., Chatzimichali, E.A., Wright, C.F., Hurles, M.E., Firth, H.V., Bevan, A.P., and Swaminathan, G.J. (2014). DECIPHER: database for the interpretation of phenotype-linked plausibly pathogenic sequence and copy-number variation. Nucleic Acids Res. *42*, D993–D1000.
40. Ordulu, Z., Wong, K.E., Currall, B.B., Ivanov, A.R., Pereira, S., Althari, S., Gusella, J.F., Talkowski, M.E., and Morton, C.C. (2014). Describing sequencing results of structural chromosome rearrangements with a suggested next-generation cytogenetic nomenclature. Am. J. Hum. Genet. *94*, 695–709.
41. Shiratsuchi, T., Nishimori, H., Ichise, H., Nakamura, Y., and Tokino, T. (1997). Cloning and characterization of BAI2 and BAI3, novel genes homologous to brain-specific angiogenesis inhibitor 1 (BAI1). Cytogenet. Cell Genet. *79*, 103–108.
42. Rutsch, F., Gailus, S., Miousse, I.R., Suormala, T., Sagné, C., Toliat, M.R., Nürnberg, G., Wittkampf, T., Buers, I., Sharifi, A., et al. (2009). Identification of a putative lysosomal cobalamin exporter altered in the cblF defect of vitamin B12 metabolism. Nat. Genet. *41*, 234–239.
43. Janssen, N., Bergman, J.E., Swertz, M.A., Tranebjaerg, L., Lodahl, M., Schoots, J., Hofstra, R.M., van Ravenswaaij-Arts, C.M., and Hoefsloot, L.H. (2012). Mutation update on the CHD7 gene involved in CHARGE syndrome. Hum. Mutat. *33*, 1149–1160.
44. Laurén, J., Airaksinen, M.S., Saarma, M., and Timmusk, T. (2003). A novel gene family encoding leucine-rich repeat transmembrane proteins differentially expressed in the nervous system. Genomics *81*, 411–421.
45. Castermans, D., Wilquet, V., Parthoens, E., Huysmans, C., Steyaert, J., Swinnen, L., Fryns, J.P., Van de Ven, W., and Devriendt, K. (2003). The neurobeachin gene is disrupted by a translocation in a patient with idiopathic autism. J. Med. Genet. *40*, 352–356.
46. Wise, A., Tenezaca, L., Fernandez, R.W., Schatoff, E., Flores, J., Ueda, A., Zhong, X., Wu, C.F., Simon, A.F., and Venkatesh, T. (2015). Drosophila mutants of the autism candidate gene neurobeachin (rugose) exhibit neuro-developmental disorders, aberrant synaptic properties, altered locomotion, and impaired adult social behavior and activity patterns. J. Neurogenet. *29*, 135–143.
47. Nuytens, K., Gantois, I., Stijnen, P., Iscru, E., Laeremans, A., Serneels, L., Van Eylen, L., Liebhaber, S.A., Devriendt, K., Balschun, D., et al. (2013). Haploinsufficiency of the autism candidate gene Neurobeachin induces autism-like behaviors and affects cellular and molecular processes of synaptic plasticity in mice. Neurobiol. Dis. *51*, 144–151.
48. Lee, S., Takeda, Y., Kawano, H., Hosoya, H., Nomoto, M., Fujimoto, D., Takahashi, N., and Watanabe, K. (2000). Expression and regulation of a gene encoding neural recognition molecule NB-3 of the contactin/F3 subgroup in mouse brain. Gene *245*, 253–266.
49. Fernandez, T., Morgan, T., Davis, N., Klin, A., Morris, A., Farhi, A., Lifton, R.P., and State, M.W. (2004). Disruption of contactin 4 (CNTN4) results in developmental delay and other features of 3p deletion syndrome. Am. J. Hum. Genet. *74*, 1286–1293.
50. Kohwi-Shigematsu, T., Kohwi, Y., Takahashi, K., Richards, H.W., Ayers, S.D., Han, H.J., and Cai, S. (2012). SATB1-mediated functional packaging of chromatin into loops. Methods *58*, 243–254.
51. Alvarez, J.D., Yasui, D.H., Niida, H., Joh, T., Loh, D.Y., and Kohwi-Shigematsu, T. (2000). The MAR-binding protein SATB1 orchestrates temporal and spatial expression of multiple genes during T-cell development. Genes Dev. *14*, 521–535.
52. Balamotis, M.A., Tamberg, N., Woo, Y.J., Li, J., Davy, B., Kohwi-Shigematsu, T., and Kohwi, Y. (2012). Satb1 ablation alters temporal expression of immediate early genes and reduces dendritic spine density during postnatal brain development. Mol. Cell. Biol. *32*, 333–347.
53. Close, J., Xu, H., De Marco García, N., Batista-Brito, R., Rossignol, E., Rudy, B., and Fishell, G. (2012). Satb1 is an activity-modulated transcription factor required for the terminal differentiation and connectivity of medial ganglionic eminence-derived cortical interneurons. J. Neurosci. *32*, 17690–17705.
54. Le Meur, N., Holder-Espinasse, M., Jaillard, S., Goldenberg, A., Joriot, S., Amati-Bonneau, P., Guichet, A., Barth, M., Charollais, A., Journel, H., et al. (2010). MEF2C haploinsufficiency caused by either microdeletion of the 5q14.3 region or mutation is responsible for severe mental retardation with stereotypic movements, epilepsy and/or cerebral malformations. J. Med. Genet. *47*, 22–29.
55. Barbosa, A.C., Kim, M.S., Ertunc, M., Adachi, M., Nelson, E.D., McAnally, J., Richardson, J.A., Kavalali, E.T., Monteggia, L.M., Bassel-Duby, R., and Olson, E.N. (2008). MEF2C, a transcription factor that facilitates learning and memory by negative regulation of synapse numbers and function. Proc. Natl. Acad. Sci. USA *105*, 9391–9396.
56. Middendorp, S., Paoletti, A., Schiebel, E., and Bornens, M. (1997). Identification of a new mammalian centrin gene, more closely related to Saccharomyces cerevisiae CDC31 gene. Proc. Natl. Acad. Sci. USA *94*, 9141–9146.
57. Arking, D.E., Cutler, D.J., Brune, C.W., Teslovich, T.M., West, K., Ikeda, M., Rea, A., Guy, M., Lin, S., Cook, E.H., and Chakravarti, A. (2008). A common genetic variant in the neurexin

superfamily member CNTNAP2 increases familial risk of autism. Am. J. Hum. Genet. *82*, 160–164.
58. Zweier, C., de Jong, E.K., Zweier, M., Orrico, A., Ousager, L.B., Collins, A.L., Bijlsma, E.K., Oortveld, M.A., Ekici, A.B., Reis, A., et al. (2009). CNTNAP2 and NRXN1 are mutated in autosomal-recessive Pitt-Hopkins-like mental retardation and determine the level of a common synaptic protein in Drosophila. Am. J. Hum. Genet. *85*, 655–666.
59. Yu, Z.K., Gervais, J.L., and Zhang, H. (1998). Human CUL-1 associates with the SKP1/SKP2 complex and regulates p21(CIP1/WAF1) and cyclin D proteins. Proc. Natl. Acad. Sci. USA *95*, 11324–11329.
60. Di Meglio, T., Kratochwil, C.F., Vilain, N., Loche, A., Vitobello, A., Yonehara, K., Hrycaj, S.M., Roska, B., Peters, A.H., Eichmann, A., et al. (2013). Ezh2 orchestrates topographic migration and connectivity of mouse precerebellar neurons. Science *339*, 204–207.
61. Chen, H., Rossier, C., and Antonarakis, S.E. (1996). Cloning of a human homolog of the Drosophila enhancer of zeste gene (EZH2) that maps to chromosome 21q22.2. Genomics *38*, 30–37.
62. Belloni, E., Muenke, M., Roessler, E., Traverso, G., Siegel-Bartelt, J., Frumkin, A., Mitchell, H.F., Donis-Keller, H., Helms, C., Hing, A.V., et al. (1996). Identification of Sonic hedgehog as a candidate gene responsible for holoprosencephaly. Nat. Genet. *14*, 353–356.
63. Anderson, E., Devenney, P.S., Hill, R.E., and Lettice, L.A. (2014). Mapping the Shh long-range regulatory domain. Development *141*, 3934–3943.
64. Choucair, N., Mignon-Ravix, C., Cacciagli, P., Abou Ghoch, J., Fawaz, A., Mégarbané, A., Villard, L., and Chouery, E. (2015). Evidence that homozygous PTPRD gene microdeletion causes trigonocephaly, hearing loss, and intellectual disability. Mol. Cytogenet. *8*, 39.
65. Uetani, N., Kato, K., Ogura, H., Mizuno, K., Kawano, K., Mikoshiba, K., Yakura, H., Asano, M., and Iwakura, Y. (2000). Impaired learning with enhanced hippocampal long-term potentiation in PTPdelta-deficient mice. EMBO J. *19*, 2775–2785.
66. Zweier, C., Peippo, M.M., Hoyer, J., Sousa, S., Bottani, A., Clayton-Smith, J., Reardon, W., Saraiva, J., Cabral, A., Gohring, I., et al. (2007). Haploinsufficiency of TCF4 causes syndromal mental retardation with intermittent hyperventilation (Pitt-Hopkins syndrome). Am. J. Hum. Genet. *80*, 994–1001.
67. Kawabe, H., Sakisaka, T., Yasumi, M., Shingai, T., Izumi, G., Nagano, F., Deguchi-Tawarada, M., Takeuchi, M., Nakanishi, H., and Takai, Y. (2003). A novel rabconnectin-3-binding protein that directly binds a GDP/GTP exchange protein for Rab3A small G protein implicated in Ca(2+)-dependent exocytosis of neurotransmitter. Genes Cells *8*, 537–546.
68. Gao, S., Alarcón, C., Sapkota, G., Rahman, S., Chen, P.Y., Goerner, N., Macias, M.J., Erdjument-Bromage, H., Tempst, P., and Massagué, J. (2009). Ubiquitin ligase Nedd4L targets activated Smad2/3 to limit TGF-beta signaling. Mol. Cell *36*, 457–468.
69. Buj-Bello, A., Biancalana, V., Moutou, C., Laporte, J., and Mandel, J.L. (1999). Identification of novel mutations in the MTM1 gene causing severe and mild forms of X-linked myotubular myopathy. Hum. Mutat. *14*, 320–325.
70. Senderek, J., Müller, J.S., Dusl, M., Strom, T.M., Guergueltcheva, V., Diepolder, I., Laval, S.H., Maxwell, S., Cossins, J., Krause, S., et al. (2011). Hexosamine biosynthetic pathway mutations cause neuromuscular transmission defect. Am. J. Hum. Genet. *88*, 162–172.
71. Begemann, M., Zirn, B., Santen, G., Wirthgen, E., Soellner, L., Büttel, H.M., Schweizer, R., van Workum, W., Binder, G., and Eggermann, T. (2015). Paternally Inherited IGF2 Mutation and Growth Restriction. N. Engl. J. Med. *373*, 349–356.
72. Gicquel, C., Rossignol, S., Cabrol, S., Houang, M., Steunou, V., Barbu, V., Danton, F., Thibaud, N., Le Merrer, M., Burglen, L., et al. (2005). Epimutation of the telomeric imprinting center region on chromosome 11p15 in Silver-Russell syndrome. Nat. Genet. *37*, 1003–1007.
73. Jungbluth, H., Wallgren-Pettersson, C., and Laporte, J. (2008). Centronuclear (myotubular) myopathy. Orphanet J. Rare Dis. *3*, 26.
74. Joseph, M., Pai, G.S., Holden, K.R., and Herman, G. (1995). X-linked myotubular myopathy: clinical observations in ten additional cases. Am. J. Med. Genet. *59*, 168–173.
75. Starr, J., Lamont, M., Iselius, L., Harvey, J., and Heckmatt, J. (1990). A linkage study of a large pedigree with X linked centronuclear myopathy. J. Med. Genet. *27*, 281–283.
76. Jeong, Y., El-Jaick, K., Roessler, E., Muenke, M., and Epstein, D.J. (2006). A functional screen for sonic hedgehog regulatory elements across a 1 Mb interval identifies long-range ventral forebrain enhancers. Development *133*, 761–772.
77. Gordon, C.T., Attanasio, C., Bhatia, S., Benko, S., Ansari, M., Tan, T.Y., Munnich, A., Pennacchio, L.A., Abadie, V., Temple, I.K., et al. (2014). Identification of novel craniofacial regulatory domains located far upstream of SOX9 and disrupted in Pierre Robin sequence. Hum. Mutat. *35*, 1011–1020.
78. Bianchi, D.W., Parker, R.L., Wentworth, J., Madankumar, R., Saffer, C., Das, A.F., Craig, J.A., Chudova, D.I., Devers, P.L., Jones, K.W., et al.; CARE Study Group (2014). DNA sequencing versus standard prenatal aneuploidy screening. N. Engl. J. Med. *370*, 799–808.
79. Norton, M.E., Jacobsson, B., Swamy, G.K., Laurent, L.C., Ranzini, A.C., Brar, H., Tomlinson, M.W., Pereira, L., Spitz, J.L., Hollemon, D., et al. (2015). Cell-free DNA analysis for noninvasive examination of trisomy. N. Engl. J. Med. *372*, 1589–1597.
80. Wapner, R.J., Martin, C.L., Levy, B., Ballif, B.C., Eng, C.M., Zachary, J.M., Savage, M., Platt, L.D., Saltzman, D., Grobman, W.A., et al. (2012). Chromosomal microarray versus karyotyping for prenatal diagnosis. N. Engl. J. Med. *367*, 2175–2184.
81. Arbabi, A., Rampášek, L., and Brudno, M. (2016). Cell-free DNA fragment-size distribution analysis for non-invasive prenatal CNV prediction. Bioinformatics *32*, 1662–1669.
82. Drury, S., Williams, H., Trump, N., Boustred, C., Lench, N., Scott, R.H., and Chitty, L.S.; GOSGene (2015). Exome sequencing for prenatal diagnosis of fetuses with sonographic abnormalities. Prenat. Diagn. *35*, 1010–1017.
83. Pangalos, C., Hagnefelt, B., Lilakos, K., and Konialis, C. (2016). First applications of a targeted exome sequencing approach in fetuses with ultrasound abnormalities reveals an important fraction of cases with associated gene defects. PeerJ *4*, e1955.
84. Kearney, H.M., Thorland, E.C., Brown, K.K., Quintero-Rivera, F., and South, S.T.; Working Group of the American College of Medical Genetics Laboratory Quality Assurance Committee (2011). American College of Medical Genetics standards and guidelines for interpretation and reporting of postnatal constitutional copy number variants. Genet. Med. *13*, 680–685.

The American Journal of Human Genetics, Volume *99*

Supplemental Data

Structural Chromosomal Rearrangements Require Nucleotide-Level Resolution: Lessons from Next-Generation Sequencing in Prenatal Diagnosis

Zehra Ordulu, Tammy Kammin, Harrison Brand, Vamsee Pillalamarri, Claire E. Redin, Ryan L. Collins, Ian Blumenthal, Carrie Hanscom, Shahrin Pereira, India Bradley, Barbara F. Crandall, Pamela Gerrol, Mark A. Hayden, Naveed Hussain, Bibi Kanengisser-Pines, Sibel Kantarci, Brynn Levy, Michael J. Macera, Fabiola Quintero-Rivera, Erica Spiegel, Blair Stevens, Janet E. Ulm, Dorothy Warburton, Louise E. Wilkins-Haug, Naomi Yachelevich, James F. Gusella, Michael E. Talkowski, and Cynthia C. Morton

Supplemental Note

Case Reports

DGAP239[1]

46,XY,t(6;8)(q13;q13)dn.arr(1-22)x2,(XY)x1.seq[GRCh37/hg19] t(6;8)(q13;q12.2)dn

Prenatal History*:* A 37 year-old G2P0SAB1 female conceived after *in vitro* fertilization (IVF) and had normal first trimester screening. Starting in the second trimester, the following abnormal findings were detected: hypoplastic right ventricle and tricuspid atresia (18.8 weeks), polyhydramnios with a small, intermittently undetected stomach and suspicion of esophageal atresia (27.3 and 30.4 weeks), flexed extremities, protruding upper lip, and micrognathia with initiation of multiple periodic therapeutic amnioreductions (33.3 weeks), and undescended right testicle (35.3 weeks). The differential diagnosis during the prenatal period included arthrogryposis, Stickler syndrome, and trisomy 18. A sample of the initial therapeutic amniocentesis fluid at 33.3 weeks was collected for cytogenetic analysis and DNA extraction.

Postnatal History: At 36.2 weeks, during a therapeutic amnioreduction for polyhydramnios, poor fetal movements were noted and an emergent C-section was performed. The birth weight was 2985 grams (68th percentile), length was 45 cm (21st percentile), and head circumference was 33.5 cm (78th percentile). General examination showed a dusky, lethargic male on the ventilator with generalized edema. The chin was slightly retrognathic and there was a high arched palate. Ears were slightly retroverted with 'snipped off' helix, prominent antihelix and patent canals. Neck was short and edematous. Genitalia appeared male, with an underdeveloped male phallus and impalpable testes. Extremities had low tone with weak grasp and clenched fists with cortical thumb. Skin showed scattered ecchymoses and duskiness. After initial stabilization of respiratory and cardiac status, the newborn was transported to the Neonatal Intensive Care Unit (NICU) for further care. Choanal atresia was confirmed by maxillofacial CT scan. Esophageal atresia and tracheoesophageal fistula were confirmed by chest radiography and CT scan. Bilateral optic nerve hypoplasia was noted on ophthalmic examination, absence of the semicircular canals was detected in the ear complex after CT, and mild bilateral hydronephrosis was noted by ultrasound. Cardiovascular system evaluation with echocardiogram revealed tricuspid atresia, hypoplastic right ventricle, atrial and ventricular septal defects with mostly left to right flow, patent ductus arteriosus, small pulmonic valve annulus and normal branch pulmonary arteries. Neurologically, the newborn initially presented with poor tone and showed signs of encephalopathy (detected by EEG) with intermittent decorticate posturing. Clinical seizure activity was not observed. Cranial MRI suggested malformation of the brain including simplicity of the gyri in the frontal and prefrontal areas and also migrational defects. The infant's cardiopulmonary status started to deteriorate by day 8, and on day 10, the infant was removed from the ventilator to allow a natural death.

The spectrum of the infant's clinical findings detected in the postnatal period was consistent with a diagnosis of CHARGE syndrome.[2-4] Of note, optic nerve hypoplasia can be considered in the spectrum of ocular coloboma, a major characteristic finding in CHARGE syndrome.[5-7] On the basis of the newborn screening and metabolic tests, the presence of any metabolic disease was excluded.

Sequencing Results and Interpretation of Convergent Genomic Evidence: Sequencing of the prenatal DNA sample identified the translocation breakpoints directly disrupting *CHD7* at 8q12.2 and *LMBRD1* at 6q13. While biallelic losses of *LMBRD1* are associated with methylmalonic aciduria and homocystinuria, cblF type (a metabolic syndrome without any phenotypic overlap with DGAP239), haploinsufficiency of *CHD7* is well known to be associated with CHARGE syndrome (mutated in more than 90% of the cases), correlating with the postnatal diagnosis of CHARGE syndrome in DGAP239. An analysis of the protein-coding genes localized in

the same TAD as the breakpoints did not reveal any additional monoallelic or imprinted genes associated with an abnormal phenotype (Figure 2A, Table 4).

BLA(S)T Outputs of Sequencing Results:

Rearrangement_A (on der(6))

```
  1  GTTGTTGTAT  TGCTTTTTGT  GTTTTTTTTA  AATTGTTTCT  TTGTTATCTT  TTATTTTTCC
 61  CAAATTATTT  CTGACCCAAA  GTTGGCTGAA  TCCATGGATC  TGGAACCCAT  TAATATGGAG
121  GGCTAACTGT  ATACCCAACT  GCTTATGAGA  CCTCCACCTG  AACATTTTTG  AGACATCTCA
181  AGTCAACTAA  TCATTTTTTT  TTACAATTTT  TCTAACCTTA  GTACTTTTTT  TTTTTTTTTT
241  CCCTGAGACA  GAGTCTTGCC  CTGTCGCCTG  GGTCAGAGTG  CAGTGGCACG  ATCTCAGCTC
301  ACTGCAACTT  CCACCTCCCA  GGTTCAAGTG  ATTCTCCTGC  CTCAGCCTCC  CAAGTAG{CT}T
361  TAAAGTATAT  GCAGAGTCTG  ATACCTTTTC  TCTCCACTTC  TACCACCCGG  GTCCAAGTGG
421  CCTTTTTTCC  TTGCCGGTGT  TACTGCAGTA  GCTCCCCTAC  TGCTCTCCCT  GCTGTTGCCT
481  GTGTTGCCTG  CAGTCTTTCC  AATGTTAGCA  GTCAAAGTCA  TCTCTCAGAG  CCAGAGCTGG
```

Score	Start	End	qSize	Identity	Chro	Strand	Start	End	Span
357	1	359	540	99.8%	6	(+)	70405510	70405868	359
183	358	540	549	100%	8	(+)	61628671	61628853	183

BLA(S)T Output: 6q13(+)(70,405,86{7-8})::8q12.2(+)(61,628,67{1-2})

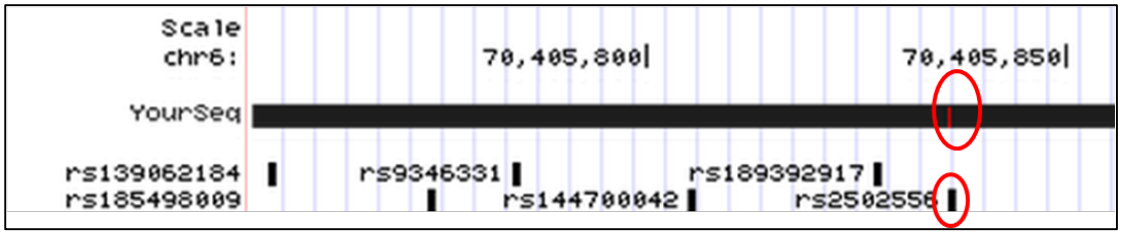

Figure S-DGAP239. BLA(S)T Output, Rearrangement_A on der(6): Circled mismatch represents a SNP (dbSNP build 141, rs2502556).

Rearrangement_B (on der(8))

```
  1  GGGATCCGCC  TGCCTTGGCC  TCCTAAAATG  CTGGGATTAC  AGGCGTGAGC  CACCGCGCCC
 61  AGCCCCTTCC  TCTTTTTGGC  TTCCACTTGG  CCAAAGGAGC  TTCCCTTTGG  GGCCGCGTCT
121  GAGTCATGTT  AGCCGCTGGT  TCAAGGGAGC  CATCTGAAAC  TCCTTGGAGC  AGGGTTTCTC
181  CTGTATATGG  CAATACTCTA  CCTTAGAAAA  ACAAAACAAA  ACAAAACAAA  ACGTCAAGTT
241  ACATGGTATA  ATGGAAAAAA  ACCCTAAACT  TGGGCTAGAA  AATATAGGCC  ACTATTTTGT
301  TTCTAATACC  ACTATGTATA  TGGACAGAAC  AGTTAACTGT  CCACGCCCTG  TGTCTTCCTT
361  CGTGAAAGGT  GGTGACACTG  TACCTTCACA  GCCTACTTCA  TAGGACTTTG  GTGTAAAATG
421  AGACAGCAGA  TGTTAAAGTA  CCTTCCGAGA  CCATTGTTTC  CAGAACCTTC  ATCACATTGT
481  GGTATTAGAA  ACCTTGGAGT  CCTCCTTGAC  TCTTTCACAA  GCTACATTGA  ATTTGTTCTC
541  AAAGCCTCTG  GCT{CTG}GGAT  TACAGGGGTG  CCCCACCACC  CTCAACTAGT  TTTTGTATTT
601  TTAGTAGAGA  CAAAGTTTCG  CCATGTTGGC  CAGGCTGGTC  TCAAACTCCT  GACCTAAGGT
661  GATCCGCCTG  CCTCGGCCTC  CCAGTGTATT  TTTTATCTCA  GCTGGTAACA  CCAAAATTAA
721  TCAAAGTACT  CAGTAACTAG  AGTGTCATGC  TAGAATCTTC  TGTTTCTCTC  ACCATTGCTC
781  TACAACCAAT  CAGAAATTCT  TTCAATTTAC  TTCTTAAATT  GCTTTATTTC  ACACCCTCAT
841  GACCACTGTT  TAGTTCAGGC  TTTCAACTCT  CTTGGATTAT  TTTAGATAGC  TCTCCCTCCC
901  CTAAG
```

Score	Start	End	qSize	Identity	Chro	Strand	Start	End	Span
556	1	556	905	100%	8	(+)	61628114	61628669	556
352	554	905	905	100%	6	(+)	70405867	70406218	352

BLA(S)T Output: 8q12.2(+)(61,628,66{7-9})::6q13(+)(70,405,86{7-9})

Next-Gen Cytogenetic Nomenclature:

Short System

46,XY,t(6;8)(q13;q13)dn.seq[GRCh37/hg19] t(6;8)(q13;q12.2)dn

Detailed System

46,XY,t(6;8)(q13;q13)dn.seq[GRCh37/hg19] t(6;8)(6pter->6q13(70,405,86{7-8})::8q12.2(61,628,67{1-2})-8qter;8pter->8q12.2(61,628,66{7-9})::6q13(70,405,86{7-9})->6qter)dn

DGAP247

46,XY,inv(8)(q13q24.1)dn.arr(1-22)x2,(XY)x1.seq[GRCh37/hg19] inv(8)(q11.21q24.23)dn

Prenatal History: A 41 year-old G3P1TAB1 female had normal first trimester screening (low risk for trisomies 13, 18, and 21, normal nuchal translucency results with normal appearing nasal bone at 12.5 weeks ultrasound). At 16.3 weeks, amniocentesis was performed for advanced maternal age. Pregnancy continued without any complications with normal ultrasound examinations at 32 and 36 weeks.

Postnatal History: The mother presented with spontaneous labor at 38 weeks and delivery occurred without complications. The newborn examination was normal. At 31 months of age, the mother reported that her son is healthy and continues to develop normally.

Sequencing Results and Interpretation of Convergent Genomic Evidence: Sequencing of the prenatal DNA sample identified the inversion breakpoints within a non-genic region at 8q11.2, and within *KHDRBS3* at 8q24.23, disrupting this gene with consequent decreased RNA expression (Figures S1 and S2). Although *KHDRBS3* (KH domain-containing, RNA-binding, signal transduction-associated protein 3) has a borderline haploinsufficiency index of 10.52%, it is not reported to be associated with an abnormal phenotype.[8] An analysis of the protein-coding genes localized in the same TAD as the breakpoints did not reveal any additional monoallelic or imprinted genes associated with an abnormal phenotype, correlating with the normal clinical phenotype of DGAP247 (Figure 2B, Table 4).

BLA(S)T Outputs of Sequencing Results:

Rearrangement_A (at proximal breakpoints of inv(8))

```
  1  TTTGACAAAC  CTGACAAAAA  CAAGAAATGA  GGAAAGGATT  CCCTATTTAA  TAAATGGTGC
 61  TGGGAAAACT  GGCTAGCCAT  ATGTAGAAAG  CTGAAACTGG  ATCCCTTCCT  TACACCTTAT
121  ACAAAAATTA  AATCAAGATG  GATTAAAGAC  TTAAATGTTA  GACCCAAAAC  CATAAAAACC
181  CTAGGAATAA  TGCAAACTCA  GAGTACGAAT  CTGAAGTCTA  TGCTTTATAC  TACTTAGTTC
241  CAGGGACTAA  TTAGCTTCAG  ATTCCGAAGG  GCAGAAAATT  CCCTCCATTT  TCTCCCATAG
301  CCACCATGAC  AACATCTTAC  TACACCCCAA  TCTGACGGCA  ATGACAGCCA  GCATGGGCAG
361  TTACAAACCA  CAACAAACCA  CTAATGGCAG  CAGAATGTGT  TTACTTGCCA  CAATCCATCA
421  TGCTTTGGGT  TCAGTGCTGT  ATAATGCAAC  TGTAATAATT  ACTGGTTTGA  GAAGAAGATA
481  TTTTCAGACA  GGTCAGACCA  CTGTGCCACA  TGTTTAATGT  AAAAGAAAAG  AGTCCATAAA
541  TATAATCAGC  AACTTTCAAA  TATCAGCCAG  TTGCAAAGAG  TATTTAATTA  ATAAATACAA
601  TTCGATAGAG  AAAACCCTTC  AGTTTTGACC  TTTCTTTTTA  ATGCAAAAGA  GATACAGGGT
661  TGGGGGGTGG  AGAAAGATAC  TTGATGTCTA  GAAATGCTGA  GAAACAAAAA  AAACAAATAA
721  TGATATTGTC  TCCAGGAATA  AGCATGAGAA  CAACAAAGCA  CTACCTGTTA  TTTTACGTAC
781  ATCGTTCTTT  CCTAGATGTT  CTGATGGAAA
```

Score	Start	End	Qsize	Identity	Chro	Strand	Start	End	Span
624	185	810	810	99.9%	8	(-)	136495195	136495820	626
184	1	184	810	100%	8	(+)	51889318	51889501	184

BLA(S)T Output: 8q11.21(+)(51,889,501)::8q24.23(-)(136,495,820)

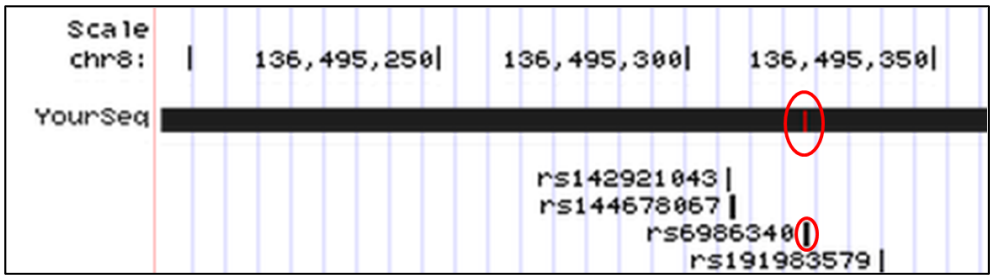

Figure S-DGAP247. BLA(S)T Output, Rearrangement_A at proximal breakpoints of inv(8): Circled mismatch represents a SNP (dbSNP build 141, rs6986340).

Rearrangement_B (at distal breakpoints of inv(8))

```
  1  TTGGCTTCTG  TTGCCATTGC  TTTTGGTGTT  TTAGACATGA  AGTCCTTGCC  CATGCCTATG
 61  TCCTGAATGA  TATTGCCTAG  GTTTTCTT(TA TTCTT)(TATTC TT)(TATTCTT)(T ATTCTT)TACT
121  TTTCCTTTAT  GAACAGAGGA  GGATATTCAT  GTCATGAGGG  TATCATATCC  TTATGATAGA
181  GGATATTTGT  GTGATGAGGG  CATCAGCCTT  AGGTGCCTGG  TTCTGTCCCC  TGCATGGCTT
241  CCTCCTGTCC  ATCTGCCGTC  TCTTGCAGGG  CTGAACTTAC  TCTTCCAGAT  TTGGAGATAC
301  TTGGAGTGTT  TGATGCTTGA  ATCCTGTCAT  GACCTGCTTA  TTCTCTCTCC  CTATCTAGGG
361  CTGTTGGGAC  TGTCTGTTTC  TGGGCCTGGA  CAGGACATTT  TTAGATATGT  TTAGAGCATA
421  AATGAAGAAT  TCCCATTGGT  TTTGATGTAA  GATGACTTTG  AATGTTCACT  ATTTTTGGAA
481  GACAGGATAG  CATGGTGATG  AAGATGAGGC  CTCTGGAATT  GGACCGCTTA  GGTTTGGGTC
541  TGTCTTATCC  CTGTGGCTTA  CTAGCTGTAT  GTCCTGGGGG  AAGTAATTTA  ACCCCTCACT
601  ACCTACATTT  CCTCAGTAAA  TTAGAGGTAA  AATGTGGAAT  AGGTAAAAAT  AACCACCACA
661  AAGAGTTAAT  GTGAAGTAAT  ATGCTAACAT  ATGTAAAGCA  TTGAGAAATA  AAAATAAAAT
721  CCTAAGCCAC  CCAACTGACT  GGGTAGACCC  CTCTTG
```

Score	Start	End	Qsize	Identity	Chro	Strand	Start	End	Span
648	109	756	756	100%	8	(+)	136495815	136496462	648
88	1	88	756	100%	8	(-)	51889502	51889589	88

BLA(S)T Output: 8q11.21(-)(51,889,502)::TATTCTTTATTCTTTATTCT::8q24.23(+)(136,495,815)

or

BLA(S)T Output: 8q11.21(-)(51,889,502)::8q24.23(136,495,816-136,495,822)x4::8q24.23(+)(136,495,823)

Next-Gen Cytogenetic Nomenclature:

Short System

46,XY,inv(8)(q13q24.1)dn.seq[GRCh37/hg19] inv(8)(q11.21q24.23)dn

Detailed System

46,XY,inv(8)(q13q24.1)dn.seq[GRCh37/hg19] inv(8)(pter->q11.21(51,889,501)::q24.23q11.21(136,495,820-51,889,502)::TATTCTTTATTCTTTATTCT::q24.23(136,495,815)->qter)dn

or

46,XY,inv(8)(q13q24.1)dn.seq[GRCh37/hg19] inv(8)(pter->q11.21(51,889,501)::q24.23q11.21(136,495,815-51,889,502)::q24.23(136,495,816-136,495,822)x4::q24.23(136,495,823)->qter)dn

DGAP248

46,XY,t(2;13)(p13;q14)dn.arr(1-22)x2,(XY)x1.seq[GRCh37/hg19] t(2;13)(p12;q13.2)dn

Prenatal History: A 44 year-old G1P0 female had normal first trimester screening. At 10.9 weeks, CVS was performed for advanced maternal age. At 17.3 weeks, fetal ultrasound was interpreted to be normal. At 19.4 weeks, the pregnancy was terminated prior to an appointment to receive the results of sequencing. The mother stated that she decided to end the pregnancy as the couple was conflicted about continuing the pregnancy for personal and psychosocial reasons, and that it was a multi-layered decision. No fetopsy was performed.

Sequencing Results and Interpretation of Convergent Genomic Evidence: Sequencing of the prenatal DNA sample identified the translocation breakpoints within a non-genic region at 2p12, and within *RFC3* at 13q13.2, disrupting this gene with consequent decreased RNA expression. *RFC3* encodes the 38 kDa subunit of replication factor C complex,[9] with a predicted haploinsufficiency index of 4.93% (likely to be monoallelic)[8], however without any known abnormal phenotypic associations. In addition, 13q13.2 breakpoints are 973 kb upstream to *NBEA,* a candidate haploinsufficient gene for autism based on animal models and disruption in a patient with idiopathic autism,[10-12] located within the same 2.16 Mb TAD with the breakpoints. The 2p12 rearrangement is located within a TAD that includes *LRRTM4*, a gene with low haploinsufficiency index with no reported abnormal phenotypic association. However, structure and expression profiles of *LRRTM* mRNAs in mice suggest a role in development and maintenance of the vertebrate nervous system.[13] These sequencing results remain of unknown clinical significance, as the pregnancy was terminated and an assessment of potential autism-like behavior would not have been possible in a fetopsy had it been performed (Figure 2C, Table 4).

BLA(S)T Outputs of Sequencing Results:

Rearrangement_A (on der(2))

```
  1    AAATTTGTAC   GGTGGGTGAA   CTGTGAGCTG   GAGTGTTTGA   GTTTGACCTG   GTAAAGTCAA
 61    CACAATGCCG   GCATTAGTAT   TCAGATGAAA   TCTCAGCTCC   TGTGAACAAG   CTGCCATGCA
121    GTCAATTTGT   CAAGATAAAA   CTTCAGAGCC   TTGTTCTGTG   TCTCTTCTCT   TTAATAACCA
181    GAACTTCCAA   GACAACGTAA   GAGGCAATTT   CAAGGATATT   GACGACAATC   TTCTTTCTGA
241    AAGGGTTGCA   CTGAATATAC   TGGCAAAGTG   CTTAGTCAAG   CACTTTATAA   TTTACAAAGT
301    GTCCTCTCCG   AATTTTGCTG   TTTGGTCTGC   ACAATCATTT   CTTGGAGTTG   AGAACATTTT
361    TCAACAATGT   TGGATACTAA   TTATTCTACT   GATTATTAAG   TACTTCATGC  A{TG}TAATCCC
421    AGCACTTTGG   GAGGCTGAGG   CGGGCGGATC   ACAAAGTCAG   GAGATCGAGA   CCAACCTGGC
481    GAACACGGTG   AAACCCCGTC   TCTACTAAAA   ACACAAAAAA   AATTAGCTGG   GCGTGGTGGC
541    GGGCGCCTGT   AGTCCCAGCT   ACTCGGGAGG   CTGAGGCAGG   AGAATGGTCT   GAACCCGGGA
601    GGCGGAGCTT   TCAGTGAGCC   GAGATCGCGC   CACTGCAGTC   CAGCCTGGGC   GACAGAGATG
661    GACTCTGTCT   CAAAAAAATA   AAATAAAATA   AAATAAATAA   AGGGATATTA   CAGAAATAAC
721    AGGCCTAGAG   TTCT
```

Score	Start	End	Qsize	Identity	Chro	Strand	Start	End	Span
411	1	413	734	99.8%	13	(-)	34542731	34543143	413
317	412	734	734	99.1%	2	(+)	78301911	78302233	323

BLA(S)T Output: 13q13.2(-)(34,542,73{2-1})::2p12(+)(78,301,91{1-2})

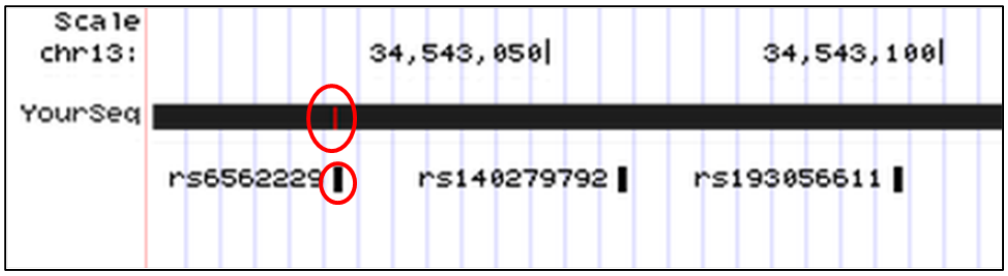

Figure S-DGAP248_1. BLA(S)T Output, Rearrangement_A on der(2): Circled mismatch represents a SNP (dbSNP build 141, rs6562229).

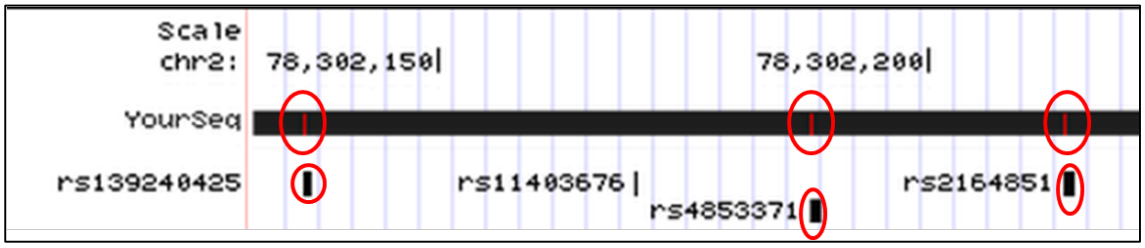

Figure S-DGAP248_2. BLA(S)T Output, Rearrangement_A on der(2): Circled mismatches represent three SNPs (dbSNP build 141, rs139240425, rs4853371, and rs2164851).

Rearrangement_B (on der(13))

```
  1    CACCTGGCTA   ATTTTTGTAA   TTTTCGTAGA   GACGAGGTTT   CACAATGTTG   GCCAGGCTGG
 61    TCTCAAACTC   CCGACCTCAA   GTGATCCTCC   CACCTCGGCC   TCCTGCAGTG   CTGGGATTAC
121    AGGTGTGCCA   CCACGCCTGG   CCCAGCATTT   ACTCTTTACA   AATGTAGCTG   AGAACATGGG
181    GATCAGATGG   TAATTTAACT   AAATGATCAA   CGAGTAGGTT   CACAGAATGA   AGGACAACCA
241    GACTTTACCA   AAGCTTAGGT   TGCCTTGTTT   TTAGCCAATC   AAACAATCAA  AAGTTTTTC{T
301   GTG}AGCCACC   GTGCGCCCGG   CCTGTAATAT   CTCTTTGTTG   ATTAGCCTCC   TAGCCATATC
361    CCCGCTACTG   AATTATCTAT   CTTCCCCTTT   TATCTAAATT   CTCTGCTGCA   TCATTTTAAT
421    CATTCTCTTG   CCAACATCTC   AAATTCTTTT   CCTTATTTGC   ATGCCTATTA   CATGCTGCCA
481    GTTAAACTGT   GATTTTGTAA   AAGTCTAAAT   GTTGGCTTCT   CAGCTTTTCC   ATCTAGCTTT
541    CAAAAGCCAC   TGGAAAAAAG   AACAACTTTA   AGTTTTATTG   TATTCTTAAT   TGACAAATAA
601    TGATTGCACA   TATTTATTAA   GTAAGACTGG   TGGTATTATG   CTGCCCATGT
```

Score	Start	End	Qsize	Identity	Chro	Strand	Start	End	Span
351	300	650	650	100%	2	(-)	78301558	78301908	351
301	1	303	650	99.7%	13	(+)	34542421	34542723	303

BLA(S)T Output: 13q13.2(+)(34,542,7{20-23})::2p12(-)(78,301,90{8-5})

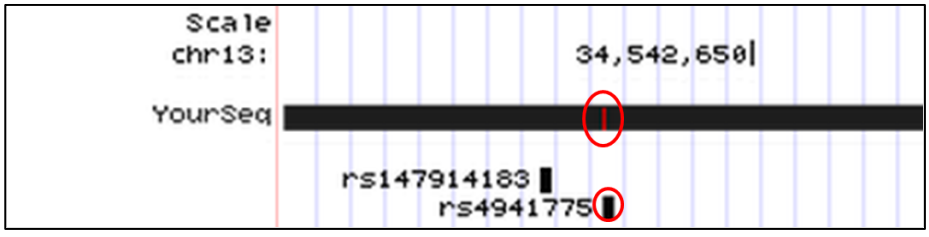

Figure S-DGAP248_3. BLA(S)T Output, Rearrangement_B on der(13): Circled mismatch represents a SNP (dbSNP build 141, rs4941775).

Next-Gen Cytogenetic Nomenclature:

Short System

46,XY,t(2;13)(p13;q14)dn.seq[GRCh37/hg19] t(2;13)(p12;q13.2)dn

Detailed System

46,XY,t(2;13)(p13;q14)dn.seq[GRCh37/hg19] t(2;13)(13qter->13q13.2(34,542,73{2-1})::2p12(78,301,91{1-2})->2qter;13pter->13q13.2(34,542,7{20-23})::2p12(78,301,90{8-5})->pter)dn

DGAP258

46,XY,inv(6)(p23q13)dn.arr(1-22)x2,(XY)x1.seq[GRCh37/hg19] inv(6)(p25.3q16.1)dn(q15q15)pat
or
46,XY,inv(6)(p23q13)dn.arr(1-22)x2,(XY)x1.seq[GRCh37/hg19] inv(6)(p25.3q16.1)dn,inv(6)(q15q15)pat

Prenatal History: A 28 year-old G1P0 female conceived after IVF and had abnormal maternal first trimester serum screening with an increased risk of chromosomal abnormality. Amniocentesis was performed at 15.9 weeks and the twins were determined to be monozygotic based upon SNP microarray results. The twin fetuses had normal ultrasound findings at 12 and 20 weeks.

Postnatal History: The twins were born prematurely at 33 weeks by C-section due to breech/breech presentation. Birth weights were 3 pounds 3 ounces and 3 pounds 4 ounces. They spent one month in the NICU for growth monitoring and did not require intubation nor have any illness or major complication during the NICU stay. At 2.5 years of age, the mother reports that the twins continue to be healthy without any hospitalization or developmental delay.

Sequencing Results and Interpretation of Convergent Genomic Evidence: Sequencing of the prenatal DNA sample identified the inversion breakpoints in non-genic regions at both 6p25.3 and 6q16.1. In addition, a paternally inherited cryptic rearrangement at 6q15 was identified. Due to the length of the sequencing reads, it was not possible to determine whether both of the breakpoints on 6q reside in the same paternally inherited chromosome, however, given their relative close proximity and localization within the same 2.21 Mb TAD, this is a likely possibility. An analysis of the protein-coding genes localized in the same TAD as the breakpoints did not reveal any additional monoallelic or imprinted genes associated with an abnormal phenotype, correlating with the normal clinical phenotype of DGAP258 (Figure 2D, Table 4).

BLA(S)T Outputs of Sequencing Results:

Rearrangement_A (on proximal part of inv(6))

```
  1    TCTGCACTCT   CATGTTTGTT   GCAGCACTCT   TCACAATAGC   CAAGATTTGG   AAGCAACCTA
 61    AGTGGCCAGG   AACAGATGAA   TGGATAAAGA   AAATGTGGTA   CTTATACACA ATGGAGTAC{T}
121    GGAAGACCAC   AAAAAGCACC   CTCCCTGAGA   GCAGGCCTCT   CCCAGTGAAA   TGCAAGTTCC
181    AGGAAATGAC   TGAGTTGTCC   CATGTGCAGC   CGAGTCCATC   ATGAGGTGCA   GGGAGATT
```

Score	Start	End	Qsize	Identity	Chro	Strand	Start	End	Span
120	1	120	238	100%	6	(-)	93191547	93191666	120
117	120	238	238	99.2%	6	(+)	776786	776904	119

BLA(S)T Output: 6q16.1(-)(93,191,54{7})::6p25.3(+)(776,81{6})

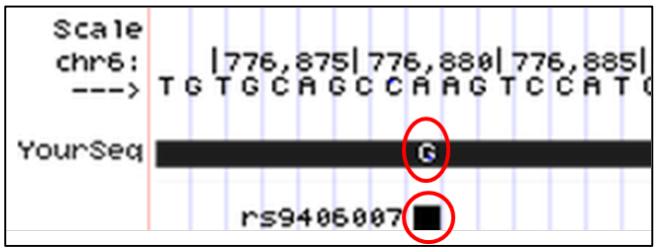

Figure S-DGAP258_1. BLA(S)T Output, Rearrangement_A on proximal part of inv(6): Circled mismatch represents a SNP (dbSNP build 141, rs9406007).

Rearrangement_B (on distal part of inv(6))

```
  1    GTTGTTGCAA   ATGACTGAAT   CTCATTTATT   TTTATGTTTG   AGCATGTACA   GCTAATTAAG
 61    ATTCTGACTG   GGTTTAGGAT   CAAAGAAAGC   TGTCCCATTG   CATTCCCACA   TTCTTCCTTC
121    TTCTTTCAAT   GTCTTCCAAG   ATCTATTTTA   AACGGGAAGT   GTTGTGTACT   TTTCAGGGGC
```

Score	Start	End	Qsize	Identity	Chro	Strand	Start	End	Span
138	43	180	180	100%	6	(-)	776650	776787	138
42	1	42	180	100%	6	(+)	93191504	93191545	42

BLA(S)T Output: 6q16.1(+)(93,191,545)::6p25.3(-)(776,787)

Rearrangement_C

Cryptic inversion spanning 6q15(92,254,978~-92,235,543~)

Next-Gen Cytogenetic Nomenclature:

Short System

46,XY,inv(6)(p23q13)dn.seq[GRCh37/hg19] inv(6)(p25.3q16.1)dn(q15q15)pat
or
46,XY,inv(6)(p23q13)dn.seq[GRCh37/hg19] inv(6)(p25.3q16.1)dn,inv(6)(q15q15)pat

Detailed System

46,XY,inv(6)(p23q13)dn.seq[GRCh37/hg19] inv(6)(qter->q16.1(93,191,54{7})::p25.3q15(776,81{6}-92,235,543~)dn::q15(92,254,978~-92,235,543~)pat::q15q16.1(92,254,978~-93,191,545)dn::p25.3(776,787)->pter)
or
46,XY,inv(6)(p23q13)dn.seq[GRCh37/hg19] inv(6)(qter->q16.1(93,191,54{7})::p25.3q16.1(776,81{6}-93,191,545)::p25.3(776,787)->pter)dn,inv(6)(pter->q15(92,235,543)::q15(92,254,978-92,235,543)::q15(92,254,978)->qter)pat

DGAP259

46,XX,t(3;18;5;7)(p25;p11.2;q13.3;q32),t(9;18)(p22;q21)dn.arr(1-22,X)x2.seq[GRCh37/hg19](3,5,7,9,18)cx,der(3)t(3;7)(p24.3;q36.3)dn,der(5)t(5;7)(q14.3;q35)t(3;7)(p24.3;q36.3)t(3;18)(p26.3;p11.31)dn,der(7)t(5;7)dn,der(9)t(9;18)(p23;q21.3)dn,der(18)t(3;18)inv(18)(p11.31q21.3)t(9;18)dn

Prenatal History: A 28-year-old G1P0 female had abnormal fetal imaging findings of bilateral ventriculomegaly and colpocephaly, with partial agenesis of the corpus callosum observed by ultrasound and MRI. Amniocentesis was performed at 21 weeks. The pregnancy was terminated at 22 weeks due to the abnormal imaging findings. Fetal autopsy showed microencephaly (40 g vs normal 75 g for the gestational age), ventriculomegaly, agenesis of the corpus callosum, left renal aplasia and hypoplasia of the right kidney.

Sequencing Results and Interpretation of Convergent Genomic Evidence: Sequencing of the prenatal DNA sample identified all of the breakpoints of this complex aberration with nine rearrangement sequences located at 3p26.3, 3p24.3, 5q14.3, 7q35, 7q36.3, 9p23, 18p11.31, and 18q21.3. An analysis of the protein-coding genes localized in the same TAD as the breakpoints revealed multiple genes associated with phenotypes overlapping with DGAP259. In particular, the breakpoints at 7q36.3 disrupt the regulatory region of *SHH* that is associated with holoprosencephaly (Supplemental Table 2), which is consistent with the cerebral malformation phenotype of DGAP259.[14] The breakpoints at 5q14.3 are located within the same TAD as *MEF2C*, a haploinsufficient region associated with cerebral malformation and hypoplastic corpus callosum,[12; 15] as observed in DGAP259. Furthermore, two well-known genome organizer and chromatin regulator protein encoding regions, *SATB1*[16; 17] and *EZH1*[18] reside in the vicinity of *TBC1D5* and *CNTNAP2,* which are disrupted in the respective breakpoints at 3p24.3 and 7q35 and might be relevant to the complex chromosome aberration of DGAP259 (Figure 3, Table 5).

BLA(S)T Outputs of Sequencing Results:

Rearrangement_A (on der(3))

```
  1    TGCTCGTCCC  ACCCCAGCGT  GGGGTGTGGA  GAGGTGGGCC  AGTAGGAGGG  GTTTGGCTGT
 61    GGAGGCAGCT  TCCTCCCAAA  TGGTTTAGTG  CAGTTCTCCC  ATAGTGCCTG  AGGTCCCCCT
121    CTCTAGAGAC  GATTCATTCT  GGCCGACTTA  CATTCATTTG  TTAAAAAGCC  AGGACACCCC
181    TTGAGTTTCC  CCTCACTGAA  GGCATCTTGT  TCCCCTTTGT  CCTTCCCCAC  CATGTTATGA
241    GGAAGCACAA  GAGGTCTCCC  CAGAAGCCTG  GGCCATGCCC  TTGAACTTCT  CAGACTGGAG
301    AACCGTGAGC  AAAATATACC  TTTTTTCTTT  ATAAATTACC  CAGTCTGAGG  TATTATTTTA
361    TAGCAAGGCC  CATCCAACAA  GTTTATGCTA  CTTAAATAAA  GTTCCTTTCA  ATAAAAGATG
421    CCACAGTGGC  ACACAGTTAA  CTATGAGGAA  ATTTTTTTAA  CTATATTTAT  TTTTGTGTCA
481    AAGGCTTAGG  TGTGCATTAG  ACAACCATTT  ATTAATTTTA  ATTTTGCTTG  GAATAAACAC
541    CCTGACAAAC  AGCATTTCAA  TTCAGGCTGC  TATACAACAG  AATCATTTAC  TTTCAGATAC
601    AATCATGCAG  TAACACCACA  AGCTCCTGCT  TCACAAATTG  CTCAATCCCC  AATCCCCAAA
661    TACTATAGAA  GATGGCTTAT  ATATAAGTTA  TACAAGACAT  GCATTCTAAT  ATTCAAGCCA
```

Score	Start	End	Qsize	Identity	Chro	Strand	Start	End	Span
363	1	367	720	99.5%	7	(-)	155701797	155702163	367
353	368	720	720	100%	3	(+)	17392144	17392496	353

BLA(S)T Output: 7q36.3(-)(155,701,797)::3p24.3(+)(17,392,144)

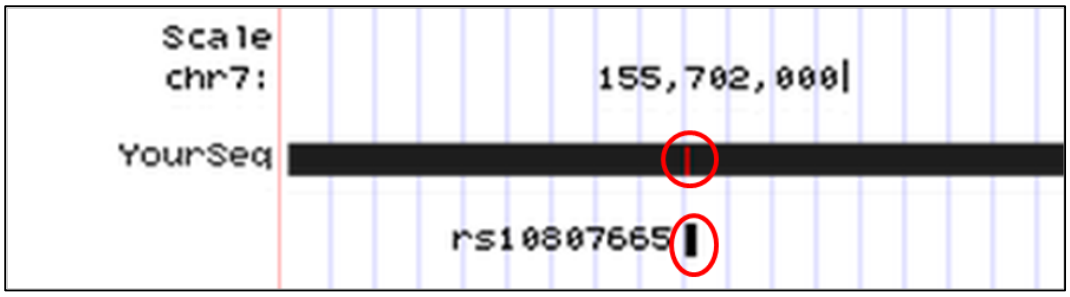

Figure S-DGAP259_1. BLA(S)T Output, Rearrangement_A on der(3): Circled mismatch represents a SNP (dbSNP build 141, rs10807665).

Rearrangement_B (on der(5))

```
  1   AGCAGTAAAA   GGCACTAGCT   GGGTAGGTAG   TTATCAAGAA   TGACAAATAT   CCTAAAGTTG
 61   TTAAATCTCC   CATTCTGAGG   AGTTGAAGTG   GGAAATGGAG   AGATTATTCA   ACTCTATCAA
121   CATCTGATAC   AGTAATTTGA   CTTACTTAAT   CATTATGTCT   CATCTTCCAT   TATTAATTTA
181   AACAATTTTG   GAATTTATGT   ATTCACGAAT   CAGACTTGTG   TGATAGTAAA   TACGCATTAA
241   AAATAGTATT   TTGTGGAATA   TTTCAGAACT   TGTACTTTTT   ACCATTTGTT   CTTAGGCAGG
301   TAGAATCAAG   TAGTTCACTA   AGGCTTGAAT   AATAGAGGGT   AAACCTCCTA   GTTCTAAGAT
361   GTCTGATATC   TGCTCTGTAA   AAAAATAAAA   TAAAATCACC   CAAATTTCAC   TACAATAAAA
421   CAAGAGCCAT   TTTATTATGC   TCAAACAATC   CATGGGTCAG   AACAAGGCAG   AGTGGATATG
481   GCTTATTCTA   TTATCATGCT   CTATGTCTGC   AGCATTAATT   GAGGAAACTC   AAATGATGGA
541   GATTACCAGT   GTTGCTGGGG   TGTGGAATGA   GCTAGAAGCT   CGTTCATTCA   CATAAATGTT
601   GCC{TGCTCCA AA}GCTGTACC   GAGTCAGTGG   CGGAGGCCGG   GTGAGCGTGG   GGAAGGGCAT
661   CAGACACGGT   ATACCTGCTC   CACCTTTCCC   TTTTGTTTTG   TTGTCACAAG   AGGCACTACT
721   TCGCTGCCTC   CGTCTCCTCT   GTGGGTGGAA   AGGATGGACC   CAAAGGAACA   GAACGCTGTG
781   GCCACTCGAC   GATGGTTTTG   ATAGGGACTT   ATCTTGCTCT   CTCTCCCTGG   ACACTCT
```

Score	Start	End	Qsize	Identity	Chro	Strand	Start	End	Span
611	1	612	837	100%	5	(+)	88755635	88756256	622
232	604	837	837	99.6%	7	(+)	147718911	147719144	234

BLA(S)T Output: 5q14.3(+)(88,756,2{48-56})::7q35(+)(147,718,91{1-9})

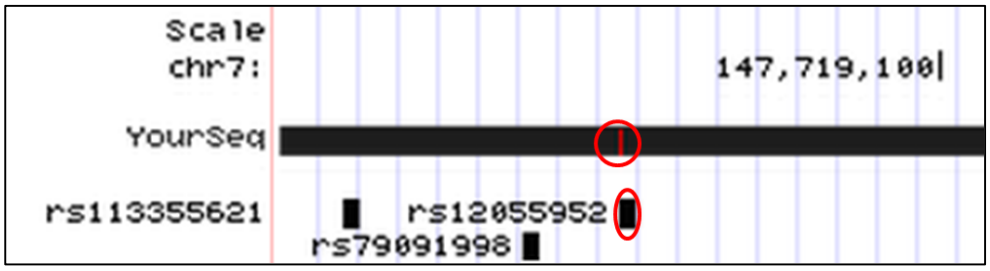

Figure S-DGAP259_2. BLA(S)T Output, Rearrangement_B on der (5):. Circled mismatch represents a SNP (dbSNP build 141, rs12055952).

Rearrangement_C (on der(5))

```
  1   GGCCTCACTC   AGTGCCCTCG   GGTCTGGAGA   CATGAATCAC   GAACCCTCCC   ACCAGCCCCA
 61   GGATTTGGTC   AGTTATAAAA   ATATCCGGAT   TTGGCATGGG   GCGGATTCAG   GAACCGAAGT
121   TTGCTCTTGC   CCTGTTCTTG   CAGTATTGGA   TTGTACAATT   ATAGCTCTTT   AGAAGTTTCC
181   TAATATGCCA   CAAGATGTCA   AGCAGCAGCA   CCAAGATTAA   TACTTTTTTT   AATGACCATT
241   GCTGACTTTG   ACCTTGAAGT   GTGTGGTGTG   TTCTGAGAGC   ATATTTCCTC   CCCTCTGCTT
301   TGCAGCTCCT   GGATTTTGAA   AAATTAACTC   CTTGCTCTCA   TCTGAACAGT   TCACCTAAGG
361   TGTTCACTTG   TTCTGTTTAC   CTTGAGCTAA   AGTGTTTTAG   AGAGAGAGGG   AGAGGGAGGA
421   GGGAGGTAGA   GAAAAGGAGA   GGGGAGGTGG   AGAGGTAGGG   GGAGAGGAAG   GAAGGTGGGA
481   AGGAAGGGGA   GGGAGAGGTA   GGGAGAAGGG   GAGAACAAAT   GATGATTTGT   TAATGCAAAT
541   GTGTCGCGAA   TGACTGGTAG   TACATCTGTC   TCTTCATCCA   TAGGCCATTA   CTGAGCAACG
601   TTAGCACATG   ATTGTAAAAA   AGGAGAAATC   ATTACATGCA   GGTAGTACAC   ATTCAATCAA
661   TTCTGAGCTT   ATGTCTCTGG   TGAAATAAAA   AAGTATATAA   TGTAAATGAT   ATTTAATCTG
721   AATAACAAAA   AAGCAGCTCT   TTGACTCTGG   CTCAAGCTGT   TAGGTGAGGT   GACTGCTGTT
```

```
 781   TGGGATTGAT   GTTTATTGGT   GGCCCAGTGG   GGAAAGGCTA   TCACTTTTAT   TCTTTGTCAT
 841   TCCTCCCATG   CGTTTCTCTA   ACCCACATCA   TATTTTAAGT   TCTGTTTTCC   TTTTTTTTCT
 901   TATCTATTTT   TTTCTTTTCA   TTATTTCTTT   CTTTTGGGGA   GTAGTTTGTG   GGATAGTGGT
 961   AAAAAATGGG   TGCTGATGAC   CACCAGTGTG   AGCATGCTAA   GCAAGCAATG   ACAATTAATA
1021   CAACAACAAC   AAAAGTTGTA   CGATTAGCTT   CAGCTCCATA   AGTGTCTAAT   GAGCCATTTG
1081   TCAGTCTTTT   GGTGAAATAA   ACTACTCTAT   CTTAATTCTC   CACTCTTGCA   GTAAATAAAT
1141   AAAAGTTATG   AAACACCCGG   GCAACAATAA   AATATAATTT   ATTTCATAGG   GCATGACAGA
1201   ACTCTTTACA   TATCTAAAAT   GAACATGTTA   TTTACAAATG   ACTTGTGATA   CTCATATAAA
1261   CCATGGATCT   GTGTGTTAAC   TGCTTTCATT   AGGGAGATAT   GCATTTTTTT   CCTAATTGTT
1321   TAATCGTTTA   AATGTATCAT   TACTCCTAAA   GGCATGTGAG   TTAAAGTGAC   TTCTCTTGGT
1381   GCGATTAACT   CATAAGGCTA   AGAAGAACCT   CAGAAATGAG   CTCTTCTGCA   GCTGAAGACA
1441   TTAAGAATTT   AATGGAAAGG   ACAAAACAAT   AATTTTCATT   TGGGAACCTC   TCAGCTCTCT
1501   GCTGATTATC   TTCCTGCCCT   TATTTATTTT   TAGGAACCCC   A
```

Score	Start	End	Qsize	Identity	Chro	Strand	Start	End	Span
511	1	511	1541	100%	7	(+)	155700363	155700873	511
1025	517	1541	1541	100%	3	(-)	17391112	17392136	1025

BLA(S)T Output: 7q36.3(+)(155,700,873)::AGAAC::3p24.3(-)(17,392,136)

Rearrangement_D (on der(5))

```
   1   TTTCTATGGC   TGCTACCACC   ATTATCTCCA   TCCCTTTAAG   AGGCCCAGGT   TCTGATGTGC
  61   CCATGCCCTC   AGGACTCCAG   GACTATGACT   ACCCAGGCAA   GCATGTGCAC   ACCTGCACAC
 121   CACACCAACT   GCTGTGCACG   CATGCCGACT   GCTGGGTCTT   TAAGCCTGAA   CTTGTGTGTG
 181   CAGGAGCTGC   CACATATGCA   TGTGGGTATG   GTGAAGCAGC   AGCAGCAGCA   GCTCATGCAC
 241   ACACAGGTTA   CAAATAAATT   CTTAATCATT   TTACCTCTCA   ATTTGTGTTT   AGTATGTACA
 301   AAACACAAAT   TGAGAGGTAA   AATGATTAAG   AATTTCAAGA   CAGTCACAGC   AGAATATTTC
 361   AAACATGGGG   ACTTCCTCAG   CACAGGGCTC   TGTGTGACTG   GATTGTATGT   CCATGAAACC
 421   AGCTCTGGAT   GTCACGCTAA   GAAATATATT   CTTACATAGT   AGAGAGTAGC   ATAGTAAAGA
 481   GTAGCATGGT   GGTTATCAGA   GGCTGGTGGG   AG{G}CAGCCCG   AGTTTCCCAA   TGCACCAAAG
 541   CAGAAGCTTT   TTGGAAACCT   ATATATTTTT   TCATACTATT   GGGAATTTCT   TCAGAATATG
 601   AAGGCTTTAT   CGAATTGTGT   CTGAAATGAA   TTTCATTTAA   ATACTGAATT   AATTGAAAGC
 661   TTTGCTTCTG   AATATTTTTC   CATAGATTTC   ACGGTGCTTT   AGAAATTTCA   TTTTGCCTCA
 721   TGTTTTAGTA   CTGGCAATAA   CTGCCAGTAA   TAGAAGTGGC   AGTGTTGAGG   GAAATGGTGG
 781   TGGCGAGTGT   GGGATGGTCT   CAGTGGGCAG   CTTTCTTACG   ATGAGGAGAG   GCGGGGCGTG
 841   ACTGGTTCTA   TCGTGTTTTC   ACTGGGACCA   GGACTCACTG   TGGAAGGGCA   GGAAGTACCA
 901   CTTAGTGGTG   AGAACAGCAC   GCAGGCTCCA   GTTTACCATT   CTGGTGATTT   GACTTTAATG
 961   AAGCCCTTTG   GAATTTTGAC   TG
```

Score	Start	End	Qsize	Identity	Chro	Strand	Start	End	Span
470	513	982	982	100%	18	(-)	6374582	6375051	470
513	1	513	982	100%	3	(-)	1408996	1409508	513

BLA(S)T Output: 3p26.3(-)(1,408,99{6})::18p11.31(-)(6,375,05{1})

Rearrangement_E (on der(7))

```
   1   GTAGACTGTT   GAGTGAATTT   CTAATAATAA   AGCCAAAAGG   AAAAATAATG   GCAATATGAT
  61   TGGACAAGCA   GTTTCAGAAT   CAAGGTAGGA   TGCCTTTTTG   TTGGTGGAGG   TTTTTTGTTT
 121   TTGTTTTGTT   TTTGGACTTA   TTCTCCCTCA   TATCAAATAA   ATTTATTAAA   CACACCTGAA
 181   CACTTGTTAT   GTGCCACTGT   CGGCCACGTA   TTAGGGACAC   GGAAGAACAA   TAAGACATAC
 241   TCCCTACCAA   AAGAGGCTTA   TGGTTTAGAA   GGAAGACACA   GTCTTGTAAA   CAGGTAAGTA
 301   AAATAAAATG   TGAGCTGCAC   TATGCTGGAA   GTCAGCCCAG   GGTGGCCCAA   GTAGACCATA
 361   GCCAGTCTAC   ATAAATAGGG   AGACACGGGG   GACAGCTTTC   TAGATGTCCC   TAACGCTGAA
 421   TCCTAAAAGA   TGAGAAGCAT   TTCTAGGGTG   CCAGAGTGGA   GAAAACACCT   GACTTGTGGG
 481   AGAACGGAAG   GCCTCGTGTT   CATTCAATGG   ATCAACTATC   ATTGGGCATC   TCCACCTGCG
 541   AGAGACGGCG   CTAGCCCCTG   GGGATCCAGT   CCCCGGTGAG   CTGGAAAGCT   ACTCTGTGCT
 601   CTCAGAGGAC   TTGGAACAGA   GAATGCAGAC   AGGGTGGCAG   GAATGCAGGA   ATGTGCTCAC
 661   AGTGCAGGAA   CCCGGTGGCT   CGCAGAGAAG   GGCACCAAAC   TTAGACCTGG   GAGATCAGGA
 721   CCCTCTCCCC   CAAAACCTGG   A{GG}TTGGAAT   ACCTCCAAAT   CTGAACTCAG   CTTTGACTGT
```

```
 781   CAATGGAGTG   CAGCTTGTGA   CCTCTCCATG   TAGTTTGAGC   CTTTCAAAAA   ATGAAGTGTG
 841   GCTACCTACA   ACCAACTGAT   TTTCAAAAAG   TCAACAAAAA   TATGAAGTGG   AAAAAGGACA
 901   CTCTATTCAG   TAAATGGTAC   TGAAACAATT   AAATAGCCAT   ATGCAGAAAA   ATGAAACTGG
 961   ACCCCTATCC   TTTACCATAT   ATAAAATTAA   CTCAAGATTA   ATAAAGACTT   ATATGCAAGA
1021   CCTGAAACTA   TAAAAATCTT   ATAGGAAAAA   CTCTTCCAGA   CTCTGGCATA   AGCAAAGATT
1081   TTATGACCAA   GACCTCAAAA   GCAAATGCAA   CAAAAAGAAA   AATAGACAAA   TGGGACTTAA
1141   TTAAAGAGCT   TCTGCACAGC   AAGAAAAAAT   AATAATAATA   ATAAACAGAG   TAAACAAACA
1201   ACTTACAAAA   TGGGAAAAAA   TATTTGCAAA   CTATGTGTCT   GACACAGAAC   TAACATCCGG
1261   AATCCAGAAG   CAACTCAAAA   CAACTCAAGA   AGAAAAAAAC   AATCCCATTT   AGAAGTGGAC
```

Score	Start	End	Qsize	Identity	Chro	Strand	Start	End	Span
743	1	743	1320	100%	7	(+)	147718166	147718908	743
577	742	1320	1320	99.9%	5	(+)	88756239	88757077	579

BLA(S)T Output: 7q35(+)(147,718,90{7-8})::5q14.3(+)(88,756,2{39-40})

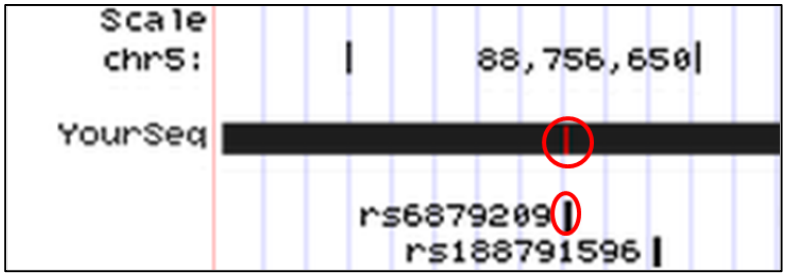

Figure S-DGAP259_3. BLA(S)T Output, Rearrangement_E on der(7): Circled mismatch represents a SNP (dbSNP build 141, rs6879209).

Rearrangement_F (on der(9))

```
   1   AGCCTCATCT   CATTATAGCA   GATGGCATCA   TTCCAAAAGA   AAATAAAAGA   AAAAAATTAA
  61   ATTGATTACT   ATGTCAACCT   TGGCATCCAT   ATGCCAAATT   GTTTTTTGAT   AAGAGCTAAG
 121   TATTAGGTAG   AAACTCGAGA   AAAATTATTT   TCTCAATTCC   AAATTCTTGC   TATAAGAATT
 181   TCTTAAGTTC   ATAGATGCAT   ATTTAAACAA   TCTGAGTATT   TCCAAAATAA   CCAGCTTTTA
 241   AACTTTCCTT   CTAAGGAGAC   CAATTTATTC   ATCTACTAAG   TACCTTGTTT   CTTCCCTCAA
 301   ATTACTCCAT   TTCATCTAAA   CTATTTGTCA   CATATGTAAA   AACAGATATA   ATATATAGTC
 361   AATTACCAGC   AATAGAGCTT   TGGGTTTGAG   TTTGGGAGGT   GTAGAATTTC   AGAAAATGTT
 421   AGGTTATTAC   AGCAGTGAGT   CAGCTTGTAG   TTTGAATCAG   CAAGGATCAT   TATCTATCAA
 481   AACATCAGTA   TGGTTTACCT   ACTGCTCTCA   TTC{A}CTATTA   AGTTTTCTGT   TTATTTTTCT
 541   GCTGGCTCGC   TATGATGTAT   CAGAATGTAG   GTATTATTAT   CTGTTTATAC   TGAGAATCAA
 601   TGTGTTTTTC   AACAATTTTC   AAAGGTATCA   GCCAGCTATC   ATCTAGTTGA   ATATGCCTTC
 661   TTCCTCCTCT   TTATACTATC   CTATAAAAAA   TAGTAGTCCC   TCTCTTATCC   ACAGGGCGTA
 721   CATTCTAAGA   CCCTCAGTGG   ATGCCTGAAA   CTGCAGATAG   TACTGAACCC   TACGTACACT
 781   GTGTTTTTTC   CTATACATGC   ATATCTATAA   TAAAGTTTAA   AATTAGTTTA   TAAATTAGGC
 841   ACAGGAAAAG   ATGAACAACA   ATAACTAAGA   ATAGAACAAT   TATAAAAGTA   TATTGTAGTA
 901   CAATAATGTG   GTCTTTCTCT   CTCTCAGAAC   ACCTTGTTGT   ACTATACCAC   AGGTTGGCTG
 961   AAACTATGGA   AAGCAAAACT   GTGGATAAGC   TGGGGAGGTG   CAGGGGGCTC   ATATAGAGTA
1021   TATACTGTTG   TGGACATTTA   TACACTGGCC   TACATTTTTT   ACCCTCTCAT   AATTTCCATC
1081   TCTTTGCCCA   TCTGTGCTTA   ATTCTAAATA   ACTTCTTCAG   GTCTGAATAA   ATTT
```

Score	Start	End	Qsize	Identity	Chro	Strand	Start	End	Span
514	1	514	1134	100%	18	(-)	54660138	54660651	514
621	514	1134	1134	100%	9	(+)	9646475	9647095	621

BLA(S)T Output: 18q21.31(-)(54,660,13{8})::9p23(+)(9,646,47{5})

Rearrangement_G (on der(18))

```
  1   AATGAACTCT   TTGAGAGAGC   AATCAATGGC   CTCATGGCTA   TTAGACAGCC   ATCTGCACAG
 61   GATGAGGACA   GGTCTGCCTG   TGGTGGGTGG   AGAGGATACA   GCAGTTAAAA   TGTTCTTGTC
```

```
121   CAAGCACCTC   TTCACCCACA   CAGGAGGCTA   CTCCCAGGAG   GAACTATGCA   TCCCCTTTTT
181   CTGGATAATA   AGCATGCTTA   TGTAGAGCTA   CTTCTTTTCA   AATACAGTCT   ATTTTTCACA
241   CTGCAGATAA   TGGTATGTCA   TCATATCACT   CCTCTGCTTC   ATACTTCCAA   AGTTTTTAAC
301   TTTTTCAGCA   AAAAATGCAT   TTCTAAAATT   TTTAATTGAT   GAATAGTAAT   TTTGTTTTAT
361   GTATTTGTGG   GATATAATGT   GATATTTTGA   TACATGTTTA   CATTGTGTAA   TGATTAAATC
421   AAGCTAGTTA   ACACAGCCAT   CACTTCACAT   CCTATCATTT   TTTTGTGATG   AGAATTAAAA
481   TCCTCATTGG   GTAATTTTGA   AATATGTATT   ACATTAACTG   TAGTCACCAT   GCTGTGCCGT
541   AGGTCTCTAA   AACTTATTCC   TCCCATCTGA   AACTTAGTAC   GCTGTGAACA   ACATCTCCTC
601   ATTTTTGTGT   TTCTGCTTCT   GGAAATAGGA   GATAGAGATT   TTAGCTACAG   CAATCAGAAT
661   CCACCCTGGA   GTGTGCTGTT   TTCCTGTGAT   AGCAAGAAAA   TGTTCCATTT   GAAAACTGCT
721   CCACAAAGAA   TCATCAGAAA   CCACAGAAAA   CAAATGATGG   TGTTGGCGGC   TT
```

Score	Start	End	Qsize	Identity	Chro	Strand	Start	End	Span
603	1	603	772	100%	3	(+)	1408382	1408984	603
169	604	772	772	100%	18	(-)	6559443	6559611	169

BLA(S)T Output: 3p26.3(+)(1,408,984)::18p11.31(-)(6,559,611)

Rearrangement_H (on der(18))

```
   1   ATTGACGACC   TCCTGTGCCC   CAGACGTTAT   TCCAGGTGCT   GGAGATACAG   TGACAAAGAG
  61   CCCTCTCGGA   GGGCTCAAGT   AAAGGAACTA   GGATGAAAAG   TGCTGAGTGT   CATGCTAAGG
 121   GAAGCGCTGG   CTGTGGAAGT   GTCCCTCACC   TAGCCTGGGA   TCGGGGTGGT   GGTTGCAGGA
 181   GGCATCCAAG   GAAATGACAT   TTACACGGAG   GTCTGAGGGG   CAGCGAGGTG   GTGGGAAGGT
 241   GGCTCCAGGT   AGGAGGTGAG   AAGAGAGCGC   ACAAAGTCAG   GTTGTAGCAC   AGTCTGGCTG
 301   GGAAGAGAAG   TCGGCTGGTC   AGGTGGGGAG   CCAGGTCAGG   AGGTGCCTCA   GAAGCCGTGG
 361   CAGCCTGGAC   TTTATCCTTA   GGGCGGGAGA   GCCATGGAGG   GGCCATAAAT   GGGGGAGAGA
 421   GAGCCAAGCC   GTAGAGGCAT   TTTAGGTCCA   CATATGGACA   GTAAGTTTGG   AAGGTATAAA
 481   GACTGGAGTT   CCTGTATCGA   CTGGGGCAGA   TGCAGTGATC   TAGGTGGCCG   CCAGTGGAAG
 541   GCACCTGTGA   GTCAGGGTTT   GCAGTTCCTG   TGTGGACGTC   TGAATTAATT   CTGCAGATCA
 601   GACTGCGTTA   CACTGCAAG{A GCAG}AAACAC   AAATGAGGTC   TGATGGTTGA   AAACTTAATG
 661   GAAGAAAAAA   ATAGAACATT   TATGCATAGA   AATAAACACA   TACACACAAA   GGAATACAGG
 721   AAAAACTGGG   AAATCTGAAT   AAGATCAGTG   GATTGTATTA   GTGTCAATTT   CCTGGCTCTG
 781   ATATTGTACT   ACAGTTTTAC   AAGATGTTAT   CACTGGGAGA   AACTAGGTTA   AAAAGTACAT
 841   GAGATACCTC   TGTATTATTT   ATTATAATTG   CATGTGAATC   TAAAATTATC   TCAAAATAAA
 901   AAAATAATTT   TTAAAAAATT   TGGAAAAGTA   ACAAAAGGAA   AACTAAATAG   TACCTTAAAA
 961   ATAAAAAACT   ATTTAACATT   TGTATTTTGA   AAATAATTAG   AAGCATATGA   AAGAGATTGT
1021   GGCTTTTTTG   TTCATTCTTT   TATAAATTAC   T
```

Score	Start	End	Qsize	Identity	Chro	Strand	Start	End	Span
624	1	624	1051	100%	18	(-)	6375048	6375671	624
432	620	1051	1051	100%	18	(+)	6559598	6560029	432

BLA(S)T Output: 18p11.31(-)(6,375,0{52-48})::18p11.31(+)(6,559,{598-602})

Rearrangement_I (on der(18))

```
  1   GTAATTATTT   TGAAAAATGA   TGTAATGCAA   ACCTAGTCAA   ATGAAGGTAT   GATGAACCAG
 61   ACATTTTCTG   GCGCATTGTC   TTCCTCAGTC   TTGTCCTGTG   ACTTCTCTAA   GCCAATTCAA
121   TCAATTCCCA   AATATTTCAC   TGAACTAGAA   GTTCAGGGAT   ACGATAGTTA   AAAGAACCTA
181   CAGCATGCAT   TTGGTAAGTT   TCTCATGAAG   AGACATGTCC   CAGGTCTGGA   TAGTTGTTTG
241   TCCTCATTTG   GGGCCAGAGG   AAACAGGCAG   ATTTCCTTCA   AAGGACTGGT   ACTTACTCTG
301   CTAAATGGTT   TTTCAACAAT   GGAATTAGAA   AACAGCAGAA   TAACATACCT   GTGCTGGGCA
361   AATACACACA   CACACACACA   CCCACACACA   CACACACACA   CACACACCCA   CACACACACA
421   CACCCCTCCC   AAAATGGTCA   CCCTACAATT   CTATAGACTA   ACAACATCCA   AGAAAACTTT
481   CCATCAAGAG   CAGAGGCAAG   ATAACAAATC   TACAGACAAA   CAAATATTAA   GTTTACCACC
541   AACAGACCCT   CAAAAAACAA   ACTTCTAAAT   ATGTAATTTA   GGCAGAGGGA   ATACTATCAC
```

Score	Start	End	Qsize	Identity	Chro	Strand	Start	End	Span
346	255	600	600	100%	9	(-)	9646126	9646471	346
252	1	254	600	99.7%	18	(+)	54659883	54660136	254

BLA(S)T Output: 18q21.31(+)(54,660,136)::9p23(-)(9,646,471)

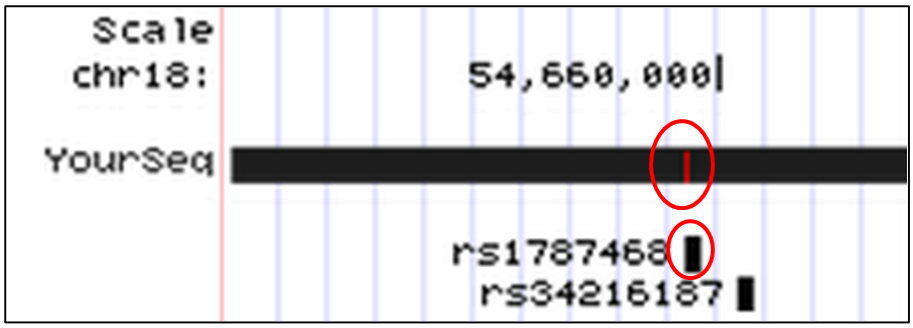

Figure S-DGAP259_4. BLA(S)T Output, Rearrangement_I on der(18): Circled mismatch represents a SNP (dbSNP build 141, rs1787468).

Next-Gen Cytogenetic Nomenclature:

Short System

46,XX,t(3;18;5;7)(p25;p11.2;q13.3;q32),t(9;18)(p22;q21)dn.seq[GRCh37/hg19](3,5,7,9,18)cx,der(3)t(3;7)(p24.3;q36.3)dn,der(5)t(5;7)(q14.3;q35)t(3;7)(p24.3;q36.3)t(3;18)(p26.3;p11.31)dn,der(7)t(5;7)dn,der(9)t(9;18)(p23;q21.3)dn,der(18)t(3;18)inv(18)(p11.31q21.3)t(9;18)dn

Detailed System

46,XX,t(3;18;5;7)(p25;p11.2;q13.3;q32),t(9;18)(p22;q21)dn.seq[GRCh37/hg19],(3,5,7,18)cx,der(3)(7qter->7q36.3(155,701,797)::3p24.3(17,392,144)->3qter)dn,der(5)(5pter->5q14.3(88,756,2{48-56})::7q35q36.3(147,718,91{1-9}-155,700,873)::AGAAC::3p24.3p26.3(17,392,136-1,408,99{6})::18p11.31(6,375,05{1})->18pter)dn,der(7)(7pter->7q35(147,718,90{7-8})::5q14.3(88,756,2{39-40})->5qter)dn,der(9)(18qter->18q21.31(54,660,13{8})::9p23(9,646,47{5})->9qter)dn,der(18)(3pter->3p26.3(1,408,984)::18p11.31(6,559,611-6,375,0{52-48})::18p11.31q21.31(6,559,{598-602}-54,660,136)::9p23(9,646,471)->9pter)dn

DGAP268

46,XY,inv(10)(p13q24)dn.arr(1-22)x2,(XY)x1.seq[GRCh37/hg19] inv(10)(p12.2p12.31)(p12.2q23.32)dn

Prenatal History: A 28 year-old G4P2TAB1 female had a previous pregnancy termination at 23 weeks due to hydrops fetalis. The father, who is of Iranian Jewish descent and the first-cousin of the mother, had two brothers who were deceased in the neonatal period. At 12 weeks of gestation, fetal ultrasound revealed abnormal nuchal translucency. Amniocentesis was performed at 17 weeks. The ultrasound findings at 15 and 22 weeks were normal. There were no complications during the pregnancy.

Postnatal History: Delivery occurred at 33 weeks at an outside facility (the reason for premature delivery is unknown). The newborn medical examination was normal. At 1 year of age, the baby was reported to be healthy and meeting all developmental milestones.

Sequencing Results and Interpretation of Convergent Genomic Evidence: Sequencing of the prenatal DNA sample identified the inversion breakpoints in non-genic regions at 10p12.31 and 10p12.2, and disruption of *CPEB3* at 10q23.32. An analysis of the protein-coding genes localized in the same TAD as the breakpoints did not reveal any monoallelic or imprinted genes associated with an abnormal phenotype, correlating with the normal clinical phenotype of DGAP268 (Figure 4A, Table 6).

BLA(S)T Outputs of Sequencing Results:

Rearrangement_A (at proximal breakpoints of the pericentric inv(10))
BLA(S)T Output: 10q23.32(-)(93,983,897~)::10p12.2(+)(23,659,495~)

Rearrangement_B (at distal breakpoints of the pericentric inv(10))

```
   1    GATGCCCCTC   TGCTCCAGAA   ATCACCAACT   CCTACTACTT   TCCCCAGCTC   TATTTTCCAC
  61    TCCTTTCATT   AGGTTACAAT   AGTAGGAACA   GACCTTAGGT   CATAACACCA   CCAAATAAGT
 121    GAATGCAGAG   TAGAAATGTT   CCCCTAAAGA   GAGGAGGTCA   TTTGAACAAA   CAGCAATACC
 181    TGTCAAGTTA   ATATTTCTGA   GTTATAACTC   CTGTACCAGA   AATGTAACAA   CATCTCACTC
 241    TTGAATCAAA   ACTTTCAGGC   CAGGTGTGGT   GACTTGTGCC   TGTAATCCCA   GCATTTTGGG
 301    AGGCCATGGC   AGGTGGATCA   CTTGAGGTCA   GGAGTTCGAG   ACCACCCTGG   ACAATATGAT
 361    GAAACCCCAT   CTGTACTAAA   AATACAAAAA   ATAGCTGGGC   ATGGTGGCAG   GTGCCTGTAA
 421    TCCCAGCTAC   TCGGGAGGCT   GAGACAGGAG   AATCTCTTGA   GCCCGAGAGG   CAAAGCCTGC
 481    AGTGAGACGA   GATCACGCCA   GTGCACTCCA   GCCTGGACAA   CAGAGCAAGA   CTCCATCTCA
 541    AAAAAATAAA   AACTCTCAAA   TTCATTTATT   TATTCAAATA   TATAATAAGC   ATCTACTACA
 601    GCTGAAGCTT   TGCTGCTGTG   GTCTGAATGT   GGTATACCCC   CAAAATGCAC   ATGTTGAAAT
 661    TTACTCCCCA   TTGTGATAGT   ATTAAGAGGT   GGGGCCTTCG   AGGAAGTAAT   TAAGTCATGG
 721    AGGCTCTGCC   CTCATTAATG   GGGTTAGAGC   TTTTATAAGA   AAGAGAGGCT   TGTAGTCCCA
 781    GCTACACAGA   AGGCTGAGGC   AGGAGGATAG   CTTGAGCCCA   GGAGTTCAAG   TCCAGAATGG
 841    GCAGTACAAT   GAGACCCCAT   CTCTTAAAAG   AGGGAGAGAG   AGAGAGAGAC   ATTGATTGAA
 901    GGGTGTGTGT   TTGCCCCTTC   TGCCATGTGA   GGACACAGAA   AGAGGCACCA   TTCATGAAGC
 961    AGAGAACGAG   CCTTTACCAG   ACAATGAATC   AGCTAGTGCC   TTTATCTTGG   ACTTTCTAGC
1021    CTCTATAATT   GTGAGAAGTA   TTAAAATTTC   TATTATTTAT   AAATTACCCC   ATCGAAGACG
1081    TTCACTTACC   TGACTTTCCA   GATTAATCTC   TGTGTTTTAT   CTTCCCTATA   AAAAATATCC
1141    ACAGCACATT   CAACAGCCGT   GACCAATAAG   ACCATAAATT   TCTGTCCAAC   AGATGAATTG
1201    CAAGCTTACC   TAGAGATGGT   AAAGGTTTGT   CTCCAAACCT   CTTTTTTTTT   TTTTTTAATT
1261    TTTCATAGAG   ATGGGATCTT   CTTATGTTGC   CCAGGCTGGT   CTCGAACTAC   CGAGTTCAAG
1321    CAATCCACCC   ACCTCAGCCT   CCCAAAGTGC   TGGGATTACA   GGTATGAGCC   ACTGCACTCA
1381    GTTCTAAACC   TTTTTAATGT   CAGTATTATT   GTAATTATGT   GACTTAAATA   TATGCAAACC
1441    AATGAAATGA   ATGCCAAAAA   ATTATTTGAT   GAAAAGCAAT   TTGAATTTGC   TAGATTTGAA
1501    TTTAGAAAAA   GCTAGATACA   ACAGCAATCA   GGTTTCATTT   ATTCAAAACG   TTATCAAAGT
1561    TCAGCAGGAA   TTCTCTCAGC   TCTGAAGAGG   GAAAAAGAGA   AATTTTAAGA   GATGTCTATG
1621    TTTTAAAATC   TTAAAACTTT   GCATTGGGTG   CCATGTTGTT   GGGTGCCATG   TAGCAGTGCT
1681    TTTACTCTGT   ATCTGTAAGC   TCCCAGATGC   ACTGTAGCAC   CCCAGGCTAG   AGTGCAATGG
```

```
1741    TGCGATCTTG  GCTCACTGCA  ACCTCTGCCT  CCCAGGTTCA  AGCGATTCTC  CTGCCTCAGC
1801    CTCCAGAGTA  GCTGGGATTC  CAGACACCCA  CCACCACGTC  CAGCTAGTTT  TTGTATTTAT
1861    AATAGAGATG  GGGTTTCACC  ATTTGGGCCA  GGCTGGTCTC  AAACTCGTGA  CCTCAGATGA
1921    TCCACCCACC  TCCACCTCCC  AAAGTCCTGG  GATTACAGGC  ATGAGCCACC  ACTCCCAGCC
1981    CAACCAGGAG  CTTTTTAAAA  GTAGATCCAC  TGTGTCCTGG  CCCAAATCCA  CCAGCTGCCT
2041    CAGAGTCTCA  CAGGCTAGGC  CTGTGTTTTT  AAGAATGCTG  TGAGTGATTC  TGACATACAA
2101    CCCAGCTTAG  GAATAACAGC  CCCACTAGGC  TGGCTGACTC  ACCTTCCCTC  TCATCTTTCT
2161    AGGACTCTGT  TTTCCCCATT  GCGGGGGATT  TCGGCTCATC  AAGTTACACC  AATTGACTCT
2221    CAGCATCACT  GAGCTTTTTC  TTTCACATCC  AGGGTGAGTT  TAAGTCAGTG  CTTCTCTGGG
2281    TCTCACAGGA  GTGGACATTC  TAAAGCCAGC  ATCTCCTCTG  AGTAACTCAC  TCCCCGATGA
2341    TGGGAGTTTG  ACTTTTCCTT  GGTTATGAGT  TACAGGATGA  AAGTCAGGTG  CAAACACTTA
2401    TTTCTTCAAG  CCAACAAATC  CTAGCACCTC  CTCGATCTCA  GAGAAGGTCA  GCAGACATGT
2461    GTGTGCCACG  TTTCTTCATC  TCAAGAGCTG  TGTATCATAG  TGGGAAACTG  GACTTGCAAA
2521    TGGCTATGCA  GGAAGAGAAG  GCTGTGTGAG  TGTCGGCCCC  TGGGTAGAGG  CTGTCTTTGT
2581    TGAAACCGTG  GTGCCCCGAC  AAAAGCCGGA  AAGCGAATCT  CCTTCTACTG  CACCTGCAGG
2641    CTCTGGGCCC  AAGCATGTTC  CGGGCGAGAG  GATATTTAGG  GATTTCTGGG  TTTAGCTTTC
2701    TCCGTTTTGC  CGTTCAGTTC  ACTCTGGCCC  TGGCTGTCTC  CAAAGGAGAG  GACTGATACC
2761    ATGGGATTAA  GTCCTTATGT  TCAAGCTCCG  GTCTGGGAAG  CTGAGTCTCC  ATCTTTTTCT
2821    GAGGCCAAGG  CATTGTTCTG  ACAACTGCCC  TTGACTCCAG  TTCCTTCAGG  ATGAGGGCCG
2881    TGGCTTTTCT  TGCCCACTCT  TCTGCTCCTG  AATCCTTCCT  CGCAGCCTCT  AACCACACTG
2941    CTAGCCCTCA  TCTCTGGCTT  GCTGCCAATT  TCCTCTGGCA  CTATCCTCCC  TAGCTGGCTG
3001    CAAACCCACC  TGTTGTTTTT  TGGGTTTTTT  AGAGATGGGG  TCTCGCTCTG  TTGCAATCAT
3061    AGCTCACTGC  AGCATCGAAC  TCTTGGGCTC  GACAATCCTC  CCACCTCAAC  CTCCTAAATA
3121    GCTGAGACTA  TAGGTGCCCA  CCACCACATC  TGGCTTATTT  TTTTATTTTT  TTGTAAGAGA
3181    TGGAGTCTCA  CTAGATTACC  CAGGCTGCTC  TCAAACTCCT  GGCCTCAAGG  GATCCTCCCA
3241    CTTCTGCCTC  CCAAAGTGCT  GGGATTACAG  GCATGAGCCC  CAGTGCCCGA  TCGCCACTTG
3301    TTTTCTCTTG  CTTACTC
```

Score	Start	End	Qsize	Identity	Chro	Strand	Start	End	Span
1598	1720	3317	3317	100%	10	(+)	21606655	21608252	1598
1698	1	1698	3317	100%	10	(+)	93980711	93982408	1698

BLA(S)T Output: 10q23.32(+)(93,982,408)::GCTCCCAGATGCACTGTAGCA::10p12.31(+)(21,606,655)

Rearrangement_C (breakpoints of paracentric inv(10))

```
   1    CATGGTTTGA  TTTGAGAAGG  AAATTGTCAA  GACTTCCTCT  CTCTCAGGCT  GGGTTTGGTT
  61    ACTGGAACAT  TTAGGACACT  TTGAGCAGCA  GGTAACTGAA  CACCAAAATT  AAACAATGCA
 121    TAAATGCATT  AGATTGTGAG  CCTGCGAGTT  TAGAGATAAG  ACACTATGTT  CTCTGGAGGA
 181    TTGGCTCAAT  TCAGTGGTTT  TAACTCCACG  TTCCTCCAAC  TCTCTGGACT  CATCCTCAAG
 241    GCCTAGAGCA  AGATGTCTGC  AGCCATTCCA  GGCCTCAGTT  ATACCAATGT  CCAGAGGGAG
 301    AGAGGGTTTC  CCCTCCAAAA  TTTCTCTCAA  GAGTGTAGGG  GAAGGGCCAG  GCTCGGTGGC
 361    TCATGCCTGT  AATCCCAGAA  CTTTGGGAGG  CCGAGGCAGG  CGGATCACCT  GAGGTTGGGA
 421    GTTCAAGACC  AGCCTGACCA  ACATGGAGAA  ACCCCCTCTC  TGCTAAAAAT  ACAAAAAAAA
 481    AAAAAAATAG  CCGGGAGTGG  TGGTGCATGC  GTGTAATCCC  AGCTACTTGG  GAGGCTGAGG
 541    TAGGAGAATC  GCTTGAACCC  GGGAGGAGGA  GGTTGCAGTG  AGCCGAGATC  GCGCCATTGT
 601    ACTCCAGCCT  GGGCAACAAG  AGCGAAACTC  CATCTAAAAC  AAAAGAATGT  AGGGGAAAAA
 661    ACCAATACCC  TTTCCTCATC  CATCACAAGG  GTCATGGCAG  ATACTCCTAT  AACAAGAGAC
 721    AGAGTAACAA  GAGAAAAGCA  TCACAAATTT  ATTTAACCAA  GGTTTACGTG  ACAGGGGAGC
 781    CTTCCAAAGT  GAAGACCTGA  AGACCCAGGG  AAGACTGTGC  TTTTGTGCTG  AGTCTGATGG
 841    AAGAAGTGAA  {CAG}AAAAAAA  AAAAAAAAAA  AAAGGCCGGG  CGCAGTGACT  CACGACTGTA
 901    ATTCCAGCAG  TTTGGGAGGC  TGAGGCGGGT  GGATCACCTG  AGGTCAGGAG  TTCAAGACCA
 961    GCCTGGCCAA  CATGGTGAAA  CCCTGTCTCT  AATAAAAATA  TAAAAAATTT  AGCCGGGTGT
1021    GGTGGTGGGC  GCCTGTAATC  GCAGCTACTC  AGGAGGCTGA  GGCAGAATTG  CTTGAACCCA
1081    GGAGATGGAG  GTTGCAGTGT  GCCGACATGG  TCCCACTGGA  CTCCAGCCTG  GGCGACAGAG
1141    TGAGATTCCA  TCTCAAAAAA  AAAAAAAGAA  AAAGCCCCTC  GTTGAAAACA  GTGTGGAGAT
1201    TATAAAAATA  GAACCACCAT  ACACTTCAGC  AACCTTGCTA  CTGGGTATCT  ACCCCCGCAA
1261    AAAAAGAAAT  CATTTTATAT  ATAAAAAAAT  ACCTGTGCTC  ATATGTTTAT  TGCAGCACTA
1321    TTCACAATAG  CAGAGTCATG  GAATCAACCT  AAGTGACCAT  CAACGGAGGG  CTGGCTAAAG
1381    AAAATGCACT  CTAAATACAC  AACAGAGGCC  GGGCGCCTGA  AAATGCACTC  TAAATACACA
1441    ACAGTGGCTC  ACGCCTGTAA  CCCAGCACTT  TGGGAGGCCG  AGGCGGATGG  ATCACGAGGT
1501    CAGGAGATCA  AGACCATCCT  GGTTAACACG  GTGAAACCCC  GTCTCTACTA  AAAATACAAA
```

```
1561    AAAAATTAGC  CGGGCGTGGT  GGTGGGCACC  TGTAGTCCCA  GCTACTTGGG  AGGCTGAGGC
1621    AGGACAATGG  CGTGAACCCG  GGAGGCGGAG  CTTGCAGTGA  GCCAAGATCG  CGCCACTGCA
1681    CTCCAGGCTG  GGCGACAGAG  CGAGACTCCG  TCTCAAAAAA  AAAAAAAAAA  AATACACAAC
1741    AGAATACTAT  TCAGGCATAA  AAAAGAAACA  ATGTCTTTTG  CAGCAACATG  GATGGAACTG
1801    GAGTCCATTA  TCTTAAGTGA  AAGAACTCAG  AAACAGAAAG  ACATTGCATG  TTCTCACTTA
1861    TAAGTGGGAG  TTGAATAATA  TGGACCCAGG  GACATAGAAT  GCAAAATAAT  AGACGCTGGA
1921    GACTTGGAGG  TGTAAGCGGG  TGGGAGGGAT  GGGAGGTTGC  TTGGTGGATA  TAAAG
```

Score	Start	End	Qsize	Identity	Chro	Strand	Start	End	Span
1125	851	1975	1975	100%	10	(-)	21605510	21606634	1125
853	1	853	1975	100%	10	(+)	23658350	23659202	853

BLA(S)T Output: 10p12.2(+)(23,659,20{0-2})::10p12.31(-)(21,606,63{4-2})

Next-Gen Cytogenetic Nomenclature:

Short System

46,XY,inv(10)(p13q24)dn.seq[GRCh37/hg19] inv(10)(p12.2p12.31)(p12.2q23.32)dn

Detailed System

46,XY,inv(10)(p13q24)dn.seq[GRCh37/hg19] inv(10)(qter->q23.32(93,983,897~)::p12.2q23.32(23,659,495~-93,982,408)::GCTCCCAGATGCACTGTAGCA::p12.31p12.2(21,606,655-23,659,20{0-2})::p12.31(21,606,63{4-2})->pter)dn

DGAP285

46,Y,inv(X)(p11.2q28).arr(1-22)x2,(XY)x1.seq[GRCh37/hg19] inv(X)(p11.21q28)

Prenatal History: A 22 year-old G1P0 female had a spontaneous conception and uncomplicated pregnancy until comprehensive ultrasound screening at 22.5 weeks, which revealed hydrocephalus, hypoplastic and irregularly shaped cerebellum, unilateral left multi-cystic kidney, and single umbilical artery. Amniocentesis was performed on the same day at 22.5 weeks. Fetal echocardiography at 23.1 weeks was reported to be normal. Follow-up fetal ultrasounds at 23.1 and 28 weeks continued to be significant for the previously reported abnormal findings. At 31.4 weeks the mother presented at an outside hospital for decreased fetal movements and intrauterine fetal demise was detected. The parents declined any post-mortem studies.

Sequencing Results and Interpretation of Convergent Genomic Evidence: Sequencing of the prenatal DNA sample identified the inversion breakpoints within *FAM104B* at Xp11.21 and within a non-genic region at Xq28. The breakpoints at Xq28 disrupt a TBR, which may result in genomic rewiring of the surrounding TADs and TBRs. *MTM1*, a hemizygous gene associated with X-linked centronuclear myopathy (a prenatal onset fatal disease with clinical findings including decreased fetal movements and hydrocephalus),[19; 20] is located in a TBR upstream to the Xq28 breakpoints, and therefore dysregulation of *MTM1* might be contributory to the phenotype of DGAP285 (Figure 4B, Table 6).

Next-Gen Cytogenetic Nomenclature:
Short System
46,Y,inv(X)(p11.2q28).seq[GRCh37/hg19] inv(X)(p11.21q28)

Detailed System
46,Y,inv(X)(p11.2q28).seq[GRCh37/hg19] inv(X)(qter->q28(150,286,207~)::p11.21q28(55,174,723~-150,284,569~)::p11.21(55,174,381~)->pter)

DGAP288

46,XX,t(6;17)(q13;q21)dn.arr(1-22,X) x2.seq[GRCh37/hg19] t(6;17)(q21;q24.3)dn

Prenatal History: A 37 year-old G3P2 female had an abnormal fetal ultrasound with a cystic hygroma identified at 11.1 weeks. CVS was performed at 11.6 weeks. At 28 weeks polyhydramnios and micrognathia were detected on ultrasound examination. At 34 weeks, fetal MRI revealed findings suggesting Pierre Robin sequence including a small jaw index consistent with micrognathia and retrognathia, glossoptosis, and suspicion for cleft palate without cleft lip.

Postnatal History: C-section was performed at 39 weeks and continuous positive airway pressure was applied after birth. Physical examination finding of cleft palate was consistent with Pierre Robin sequence, and additional findings included small low-set ears, a flat nasal bridge, hypotelorism, a short wide neck, and a large space between the 1st-2nd phalanges. The newborn received nasogastric feeding due to the cleft palate.

Sequencing Results and Interpretation of Convergent Genomic Evidence: Sequencing of the prenatal DNA sample identified the translocation breakpoints within non-genic regions at 6q21 and 17q24.3. An analysis of the protein-coding genes localized in the same TAD as the breakpoints revealed that the 17q24.3 breakpoints are within the same 1.88 Mb TAD as *SOX9* and within its well known upstream cis-regulatory region for Pierre Robin sequence.[21-23] DGAP288 had decreased *SOX9* RNA expression and an overlapping phenotype of Pierre Robin sequence (Figure 4C, 5, Table 6).

Rearrangement_A (on der(6))

```
  1    ATAACAGAAG   CATTCTTTAG   TCACCCTAAT   GATAGACAGT   GAAGCAATCT   GGTGAATGGT
 61    TAGGATGTTA   GTGGGATGGG   AGGATTTGAA   AAGGAGCAGA   TATAGTTGAG   TATTGGAAAG
121    CAAGAATTCT   GTTTGGTACA   TTTTAAGTTG   AGAAGTCAAT   TTTATGGACG   TCCAAGGAGA
181    GATATTGCTT   AGGTAGTTAA   ATGATTGAGT   CAAACATTCA   TGGGAAAGGT   GAGAGCTAAA
241    AACATAAACT   AGGGAGTTAT   TAGCTTATAA   AGTTAACCTT   TAAAGCCATG   GGATTCAACG
301    TTTCCACCTA   GAACATATGT   GTTGTTAGAG   AAAAGTGTGA   GGCTTGAGCC   CTAGAGCATG
361    ACAATACGTA   GACATCAGGA   AGACGAGAAG   GATCCAGGAA   AGGATATAGG   AAGGAGTAGC
421    CAGTGAAATA   GAAGGTAAGC   AAATGAACAA   AAATGTCCTG   GAAGAAAAGT   GAAAAAAGGT
481    TTCAAGGAGG   AGAAAGTGAT   CCACTGTGTC   CAGTGAATTT   GATGAATTAA   ATGAGGCAAG
541    AAATGAGAAT   TGATCATTGG   ATTGTTAACC   AGAGGTCACT   GGTGACTGAT   AAATTTCAGT
601    GGAGTGATCA   AGGTGAAAGC   AAGATTGGAG   AGTGTTCACA   AGATAATGAG   ACAGGAAGAA
661    CTGGAGACAG   AAATAACTCT   TTCGAAGAGT   TTTCATCTAA   {AGG}ATTTGCC   TTCAGCCATT
721    TCTCAGTTAG   GAAAAATACA   GATTCTGGGG   GAAAGTTATT   CACAGAGAAA   GTAAAAATTG
781    CCAGTGGGTC   TTTTTTTTTT   TTTCTTCCAG   AAATAAAAGG   AT
```

Score	Start	End	Qsize	Identity	Chro	Strand	Start	End	Span
703	1	703	822	100%	6	(+)	112975342	112976044	703
116	701	822	822	95.9%	17	(+)	69728017	69728137	121

BLA(S)T Output: 6q21(+)(112,976,04{2-4})::17q24.3(+)(69,728,01{7-9})

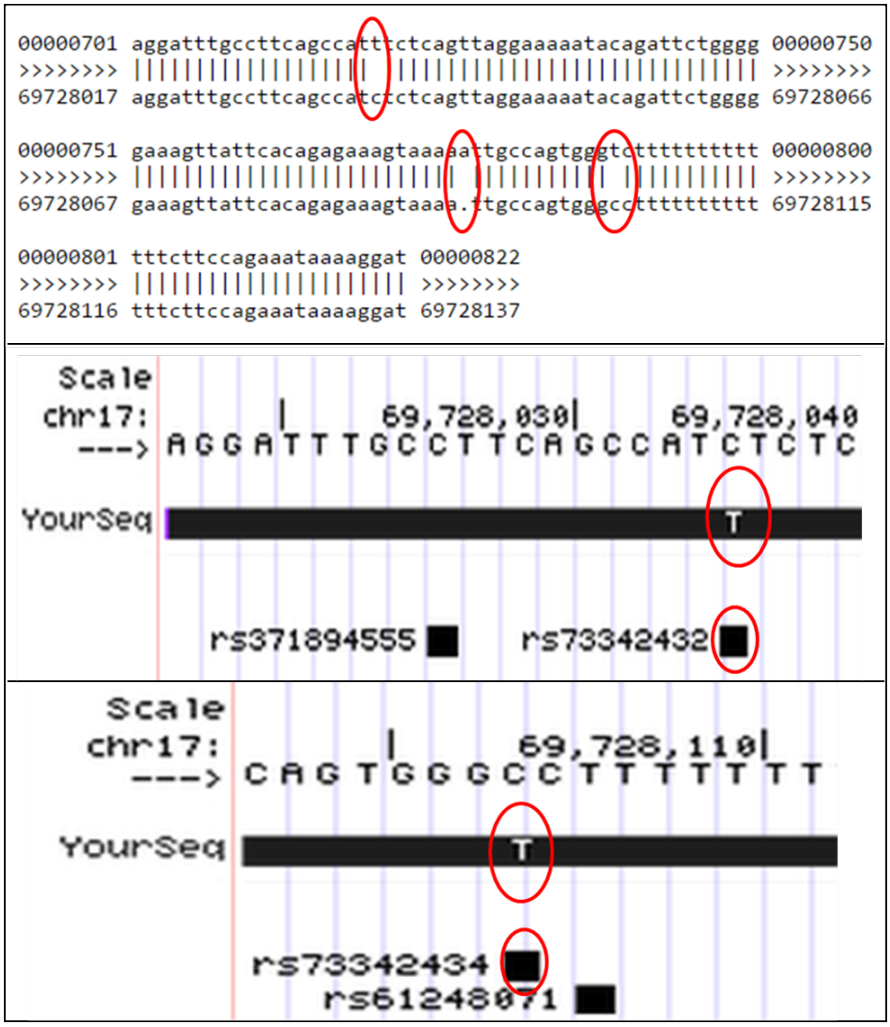

Figure S-DGAP288_1. BLA(S)T Output, Rearrangement_A on der(6): Circled mismatches represent a SNP (dbSNP build 141, rs73342432), an additional repetitive nucleotide "A", and another SNP (dbSNP build 141,. rs73342434); respectively.

Rearrangement_B (on der(17))

```
  1    CTGGGTATTT   ACAGAAAAAG   ATGTTGAGCC   TTCTTCTAGG   CAGAGACAAC   TCTTCTAGAA
 61    AATATCTCAT   ACAATAAAGA   TTGATTATCA   CATTGTTTAG   TGTGTAATTC   ATGTGTTCTC
121    AAAATTTTCC   TTAGAGGTAT   AGCAGTTACA   GACATACCCC   AAATACATAA   ATCTGTGCTT
181    GTACTAAGAG   AAACTTGGTG   TCAATTATTC   ACTTTCCAAA   AGGATTCACT   AGATGTCATC
241    CTCAGTGATT   TTCCTTAGAG   CGTTTCAGGT   GGGATTTGAG   TTATCAAACT   TGGTTTCATT
301    TGTGCTTTCG   TGAATATACC   TATTTGGTAA   GATCTGTTTT   GCCAAATTCA   GTCCAATACA
361    AATTGGTCTT   GAATCCTATT   CAAGGGAGAT   TATGTTTAAA   GGACCTGAGG   GACTTCATTA
421    TAACCACAGC   TTCTTCTACC   CCGGATGCCC   CATGGCCTAA   GACTCCCAAG   AGCAGCAGCT
481    TTCCAGCCAT   GTCCTGAGTT   TCTGGGGCAG   AGTAAAGCCC   TTTATTTTCA   TCTAAAGGGC
541    TTTAGGGAAA   TAGCTGGTAG   CTGGAAGGAA   ACATGAGATT   AAGAGAGGGT   TTATTTCATT
601    GTTTCAAAAG   TTGAGATTTA   ATGTACATAT   TATGAAATGC   ACAGATCTTA   CATGTACTTA
661    GTTCTGATAA   ATGCACATAC   CATGTGGCAT   GCACACTCTT   ATGAAGATAT   AGAGCATTTT
721    TCTCAGTCCA   GAACATTCCC   TTTTAGCCAT   TCTAGTCAAT   ACATATATCA   TCCTACTTTC
781    CCTTATCTAC   TCCATATGAA   GCAACTATTG   TTCTGATTTC   TCTCAACATA   GAACATTCTT
841    GCCTAGTCCA   AGAGTTCGTA   TCAATGGAAT   CACAGGGTGT   GTC
```

Score	Start	End	Qsize	Identity	Chro	Strand	Start	End	Span
517	1	517	883	100%	17	(+)	69727490	69728006	517
357	525	883	883	99.8%	6	(+)	112976031	112976389	359

BLA(S)T Output: 17q24.3(+)(69,728,006)::CCCTTTA::6q21(+)(112,976,031)
or
BLA(S)T Output: 17q24.3(+)(69,728,006)::6q21(112,976,045-112,976,039)::6q21(+)(112,976,031)

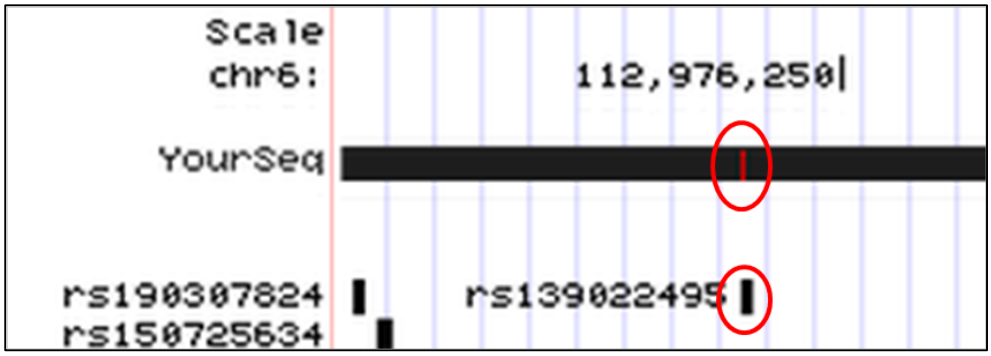

Figure S-DGAP288_2. BLA(S)T Output, Rearrangement_B on der(17): Circled mismatch represents a SNP (dbSNP build 141, rs139022495).

Next-Gen Cytogenetic Nomenclature:

Short System

46,XX,t(6;17)(q13;q21)dn.seq[GRCh37/hg19] t(6;17)(q21;q24.3)dn

Detailed System

46,XX,t(6;17)(q13;q21)dn.seq[GRCh37/hg19] t(6;17)(6pter->6q21(112,976,04{2-4})::17q24.3(69,728,01{7-9}->17qter;17pter->17q24.3(69,728,006)::CCCTTTA::6q21(112,976,031)->6qter)dn
or
46,XX,t(6;17)(q13;q21)dn.seq[GRCh37/hg19] t(6;17)(6pter->6q21(112,976,04{2-4})::17q24.3(69,728,01{7-9}->17qter;17pter->17q24.3(69,728,006)::6q21(112,976,045-112,976,039)::6q21(112,976,031)->6qter)dn

DGAP290

46,XY,t(2;7)(q33;q32)dn.arr(1-22)x2,(XY)x1.seq[GRCh37/hg19](2,7)cx,der(2)t(2;7)(q32.3;q33)inv(7)(q33q33)dn,der(7)t(2;7)dn

Prenatal History: A 38 year-old G2P2 female conceived after IVF had a high-risk pregnancy based on first trimester combined screening results. CVS was performed at 13 weeks 6 days. Ultrasound examinations at 16.4 and 18 weeks were normal. Due to a family history of congenital heart anomalies, fetal echocardiography was performed at 16.4 weeks and was interpreted to be normal. The parents decided to terminate the pregnancy at 23 weeks due to uncertainty of the clinical significance of the balanced rearrangement.

Sequencing Results and Interpretation of Convergent Genomic Evidence: Sequencing of the prenatal DNA sample identified the translocation breakpoints disrupting *HECW2* at 2q32.3 and *NUP205* at 7q33, with an additional non-genic disruption at 7q33. An analysis of the protein-coding genes localized in the same TAD as the breakpoints did not reveal any monoallelic or imprinted genes associated with an abnormal phenotype (Figure 4D, Table 6).

BLA(S)T Outputs of Sequencing Results:

Rearrangement_A (on der(2))

```
  1      ATAATACTTC   CTAAACCCAC   AGAATTTAAG   TCTTACAGAA   ATGTATAAAT   GCACAGCATG
 61      GATCATCTTT   TTAGCTAATA   TAAATGCAGT   TCATAAGAGG   AAGAAAAAAA   TTAAAATGCT
121      TTAGAAAGAA   TACTTTGAAA   TCAAGATAGA   CTATCCAGCA   AAATAAATTC   TAAAATCATG
181      CCCAACTAAA   GAAAAAGGAA   ACACGATAAA   AACACGAAAA   CAAAATAAGT   TAAAAAAAAA
241      AAAAAGCCTG   TAAGCTGCTT   AGTATTTTCA   TACTGTTAAA   ACATGTTAGT   TGTCAAAAGT
301      CCAGGAGAGT   TATAGTTGTA   ACAAACACGG   TAAGGACATT   TAATGCAAAA   TCTCTTTATC
361      CTAGGAGTTC   CCAAACTCGT   GATTTGTCTG   TAGGTTAAAA   ATTCAGGAGT   GGCTTAGCTA
421      AGTGGTCCTG   GCTCGGGTTC   GTTATGAAGT   TGCCCACCCT   TAAATTCCTT   AGAGGGCCTT
481      TTATCTCACC   ATCTGGTTCT   CTAACTTCTT   CACAAAGCAT   ATTATAGTCA   CACCCTCAGG
541      TTCATCTTTA   TACTATATCT   TCCTGAGAGT   ACCCTGAATT   TGATCTTTGT   TCAAAAGCCA
601      ATTTTTTTAA   ATTTTAGCAT   TGTTTGCCAT   CCAAAGAGGC   TGCAAACTTT   AAAACCCACC
661      AGGTCTTCAC   TGCTTTATAT   ATTATAATTT   TTCTCTGACT   TGTTTCTCTC   CTCTTGTATT
721      TTACTA
```

Score	Start	End	Qsize	Identity	Chro	Strand	Start	End	Span
369	1	373	726	99%	2	(+)	197163823	197164194	372
351	376	726	726	100%	7	(-)	135905573	135905923	351

BLA(S)T Output: 2q32.3(+)(197,164,194)::AA::7q33(-)(135,905,923)

Figure S-DGAP290_1. BLA(S)T Output, Rearrangement_A on der(2): Circled mismatch represents an additional repetitive nucleotide "A".

Rearrangement_B (on der(7))

```
  1       GCCAGGATTT   CTTATTTTCC   CAGTTGCAGT   ATCTACCATT   TTCTAACAAA   GGTAGGCCAT
 61       TATTTTCCCG   TATTTATAAG   AACACATTTA   TAATTCCATG   TTAAGTGATT   TTATTTATAC
121       AATATTTGGG   GGAATTCTGT   TCTCATTCTG   ATACTTTGGC   TTCTTTGTTA   TTTTGGGTTC
181       TTTTTGTAAT   TTCTGCTTAA   AGAAGGCTGA   TATTTTAACT   GCTAGCAAAA   ACTTATTTAA
241       ATATAGCCTA   TCAAGGATGG   AATTTGATTC   TCTTACAACA   AATAAAATTT   AAAGATTGTG
301       TTGAAGGGAT   TAGAAAATTA   ATGGGAATTT   AAAGTTTTTG   AATGAAAATT   GTTTTACAAA
361       GATTTCTGAT   TTTCTCTTCC   CAGGCTGTTT   ATGAGGAAAA   AAAAAATCCT   GGTTTATTTT
421       TGTTTCTTGT   GTTTGTATTG   AAACCAATTC   AGATCTTGAA   ATGAAAAGTT   GAAAACTAAT
481       TATGGTAGAA   AACAGTTTTA   ACTTAGTTTA   TTGACATGGC   TAACAATTAT   TCCAGGCTAA
541       TGCAGTCTTA   TCGAGATTCT   ACTTTATTTT   CTTTTTGACC   AACTTTTAAC   AGTTTTCTGA
601       ATTCAGACTA   TATTCAGACA   GTCTTAGTCT   GTTGAGTTTT   TTAAAAGTTT   AGCTTGTGTC
661       ATCTTTATGT   TTTAGGAAGT   TGAGGCTCAC   ACATGCCATA   AACAAATTTC   TATTACTAGT
721       AATTGTCAGC   ATCTAATTTA   CCTTTTAGAG   TAATGGCGTT   AGACCTCTGA   GAATTATCTA
781       ATGGCAAAAG   GTTTTTCACT   CTATTTTCAT   AAGTGTCTTA   TTTTTAGTTC   TGGGATTTTG
841       GACAGTTGTA   TCAGAATCAC   TTAAGGGGCC   TAAAACAAAA   CAAAGCAAAA   TAAAAACAGA
901       CTGCTGGGAC   CCACTCCAGA   CCTACTGAAC   CAGAATCTCT   AAGATCTGGG   TACCAAGAAT
961       ATGCATTTTA   TTTTTTAAAG   TC
```

Score	Start	End	Qsize	Identity	Chro	Strand	Start	End	Span
838	1	840	982	99.9%	7	(+)	135298971	135299810	840
141	842	982	982	100%	2	(+)	197164206	197164346	141

BLA(S)T Output: 7q33(+)(135,299,810)::G::2q32.3(+)(197,164,206)

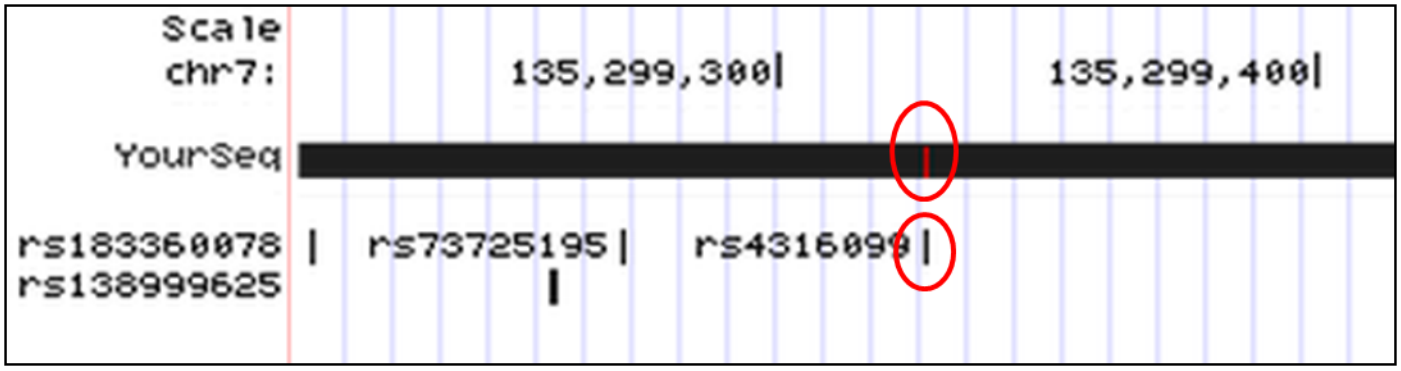

Figure S-DGAP290_2. BLA(S)T Output, Rearrangement_B on der(7): Circled mismatch represents a SNP (dbSNP build 141, rs4316099).

Rearrangement_C (on der(2))

```
   1       CAAAACAAAT   ACATAAGAAA   AATTAAACTT   AAATTGCATG   ATTTTATAAT   ACCTCAATTA
  61       ATGATGTGGT   TTAACATTTA   ATTAAGGCTG   AGAATCACTT   ATACAATAGT   TTTTATTTTT
 121       ATTTATTTAT   TTTTTATTGT   AGAGACAGGG   TCTCACTCTA   TTGCCCAGGC   TGTACTTGAA
 181       CTCCTTGCCT   CAGTGTTCCT   CCTGTCTCAG   CCTACCTAAG   CACTGGGATT   ATAGGCGCGA
 241       GCCACTGTGC   CTGGTCCTAC   AATAAGATTT   TTTTAATCCA   ATACTATTTT   AATATGCTTG
 301       ACATTGAAAC   CCTAAACTGT   GACAGTATAA   ACATAAAATT   AACCATATAA   CAATACTAAT
 361       AATAATTTCA   GGCAAAGCTA   AATGAAGTTT   TATAAAACAC   ATACCATAAT   AGGTAAGATG
 421       TTAATTTTTA   TTTTTAATTA   GGTGTAAAGA   GGGTTTCTAA   AAGCTTCTTA {A}GATAATAAA
 481       TATTTACTGC   TGCTTTAAAC   CATTAAGGTT   TGGTTTAATT   TGCTGTGTAG   CAATAGATAA
 541       TAAGTTGCCA   CTGACTTTTA   ATTATTGTAA   AATCAATGAG   GAGATGTCTG   GCCTCATAGA
 601       AGATTTACCT   GACATGAATC   AGCCCTCTTC   CTGATTCTAA   CATATAGAAA   TGATGGAAAA
 661       ACTACAAAAA   GCTTGAATAA   AATAGTCATG   TAACTGAGAA   AATGGAATCC   CTAGATAATA
 721       AAAACATAGA   GAGAAATCAC   AGTCATTTGG   GAAGGGTAAA   GTGAACGTAG   TAACCTGGCC
 781       CATTGAGGTT   TATGAGATAT   AGGATTGTGT   AAAGGATGAG   GCTGAAGTTT   TCATGCAGGG
 841       TCAGCAGCTG   GAAACAAGTC   CAATTGTATA   AGGCCAAGAG   CCTACAAGGG   TGCACTCTCT
 901       TCACAAATAT   AAAGTTTGAC   TTTCCAGCCT   GGAAAAGCAA   CAAAGAAACT   TGTTAAACAT
 961       TCAAGACTTT   TTCATCCACT   GATTATTCTT   TGTCCCTTTG   TTATGAGAGA   GTTCTTTGAA
1021       AACAAAGCAA   AGCAAGTGCA
```

Score	Start	End	Qsize	Identity	Chro	Strand	Start	End	Span
471	1	471	1040	100%	7	(-)	135299812	135300282	471
570	471	1040	1040	100%	7	(+)	135905924	135906493	570

BLA(S)T Output: 7q33(-)(135,299,81{2})::7q33(+)(135,905,92{4})

Next-Gen Cytogenetic Nomenclature:

Short System

46,XY,t(2;7)(q33;q32)dn.seq[GRCh37/hg19](2,7)cx,der(2)t(2;7)(q32.3;q33)inv(7)(q33q33)dn,der(7)t(2;7)dn

Detailed System

46,XY,t(2;7)(q33;q32)dn.seq[GRCh37/hg19](2,7)cx,der(2)(2pter->2q32.3(197,164,194)::AA::7q33(135,905,923-135,299,81{2})::7q33(135,905,92{4})->7qter)dn,der(7)(7pter->7q33(135,299,810)::G::2q32.3(197,164,206)->2qter)dn

DGAP295

46,XY,t(2;11)(p13.1;p15.5)dn.arr(1-22)x2,(XY)x1.seq[GRCh37/hg19](2,11)cx,der(2)inv(11)(p15.5) inv(11)(p15.5)t(2;11)(p13.3;p15.5)dn,der(11)t(2;11)dn

Prenatal History: A 21 year-old G2P1 female had positive first trimester serum screening for trisomies 13 and 18. Of note, the PAPP-A value was very low (0.1 percentile). cfDNA testing failed at both 12 and 14 weeks, due to low fetal fractions. Fetal ultrasonography was normal until 19 weeks, when an anatomical survey revealed severe growth restriction (~3 weeks delayed) and an amniocentesis was performed. Ultrasound examinations at 25 and 29 weeks showed decreased amniotic fluid volume and continued growth restriction. A fetal echocardiogram at 25 weeks was interpreted to be within normal limits. At 29 weeks, the mother was hospitalized after the fetal ultrasound revealed that the fetus continued to have significant intrauterine growth restriction (~10 weeks delayed).

Postnatal History: An emergency C-section occurred at 31 weeks, following an ultrasound examination with no observation of fetal movement. The newborn weighed 450 grams with an otherwise normal physical examination and was admitted and followed in the NICU. The newborn was discharged from the hospital after 21 weeks in stable condition.

Sequencing Results and Interpretation of Convergent Genomic Evidence: Sequencing of the prenatal DNA sample identified the translocation breakpoints disrupting *GFPT1* at 2p13.3 and multiple non-genic regions at 11p15.5 within a 70 kb distribution. Interestingly, the breakpoints at 11p15.5 are located within the same 600 kb TAD as *IGF2*, a region well known to be associated with Silver-Russell syndrome through imprinted loss of function (epimutation)[24], overlapping with the phenotype of DGAP295 (Figure 4E, Table 6).

Next-Gen Cytogenetic Nomenclature:
Short System
46,XY,t(2;11)(p13.1;p15.5)dn.arr(1-22)x2,(XY)x1.seq[GRCh37/hg19]
(2,11)cx,der(2)inv(11)(p15.5)inv(11)(p15.5)t(2;11)(p13.3;p15.5)dn,der(11)t(2;11)dn

Detailed System
46,XY,t(2;11)(p13.1;p15.5)dn.arr(1-22)x2,(XY)x1.seq[GRCh37/hg19] (2,11)cx,der(2)(11pter->11p15.5(1,915,057~)::11p1.55(1,936,993~-1,960,727~)::11p15.5(1,936,668~-1,915,843~)::11p15.5(1,961,361~-1,984,895~)::2p13.3(69,588,420~)->2qter)dn,der(11)(2pter->2p13.3(69,588,264)::11p15.5(1,985,019~)->11qter)dn

Supplementary Figures

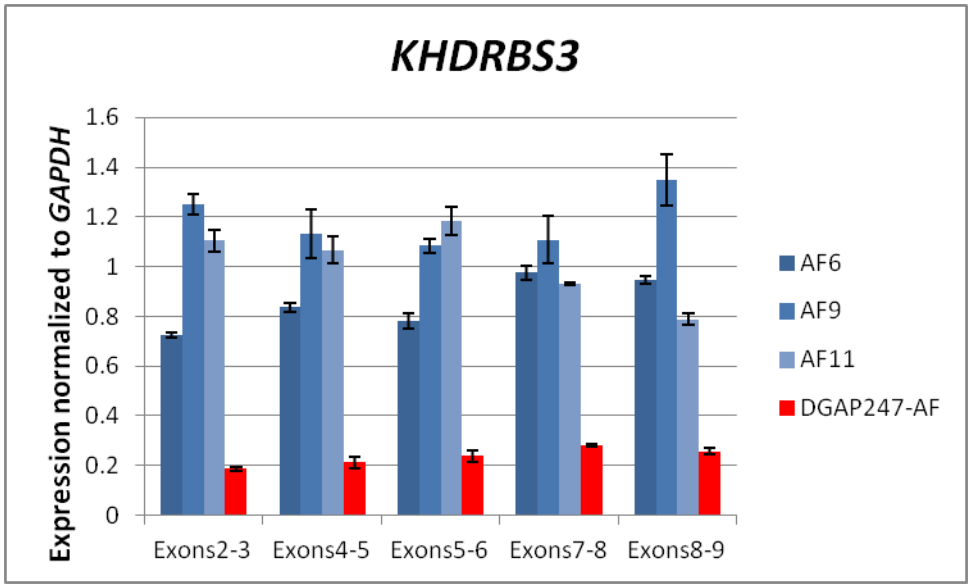

Figure S1. DGAP247 amniotic fluid *KHDRBS3* expression: Decreased expression of *KHDRBS3* in the amniotic fluid sample of DGAP247 in comparison to three amniotic fluid control samples (normalized to *GAPDH*).

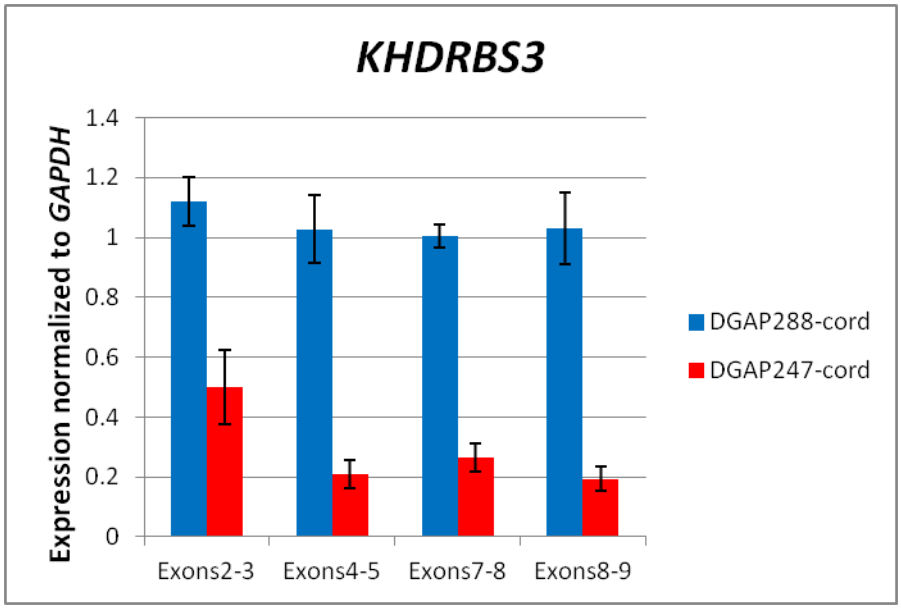

Figure S2. DGAP247 cord blood *KHDRBS3* expression: Decreased expression of *KHDRBS3* in the cord blood sample of DGAP247 in comparison to the cord blood sample of DGAP288 (normalized to *GAPDH*).

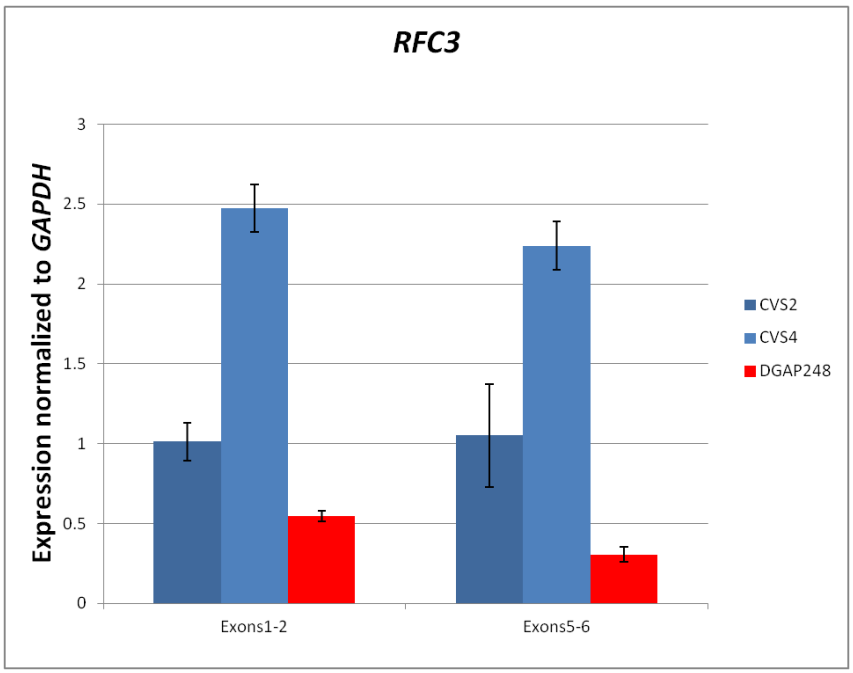

Figure S3. DGAP248 CVS *RFC3* Expression: Decreased expression of *RFC3* in the CVS of DGAP248 in comparison to two CVS control samples (normalized to *GAPDH*).

Table S1. Next-Gen Breakpoint Nucleotides of the Analyzed Cases

Case	Next-Gen Band	`Next-Gen Breakpoint Nucleotides (GRCh37/hg19)
DGAP239	6q13	Rearrangement_A: 70,405,86{7-8} Rearrangement_B: 70,405,86{7-9}
	8q12.2	Rearrangement_A: 61,628,67{1-2} Rearrangement_B: 61,628,66{7-9}
DGAP247	8q11.21	Rearrangement_A: 51,889,501 Rearrangement_B: 51,889,502
	8q24.23	Rearrangement_A: 136,495,820 Rearrangement_B: 136,495,823
DGAP248	2p12	Rearrangement_A: 78,301,91{1-2} Rearrangement_B: 78,301,90{8-5}
	13q13.2	Rearrangement_A: 34,542,73{2-1} Rearrangement_B: 34,542,7{20-23}
DGAP258	6p25.3	Rearrangement_A: 776,81{6} Rearrangement_B: 776,787
	6q16.1	Rearrangement_A: 93,191,54{7} Rearrangement_B: 93,191,545
DGAP259	3p26.3	Rearrangement_D: 1,408,99{6} Rearrangement_G: 1,408,984
	3p24.3	Rearrangement_A: 17,392,144 Rearrangement_C: 17,392,136
	5q14.3	Rearrangement_B: 88,756,2{48-56} Rearrangement_E: 88,756,2{39-40}
	7q35	Rearrangement_B: 147,718,91{1-9} Rearrangement_E: 147,718,90{7-8)
	7q36.3	Rearrangement_A: 155,701,797 Rearrangement_C: 155,700,873
	9p23	Rearrangement_F: 9,646,47{5} Rearrangement_I: 9,646,471
	18p11.31	Rearrangement_D: 6,375,05{1} Rearrangement_G: 6,559,611 Rearrangement_H: 6,375,0{52-48} and 6,559,{598-602}
	18q21.3	Rearrangement_F: 54,660,13{8} Rearrangement_I: 54,660,136
DGAP268	10p12.31	Rearrangement_B: 21,606,655 Rearrangement_C: 21,606,63{4-2}
	10p12.2	Rearrangement_A: 23,659,495~ Rearrangement_C: 23,659,20{0-2}
	10q23.32	Rearrangement_A: 93,983,897~ Rearrangement_B: 93,982,408
DGAP285	Xp11.21	Rearrangement_A: 55,174,723~ Rearrangement_B: 55,174,381~
	Xq28	Rearrangement_A: 150,286,207~ Rearrangement_B: 150,284,569~
DGAP288	6q21	Rearrangement_A: 112,976,04{2-4} Rearrangement_B: 112,976,031
	17q24.3	Rearrangement_A: 69,728,01{7-9} Rearrangement_B: 69,728,006
DGAP290	2q32.3	Rearrangement_A: 197,164,194 Rearrangement_B: 197,164,206
	7q33	Rearrangement_A: 135,905,923 Rearrangement_B: 135,299,810 Rearrangement_C: 135,299,81{2} and 135,905,92{4}
DGAP295	2p13.3	Rearrangement_D: 69,588,420~ Rearrangement_E: 69,588,264~
	11p15.5	Rearrangement_A: 1,915,057~ Rearrangement_B: 1,960,727~ Rearrangement_D: 1,915,843~ Rearrangement_C: 1,961,361~
		Rearrangement_A: 1,936,993~ Rearrangement_C: 1,984,895~ Rearrangement_B: 1,936,668~ Rearrangement_E: 1,985,019~

Table S2. Analyzed topologically associated domains (TADs) and topological boundary regions (TBRs)

Case	Next-Gen Band	TAD and TBR nucleotides [hESC, GRCh37/hg19][25] (size)
DGAP239	6q13	TBR: 69,103,279-69,343,279 (240kb) TAD: 69,343,279-70,903,279 (1.56 Mb) TAD: 70,903,279-71,743,279 (840kb)
	8q12.2	TAD: 59,557,446-60,917,446 (1.36 Mb) TBR: 60,917,446-60,957,446 (40 kb) TAD: 60,957,446-61,317,446 (360kb) TBR: 61,317,446-61,557,446 (240kb) TAD: 61,557,446-62,037,446 (480kb) TAD: 62,037,446-62,517,446 (480kb) TBR: 62,517,446-62,557,446 (40kb) TAD: 62,557,446-64,037,446 (1.48 Mb) TBR: 64,037,446-64,117,446 (80kb)
DGAP247	8q11.21	TBR: 48,677,447-48,917,447 (240kb) TAD: 48,917,447-49,837,447 (920kb) TBR: 49,837,447-49,877,447 (40kb) TAD: 49,877,447-52,757,447 (2.88 Mb) TBR: 52,757,447-52,957,447 (200kb) TAD: 52,957,447-53,317,447 (360kb) TBR: 53,317,447-53,437,447 (120kb) TAD: 53,437,447-54,797,447 (1.36 Mb)
	8q24.23	TAD: 134,490,818-135,890,818 (1.4 Mb) TAD: 135,890,818-137,770,818 (1.88 Mb) TAD: 137,770,818-139,130,818 (1.36 Mb)
DGAP248	2p12	TAD: 75,866,492-76,826,492 (960kb) TBR: 76,826,492-77,146,492 (80kb) TAD: 77,146,492-79,226,492 (2.08 Mb) TAD: 79,226,492-80,146,489 (919kb) TBR: 80,146,489-80,266,489 (120kb)
	13q13.2	TAD: 32,902,000-34,342,000 (1.44 Mb) TBR: 34,342,000-34,382,000 (40kb) TAD: 34,382,000-36,542,000 (2.16 Mb) TAD: 36,542,000-37,582,000 (1.04 Mb) TBR: 37,582,000-37,622,000 (40kb)
DGAP258	6p25.3	TAD: 135,000-1,455,001 (1.32 Mb) TAD: 1,455,001-2,735,001 (1.28 Mb) TBR: 2,735,001-2,775,001 (40kb)
	6q16.1	TAD: 90,623,279-91,183,279 (560kb) TBR: 91,183,279-91,223,279 (40kb) TAD: 91,223,279-93,463,279 (2.24 Mb) TBR: 93,463,279-93,503,279 (40kb) TAD: 93,503,279-94,143,279 (640kb)
DGAP259	3p26.3	TAD: 60,000-2,145,000 (2.085 Mb) TBR: 2,145,000-2,225,000 (80kb) TAD: 2,225,000-3,225,000 (1 Mb)
	3p24.3	TAD: 15,624,996-16,304,996 (680kb) TAD: 16,304,996-16,624,996 (320kb) TAD: 16,624,996-17,304,996 (680kb) TAD: 17,304,996-17,904,996 (600kb) TAD: 17,904,996-18,464,996 (560kb) TBR: 18,464,996-18,504,996 (40kb) TAD: 18,504,996-19,064,996 (560kb)
	5q14.3	TAD: 86,684,244-88,004,244 (1.32 Mb) TAD: 88,004,244-90,124,244 (2.12 Mb)
	7q35	TAD: 145,809,067-147,969,067 (2.16 Mb) TAD: 147,969,067-148,209,067 (240kb) TAD: 148,209,067-148,649,067 (440kb) TBR: 148,649,067-148,809,067 (160kb) TAD: 148,809,067-149,129,067 (320kb)
	7q36.3	TBR: 153,729,067-155,147,248 (1.418 Mb) TAD: 155,147,248-155,587,239 (439kb) TAD: 155,587,239-157,187,239 (1.6 Mb) TAD: 157,187,239-159,128,663 (1.94 Mb)
	9p23	TAD: 7,570,000-8,330,000 (760kb) TAD: 8,330,000-9,290,000 (960kb) TAD: 9,290,000-9,970,000 (680kb) TAD: 9,970,000-11,370,000 (1.4 Mb)

Case	Next-Gen Band	TAD and TBR nucleotides [hESC, GRCh37/hg19][25] (size)
DGAP259 (continued)	18p11.31	TAD: 3,690,000-5,090,000 (1.4 Mb) TAD: 5,090,000-6,530,000 (1.44 Mb) TAD: 6,530,000-6,930,000 (400kb) TAD: 6,930,000-7,210,000 (280kb) TAD: 7,210,000-8,530,000 (1.32Mb) TBR: 8,530,000-8,610,000 (80kb)
	18q21.3	TBR: 52,649,002-52,729,002 (320kb) TAD: 52,729,002-54,329,002 (1.6 Mb) TAD: 54,329,002-55,289,002 (960kb) TAD: 55,289,002-56,169,020 (880kb)
DGAP268	10p12.31	TAD: 21,159,994-22,239,994 (1.08 Mb) TBR: 22,239,994-22,279,994 (40kb) TAD: 22,279,994-23,399,994 (1.12 Mb)
	10p12.2	TAD: 23,399,994-24,839,994 (1.44 Mb) TBR: 24,839,994-24,879,994 (40kb)
	10q23.32	TAD: 92,650,020-93,690,020 (1.04 Mb) TBR: 93,690,020-93,770,020 (80kb) TAD: 93,770,020-94,210,020 (440kb) TBR: 94,210,020-94,410,020 (200kb) TAD: 94,410,020-95,290,010 (879.99kb)
DGAP285	Xp11.2	TBR: 55,103,275-55,143,275 (40kb) TAD: 55,143,275-56,263,275 (1.12 Mb) TBR: 56,263,275-56,303,275 (40kb)
	Xq28	TBR: 148,592,095-149,929,342 (1.337 Mb) TAD: 149,929,342-150,249,342 (320kb) TBR: 150,249,342-150,289,342 (40kb) TAD: 150,289,342-150,889,344 (600kb)
DGAP288	6q21	TBR: 112,413,307-112,493,307 (80kb) TAD: 112,493,307-114,253,307 (1.76 Mb)
	17q24.3	TBR: 68,608,405-68,648,405 (40kb) TAD: 68,648,405-70,528,405 (1.88 Mb) TBR: 70,528,405-70,568,405 (40kb)
DGAP290	2q32.3	TAD: 196,211,755-196,931,755 (720kb) TAD: 196,931,755-198,251,755 (1.32 Mb) TAD: 198,251,755-198,651,755 (400kb)
	7q33	TAD: 134,309,460-134,949,460 (640kb) TAD: 134,949,460-136,829,460 (1.88 Mb) TAD: 136,829,460-137,309,460 (480kb)
DGAP295	2p13.3	TAD: 69,186,496-69,546,496 (360kb) TBR: 69,546,496-69,586,496 (40kb) TAD: 69,586,496-70,106,496 (520kb) TAD: 70,106,496-70,506,496 (400kb)
	11p15.5	TAD: 850,000-1,523,424 (673kb) TBR: 1,523,424-1,603,424 (80kb) TAD: 1,603,424-2,203,424 (600kb) TAD: 2,203,424-2,443,424 (240kb)

Table S3. Convergent Genomic Analysis of DGAP239 6q13 breakpoints

DGAP239: 6q13 breakpoints on Rearrangement_A: 70,405,86{7-8} and Rearrangement_B: 70,405,86{7-9}							
Genes	**Nucleotides (GRCh37/hg19)**	**Description**	**OMIM[26]**	**OMIM Morbid[26]**	**DDG2P[27]**	**%HI[8]**	**Notes**
ADGRB3	69345259-70099403	Adhesion G Protein-Coupled Receptor B3	+	-	-	3.02	No reported phenotypic association Homologous to *ADGRB1*, an angiogenesis inhibitor that is a candidate for involvement in development of glioblastoma.[28]
LMBRD1 (Disrupted)	70385694-70507003	LMBR1 Domain Containing 1	+	+	+	12.92	Biallelic loss of function (autosomal recessive) is associated with Methylmalonic Aciduria and Homocystinuria, cblF type.[29] (no phenotype overlap with DGAP239)
COL19A1	70576463-70919679	Collagen, Type XIX, Alpha 1	+	-	-	26.71	
COL9A1	70924764-71012786	Collagen, Type IX, Alpha 1	+	+	+	23.89	Some evidence for haploinsufficiency (autosomal dominant, monoallelic mode) exists for the Multiple Epiphyseal Dysplasia type 6 (MED6) phenotype. However, it has been reported that although mutations in *COL9A1* can cause MED, they are not the major causes of MED and at least one additional locus exists in such cases.[30]
FAM135A	71122644-71270877	Family With Sequence Similarity 135, Member A	-	-	-	26.1	
SDHAF4	71276620-71299272	Succinate Dehydrogenase Complex Assembly Factor 4	-	-	-	63.15	
SMAP1	71377479-71571718	Small Arfgap 1	+	-	-	34.54	
B3GAT2	71566382-71666741	Beta-1,3-Glucuronyltransferase 2	+	-	-	33.88	

DDG2P: Developmental Disorders Genotype-to-Phenotype Database, +: Confirmed DDG2P gene, HI: Haploinsufficiency index (in red if <10%)
Shaded rows: Protein coding genes located within the same hESC topologically associated domain (TAD)[25] with the breakpoints

Table S4. Convergent Genomic Analysis of DGAP239 8q12.2 breakpoints

DGAP239: 8q12.2 breakpoints on Rearrangement_A: 61,628,67{1-2} and Rearrangement_B: 61,628,66{7-9}							
Genes	**Nucleotides (GRCh37/hg19)**	**Description**	**OMIM[26]**	**OMIM Morbid[26]**	**DDG2P[27]**	**%HI[8]**	**Notes**
NSMAF	59496063-59572403	Neutral Sphingomyelinase (N-SMase) Activation Associated Factor	+	-	-	39.33	
TOX	59717977-60031767	Thymocyte Selection-Associated High Mobility Group Box	+	-	-	2.83	Linkage-disequilibrium mapping of a pulmonary tuberculosis susceptibility locus near the 3' end of *TOX*[31]
CA8	61099906-61193971	Carbonic Anhydrase VIII	+	+	+	10.02	Biallelic loss of function (autosomal recessive) associated with Cerebellar Ataxia, Mental Retardation, and Dysequilibrium Syndrome 3[32]
RAB2A	61429416-61536186	RAB2A, Member RAS Oncogene Family	+	-	-	11.01	
CHD7 (Disrupted)	61591337-61779465	Chromodomain Helicase DNA Binding Protein 7	+	+	+	2.4	Haploinsufficiency (autosomal dominant, monoallelic) reported in association with CHARGE syndrome, with mutations in over 90% of cases meeting diagnostic criteria of CHARGE syndrome[33] (Consistent with the clinical diagnosis of CHARGE syndrome during the postnatal period of DGAP239)
CLVS1	61969717-62414204	Clavesin 1	+	-	-	14.59	
ASPH	62413116-62627155	Aspartate Beta-Hydroxylase	+	+	P	46.75	Biallelic loss of function (autosomal recessive) associated with Traboulsi Syndrome[34]
NKAIN3	63161150-63912211	Na+/K+ Transporting Atpase Interacting 3	+	-	-	24.34	
GGH	63927638-63951730	Gamma-Glutamyl Hydrolase (Conjugase, Folylpolygammaglutamyl Hydrolase)	+	-	-	63.59	
TTPA	63961112-63998612	Tocopherol (Alpha) Transfer Protein	+	+	-	46.94	Biallelic loss of function (autosomal recessive) associated with Ataxia with Isolated Vitamin E Deficiency[35]
YTHDF3	64081112-64125346	YTH N(6)-Methyladenosine RNA Binding Protein 3	-	-	-	6.55	No reported phenotype association

DDG2P: Developmental Disorders Genotype-to-Phenotype Database, +: Confirmed DDG2P gene, P: Probable DDG2P gene, HI: Haploinsufficiency index (in red if <10%)
Shaded rows: Protein coding genes located within the same hESC topologically associated domain (TAD)[25] with the breakpoints

Table S5. Convergent Genomic Analysis of DGAP247 8q11.2 breakpoints.

DGAP247: 8q11.2 breakpoints on Rearrangement_A: 51,889,501 and Rearrangement_B: 51,889,502							
Genes	**Nucleotides (GRCh37/hg19)**	**Description**	**OMIM**[2] 6	**OMIM Morbid**[26]	**DDG2P**[2] 7	**%HI**[8]	**Notes**
PRKDC	48685669-48872743	Protein Kinase, DNA-Activated, Catalytic Polypeptide	+	-	-	10.36	
MCM4	48872745-48890720	Minichromosome Maintenance Complex Component 4	+	+	-	13.9	Biallelic loss of function (autosomal recessive) associated with Natural Killer Cell and Glucocorticoid Deficiency with DNA Repair Defect[36]
UBE2V2	48920960-48977268	Ubiquitin-Conjugating Enzyme E2 Variant 2	+	-	-	12.96	
EFCAB1	49623348-49647870	EF-Hand Calcium Binding Domain 1	-	-	-	44.58	
SNAI2	49830249-49834299	Snail Family Zinc Finger 2	+	+	-	5.15	Haploinsufficiency (autosomal dominant, monoallelic) reported to be associated with piebaldism[37] Biallelic loss of function (autosomal recessive) associated with Waardenburg Syndrome, Type 2D[38]
C8orf22	49966870-49988649	Chromosome 8 Open Reading Frame 22	-	-	-	81.46	
SNTG1	50822349-51706678	Syntrophin, Gamma 1	+	-	-	43.69	
PXDNL	52232138-52722005	Peroxidasin-Like	+	-	-	85.15	
PCMTD1	52730140-52811735	Protein-L-Isoaspartate (D-Aspartate) O-Methyltransferase Domain Containing 1	-	-	-	21.84	
ST18	53023399-53373519	Suppression Of Tumorigenicity 18, Zinc Finger	-	-	-	15.51	
FAM150A	53446597-53478067	Family With Sequence Similarity 150, Member A	-	-	-	80.59	
RB1CC1	53535016-53658403	RB1-Inducible Coiled-Coil 1	+	-	-	10.33	
NPBWR1	53850991-53853677	Neuropeptides B/W Receptor 1	+	-	-	47.38	
OPRK1	54138284-54164257	Opioid Receptor, Kappa 1	+	-	-	28.99	
ATP6V1H	54628117-54756118	Atpase, H+ Transporting, Lysosomal 50/57 kda, V1 Subunit H	+	-	-	20.78	
RGS20	54764368-54871863	Regulator Of G-Protein Signaling 20	+	-	-	69.9	

DDG2P: Developmental Disorders Genotype-to-Phenotype Database, +: Confirmed DDG2P gene, HI: Haploinsufficiency index (in red if <10%)
Shaded rows: Protein coding genes located within the same hESC topologically associated domain (TAD)[25] with the breakpoints

Table S6. Convergent Genomic Analysis of DGAP247 8q24.23 breakpoints

DGAP247: 8q24.23 breakpoints on Rearrangement_A: 136,495,820 and Rearrangement_B: 136,495,823							
Genes	**Nucleotides (GRCh37/hg19)**	**Description**	**OMIM[2] [6]**	**OMIM Morbid[26]**	**DDG2P[27]**	**%HI[8]**	**Notes**
ST3GAL1	134467091-134584183	ST3 Beta-Galactoside Alpha-2,3-Sialyltransferase 1	+	-	-	61.67	
ZFAT	135490031-135725292	Zinc Finger And AT Hook Domain Containing	+	-	-	57.4	
KHDRBS3 (Disrupted)	136469700-136668965	KH Domain Containing, RNA Binding, Signal Transduction Associated 3	+	-	-	10.52	No reported phenotype association

DDG2P: Developmental Disorders Genotype-to-Phenotype Database, +: Confirmed DDG2P gene, HI: Haploinsufficiency index (in red if <10%)
Shaded row: Protein coding gene located within the same hESC topologically associated domain (TAD)[25] with the breakpoints

Table S7. Convergent Genomic Analysis of DGAP248 2p12 breakpoints

DGAP248: 2p12 breakpoints on Rearrangement_A: 78,301,91{1-2} and Rearrangement_B: 78,301,90{8-5}							
Genes	**Nucleotides (GRCh37/hg19)**	**Description**	**OMIM[26]**	**OMIM Morbid[26]**	**DDG2P[27]**	**%HI[8]**	**Notes**
MRPL19	75873909-75917977	Mitochondrial Ribosomal Protein L19	+	-	-	41.5	
GCFC2	75879126-75938115	GC-Rich Sequence DNA-Binding Factor 2	+	-	-	68.95	
LRRTM4	76974845-77820445	Leucine Rich Repeat Transmembrane Neuronal 4	+	-	-	7.26	No reported phenotype association Structure and expression profile of *LRRTM* mRNAs in mice suggest a role in development and maintenance of the vertebrate nervous system[13]
REG3G	79252812-79255631	Regenerating Islet-Derived 3 Gamma	+	-	-	90.1	
REG1B	79312156-79315145	Regenerating Islet-Derived 1 Beta	+	-	-	94.05	
REG1A	79347488-79350545	Regenerating Islet-Derived 1 Alpha	+	-	-	91.34	
REG3A	79384132-79386879	Regenerating Islet-Derived 3 Alpha	+	-	-	92.13	
CTNNA2	79412357-80875905	Catenin (Cadherin-Associated Protein), Alpha 2	+	-	-	2.24	No reported phenotype association

DDG2P: Developmental Disorders Genotype-to-Phenotype Database, +: Confirmed DDG2P gene, HI: Haploinsufficiency index (in red if <10%)
Shaded row: Protein coding gene located within the same hESC topologically associated domain (TAD)[25] with the breakpoints

Table S8. Convergent Genomic Analysis of DGAP248 13q13.2 breakpoints

DGAP248: 13q13.2 breakpoints on Rearrangement_A: 34,542,73{2-1} and Rearrangement_B: 34,542,7{20-23}							
Genes	**Nucleotides (GRCh37/hg19)**	**Description**	**OMIM[26]**	**OMIM Morbid[2] 6**	**DDG2P[27]**	**%HI[8]**	**Notes**
BRCA2	32889611-32973805	Breast Cancer 2, Early Onset	+	+	+	13.3	Germline mutations associated with familial Breast-Ovarian Canc Susceptibility 2[39], homozygous or compound heterozygous mutatic involved in Fanconi anemia complementation group D1[40]
N4BP2L2	33006554-33112970	NEDD4 Binding Protein 2-Like 2	+	-	-	75.5	
PDS5B	33160564-33352157	PDS5 Cohesin Associated Factor B	+	-	-	24.83	
KL	33590207-33640282	Klotho	+	+	-	16.22	Biallelic loss of function (autosomal recessive) associated w Hyperphosphatemic Familial Tumoral Calcinosis[41]
STARD13	33677272-33924767	Star-Related Lipid Transfer (START) Domain Containing 13	+	-	-	41.15	
RFC3 (Disrupted)	34392186-34540695	Replication Factor C (Activator 1) 3, 38 kda	+	-	-	4.93	No reported phenotype association
NBEA	35516424-36247159	Neurobeachin	+	-	-	6.83	Disrupted in a patient with a *de novo* translocation and idiopat autism,[10] a linkage study implicated its localization on chromosome for autism[42] and haploinsufficiency causes autism-like behaviors animal models[11; 12]
MAB21L1	36047926-36050832	Mab-21-Like 1 (C. Elegans)	+	-	-	10.38	
DCLK1	36345478-36705443	Doublecortin-Like Kinase 1	+	-	-	6.47	No reported phenotype association A microtubule-associated kinase that can under autophosphorylation[43]
SOHLH2	36742345-36871979	Spermatogenesis And Oogenesis Specific Basic Helix-Loop-Helix 2	+	-	-	71.56	
CCDC169	36801182-36871977	Coiled-Coil Domain Containing 169	-	-	-	79.84	
SPG20	36875775-36944317	Spastic Paraplegia 20 (Troyer Syndrome)	+	+	-	43.36	Biallelic loss of function (autosomal recessive) associated with Spas Paraplegia 20[44]
CCNA1	37005967-37017019	Cyclin A1	+	-	-	33.13	
SERTM1	37248049-37271976	Serine-Rich And Transmembrane Domain Containing 1	-	-	-	49.92	
RFXAP	37393361-37403241	Regulatory Factor X-Associated Protein	+	+	-	65.91	Biallelic loss of function (autosomal recessive) associated with Ba lymphocyte syndrome, type II, complementation group D[45]
SMAD9	37418968-37494902	SMAD Family Member 9	+	+	-	11.22	Haploinsufficiency (autosomal dominant, monoallelic) reported to associated with primary pulmonary hypertension, type 2[46]
ALG5	37523912-37574398	ALG5, Dolichyl-Phosphate Beta-Glucosyltransferase	+	-	-	22.12	
EXOSC8	37572953-37583750	Exosome Component 8	+	-	-	6.92	Biallelic loss of function (autosomal recessive) associated w Pontocerebellar hypoplasia, type 1C[47]
SUPT20H	37583449-37633850	Suppressor Of Ty 20 Homolog (*S. Cerevisiae*)	+	-	-	18.6	

DDG2P: Developmental Disorders Genotype-to-Phenotype Database, +: Confirmed DDG2P gene, HI: Haploinsufficiency index
Shaded rows: Protein coding genes located within the same hESC topologically associated domain (TAD)[25] with the breakpoints

Table S9. Convergent Genomic Analysis of DGAP258 6p25.3 breakpoints

DGAP 258: 6p25.3 breakpoints on Rearrangement_A: 776,81{6} and Rearrangement_B: 776,787							
Genes	**Nucleotides (GRCh37/hg19)**	**Description**	**OMIM**[26]	**OMIM Morbid**[26]	**DDG2P**[27]	**%HI**[8]	**Notes**
FOXF2	1390069-1395832	Forkhead Box F2	+	-	-	29.64	
FOXC1	1610681-1614127	Forkhead Box C1	+	+	+	9.01	Haploinsufficiency (autosomal dominant, monoallelic) reported to be associated with multiple ocular malformation syndromes including Peters anomaly (PAN), iridogoniodysgenesis anomaly (IGDA), Axenfeld-Rieger syndrome type 3 (RIEG3)[48; 49] and 6p25.3 Dandy-Walker malformation[50]
GMDS	1624041-2245926	GDP-Mannose 4,6-Dehydratase	+	-	-	3.84	Suggestive association with 6p25.3 Dandy-Walker malformation along with deletion of *FOXC1*[50]
MYLK4	2663863-2751200	myosin light chain kinase family, member 4	-	-	-	57.67	
WRNIP1	2765648-2787186	Werner helicase interacting protein 1	+	-	-	36.94	

DDG2P: Developmental Disorders Genotype-to-Phenotype Database, +: Confirmed DDG2P gene, HI: Haploinsufficiency index (in red if <10%)
Shaded row: Protein coding gene located within the same hESC topologically associated domain (TAD)[25] with the breakpoints

Table S10. Convergent Genomic Analysis of DGAP258 6q16.1 breakpoints

DGAP258: 6q16.1 breakpoints on Rearrangement_A: 93,191,54{7} and Rearrangement_B: 93,191,545							
Genes	**Nucleotides (GRCh37/hg19)**	**Description**	**OMIM**[26]	**OMIM Morbid**[26]	**DDG2P**[27]	**%HI**[8]	**Notes**
BACH2	90636248-91006627	BTB and CNC Homology 1, Basic Leucine Zipper Transcription Factor 2	+	-	-	7.84	No reported phenotype association
MAP3K7	91223292-91296764	Mitogen-Activated Protein Kinase Kinase Kinase 7	+	-	-	2.75	No reported phenotype association
EPHA7	93949738-94129265	EPH Receptor A7	+	-	-	2.77	No reported phenotype association

DDG2P: Developmental Disorders Genotype-to-Phenotype Database, +: Confirmed DDG2P gene, HI: Haploinsufficiency index (in red if <10%)
Shaded row: Protein coding gene located within the same hESC topologically associated domain (TAD)[25] with the breakpoints

Table S11. Convergent Genomic Analysis of DGAP259 3p26.3 breakpoints

DGAP259: 3p26.3 breakpoints on Rearrangement_D: 1,408,99{6} and Rearrangement_G: 1,408,984							
Genes	**Nucleotides (GRCh37/hg19)**	**Description**	**OMIM[26]**	**OMIM Morbid[26]**	**DDG2P[27]**	**%HI[8]**	**Notes**
CNTN6 (Disrupted)	1134260-1445901	Contactin 6	+	-	-	39.69	No reported phenotype association A neural adhesion molecule of the contactin subgroup of the immunoglobulin superfamily[51]
CNTN4	2140497-3099645	Contactin 4	+	-	-	6.9	A boy with t(3;10)(p26;q26)dn and characteristic features of 3p- syndrome (autosomal dominant) is reported to have a translocation breakpoint on chromosome 3 within the minimal candidate region for 3p deletion syndrome disrupting the *CNTN4* mRNA transcript at 3p26.3-p26.2[52] (relevant to cerebral and renal malformation phenotype of DGAP259)
IL5RA	3111233-3168297	Interleukin 5 Receptor, Alpha	+	-	-	87.3	
TRNT1	3168600-3192563	tRNA Nucleotidyl Transferase, CCA-Adding, 1	+	-	-	70.26	
CRBN	3190676-3221394	Cereblon	+	+	-	31.14	

DDG2P: Developmental Disorders Genotype-to-Phenotype Database, +: Confirmed DDG2P gene, HI: Haploinsufficiency index (in red if <10%)
Shaded rows: Protein coding genes located within the same hESC topologically associated domain (TAD)[25] with the breakpoints

Table S12. Convergent Genomic Analysis of DGAP259 3p24.3 breakpoints

DGAP259: 3p24.3 breakpoints on Rearrangement_A: 17,392,144 and Rearrangement_C: 17,392,136							
Genes	**Nucleotides (GRCh37/hg19)**	**Description**	**OMIM[26]**	**OMIM Morbid[26]**	**DDG2P[27]**	**%HI[8]**	**Notes**
BTD	15642848-15687329	Biotinidase	+	+	+	76.15	Biallelic loss of function (autosomal recessive) associated with biotinidase deficiency[53]
ANKRD28	15708743-15901278	Ankyrin Repeat Domain 28	+	-	-	19.04	
GALNT15	16216156-16273499	Polypeptide N-Acetylgalactosaminyltransferase 15	+	-	-	65.27	
DPH3	16299485-16306479	Diphthamide Biosynthesis 3	+	-	-	19.41	
OXNAD1	16306706-16391806	Oxidoreductase NAD-Binding Domain Containing 1	-	-	-	63.97	
RFTN1	16355081-16555533	Raftlin, Lipid Raft Linker 1	-	-	-	61.2	
DAZL	16628299-16711813	Deleted In Azoospermia-Like	+	-	-	15.92	
PLCL2	16844159-17132086	Phospholipase C-Like 2	+	-	-	38.08	
TBC1D5 (Disrupted)	17198654-18486309	TBC1 Domain Family, Member 5	+	-	-	5.84	No reported phenotype association
SATB1	18386879-18487080	SATB Homeobox 1 (Special AT-rich sequence-binding protein-1)	+	-	-	2.15	A global genome-organizer and matrix attachment region-binding protein mediating chromatin looping by tethering multiple genomic loci and recruiting chromatin-remodeling enzymes to regulate chromatin structure and gene expression[16; 17] (DGAP259 has a complex chromosome rearrangement involving five different chromosomes.) Role in cortical neurons to facilitate neuronal plasticity and regulate expression of key neuronal genes[54] and required for medial ganglionic eminence-derived interneuron differentiation, connectivity, and survival[55] (relevant to cerebral malformation phenotype of DGAP259)

DDG2P: Developmental Disorders Genotype-to-Phenotype Database, +: Confirmed DDG2P gene, HI: Haploinsufficiency index (in red if <10%)
Shaded row: Protein coding gene located within the same hESC topologically associated domain (TAD)[25] with the breakpoints

Table S13. Convergent Genomic Analysis of DGAP259 5q14.3 breakpoints

DGAP259: 5q14.3 breakpoints on Rearrangement_B: 88,756,2{48-56} and Rearrangement_E: 88,756,2{39-40}							
Genes	**Nucleotides (GRCh37/hg19)**	**Description**	**OMIM[26]**	**OMIM Morbid[26]**	**DDG2P[27]**	**%HI[8]**	**Notes**
RASA1	86563705-86687748	RAS p21 Protein Activator (GTPase Activating Protein) 1	+	+	+	2.57	Haploinsufficiency (autosomal dominant, monoallelic) reported to be associated with Parkes Weber Syndrome and Capillary malformation-Arteriovenous malformation[56]
CCNH	86687311-86708836	Cyclin H	+	-	-	7.31	Regulation of cell cycle progression, no reported phenotype association
TMEM161B	87485450-87565293	Transmembrane Protein 161B	-	-	-	9.65	
MEF2C	88013975-88199922	Myocyte Enhancer Factor 2C	+	+	+	0.26	Haploinsufficiency (autosomal dominant, monoallelic) reported to be associated with Mental retardation, Stereotypic movements, Epilepsy and cerebral malformations (MRSME)[15] and cases with hypoplastic corpus callosum[57; 58], long range regulation associated phenotype also reported in a *de novo* translocation case[22] (relevant to cerebral malformation and hypoplastic corpus callosum phenotype of DGAP259) Role in synaptic plasticity and hippocampal-dependent learning and memory[59] (9p23 breakpoints of DGAP259 disrupt *PTPRD1* with similar role)
CETN3	89688078-89705603	Centrin, EF-Hand Protein, 3	+	-	-	5.94	Present in centrosomes and lays an important role in early cleavage of frog embryos[60]
MBLAC2	89754020-89770585	Metallo-Beta-Lactamase Domain Containing 2	-	-	-	38.68	
POLR3G	89767565-89810370	Polymerase (RNA) III (DNA Directed) Polypeptide G (32kd)	-	-	-	38.97	
LYSMD3	89811428-89825401	Lysm, Putative Peptidoglycan-Binding, Domain Containing 3	-	-	-	28.58	
ADGRV1	89825161-90460038	Adhesion G Protein-Coupled Receptor V1	+	+	-	25.58	Biallelic loss of function (autosomal recessive) associated with Usher syndrome, type 2C[61]

DDG2P: Developmental Disorders Genotype-to-Phenotype Database, +: Confirmed DDG2P gene, HI: Haploinsufficiency index (in red if <10%)
Shaded rows: Protein coding genes located within the same hESC topologically associated domain (TAD)[25] with the breakpoints

Table S14. Convergent Genomic Analysis of DGAP259 7q35 breakpoints

DGAP259: 7q35 breakpoints on Rearrangement_B: 147,718,91{1-9} and Rearrangement_E: 147,718,90{7-8}							
Genes	**Nucleotides (GRCh37/hg19)**	**Description**	**OMIM[26]**	**OMIM Morbid[26]**	**DDG2P[27]**	**%HI[8]**	**Notes**
CNTNAP2 (Disrupted)	145813453-148118090	Contactin Associated Protein-Like 2	+	+	+	4.94	Susceptibility to Autism type 15[62], homozygous or comp heterozygous mutations causing Cortical Dysplasia-F Epilepsy Syndrome[63] and Pitt-Hopkins-like syndro (PTHSL1)[64] (relevant to cerebral malformation phenotyp DGAP259) (18q21 breakpoints of DGAP259 mapping one downstream of *TCF4*, a monoallelic gene in Pitt-Ho Syndrome)
C7orf33	148287657-148312952	Chromosome 7 Open Reading Frame 33	-	-	-	97.83	
CUL1	148395006-148498128	Cullin 1	+	-	-	4.3	No reported phenotype association Regulates mammalian G1/S transition by specifically targ mammalian G1 cell cycle regulators for ubiquitin-deper degradation[65]
EZH2	148504475-148581413	Enhancer of Zeste 2 Polycomb Repressive Complex 2 Subunit	+	+	+	3.07	Critical role during normal and perturbed development o hematopoietic and central nervous systems[66] and a memb the Polycomb group, which maintains homeotic repression and is thought to control gene expressio regulating chromatin[18] (In addition to the cerebral malforma DGAP259 has a complex chromosome rearrangement.)
PDIA4	148700154-148725733	Protein Disulfide Isomerase Family A, Member 4	-	-	-	70.97	
ZNF786	148766735-148787874	Zinc Finger Protein 786	-	-	-	92.01	
ZNF425	148799876-148823438	Zinc Finger Protein 425	-	-	-	92.53	
ZNF398	148823508-148880116	Zinc Finger Protein 398	-	-	-	61.58	
ZNF282	148892577-148923339	Zinc Finger Protein 282	+	-	-	64.68	
ZNF212	148936742-148952700	Zinc Finger Protein 212	+	-	-	67.39	
ZNF783	148959262-148994393	Zinc Finger Family Member 783	-	-	-	82.83	
ZNF777	149128454-149158214	Zinc Finger Protein 777	-	-	-	52.36	
ZNF746	149169885-149194908	Zinc Finger Protein 746	+	-	-	59.83	

DDG2P: Developmental Disorders Genotype-to-Phenotype Database, +: Confirmed DDG2P gene, HI: Haploinsufficiency index (in red if <10%)
Shaded row: Protein coding gene located within the same hESC topologically associated domain (TAD)[25] with the breakpoints

Table S15. Convergent Genomic Analysis of DGAP259 7q36.3 breakpoints

DGAP259: 7q36.3 breakpoints on Rearrangement_A: 155,701,797 and Rearrangement_C: 155,700,873							
Genes	**Nucleotides (GRCh37/hg19)**	**Description**	**OMIM[26]**	**OMIM Morbid[26]**	**DDG2P[27]**	**%HI[8]**	**Notes**
PAXIP1	154735397-154794794	PAX Interacting (with Transcription-Activation Domain) Protein 1	+	-	-	48.56	
HTR5A	154862034-154877459	5-Hydroxytryptamine (Serotonin) Receptor 5a, G Protein-Coupled	+	-	-	59.81	
INSIG1	155089486-155101945	Insulin Induced Gene 1	+	-	-	73.03	
EN2	155250824-155257526	Engrailed Homeobox 2	+	-	-	23.56	
CNPY1	155266901-155326557	Canopy Fgf Signaling Regulator 1	+	-	-	63.67	
RBM33	155437145-155574179	Rna Binding Motif Protein 33	-	-	-	42.71	
SHH	155592680-155604967	Sonic Hedgehog	+	+	+	0.66	Haploinsufficiency (autosomal dominant, monoallelic) associated with Holoprosencephaly type 3 (HPE3), with long range regulation associated phenotype (relevant to cerebral malformation phenotype DGAP259)
RNF32	156432975-156469824	Ring Finger Protein 32	+	-	-	75.12	
LMBR1	156461646-156685924	Limb Development Membrane Protein 1	+	+	-	24.09	
NOM1	156742417-156765876	Nucleolar Protein With Mif4g Domain 1	+	-	-	80.94	
MNX1	156786745-156803345	Motor Neuron And Pancreas Homeobox 1	+	+	+	0.84	Haploinsufficiency (autosomal dominant, monoallelic associated with Currarino Syndrome (sacral malformation)[69]
UBE3C	156931607-157062066	Ubiquitin Protein Ligase E3c	+	-	-	59.16	
DNAJB6	157128075-157210133	Dnaj (Hsp40) Homolog, Subfamily B, Member 6	+	+	-	47.78	
PTPRN2	157331750-158380480	Protein Tyrosine Phosphatase, Receptor Type, N Polypeptide 2	+	-	-	45.29	
NCAPG2	158424003-158497520	Non-SMC Condensin II Complex, Subunit G2	+	-	-	45.05	
ESYT2	158523686-158622944	Extended Synaptotagmin-Like Protein 2	-	-	-	55.86	
WDR60	158649269-158749438	WD Repeat Domain 60	+	+	+	89.69	
VIPR2	158820866-158937649	Vasoactive Intestinal Peptide Receptor 2	+	-	-	73.84	

DDG2P: Developmental Disorders Genotype-to-Phenotype Database, +: Confirmed DDG2P gene, HI: Haploinsufficiency index (in red if <10%)
Shaded rows: Protein coding genes located within the same hESC topologically associated domain (TAD)[25] with the breakpoints

Table S16. Convergent Genomic Analysis of DGAP259 9p23 breakpoints

DGAP259: 9p23 breakpoints on Rearrangement_F: 9,646,47{5} and Rearrangement_I: 9,646,471							
Genes	**Nucleotides (GRCh37/hg19)**	**Description**	**OMIM[26]**	**OMIM Morbid[26]**	**DDG2P[27]**	**%HI[8]**	**Notes**
TMEM261	7796490-7888380	Transmembrane Protein 261	-	-	-	87.18	
PTPRD (Disrupted)	8314246-10612723	Protein Tyrosine Phosphatase, Receptor Type, D	+	-	-	0.14	Homozygous microdeletion causes trigonocephaly, hearin loss, and intellectual disability, overlapping phenotypes wit the autosomal dominant 9p deletion syndrome[70] (relevant t cerebral malformation phenotype of DGAP259) Role in synaptic plasticity and hippocampal-depende learning and memory[71] (5q14.3 breakpoints of DGAP25 within same TAD as *MEF2C* with similar role)
TYRP1	12685439-12710290	Tyrosinase-Related Protein 1	+	+	+	21.84	

DDG2P: Developmental Disorders Genotype-to-Phenotype Database, +: Confirmed DDG2P gene, HI: Haploinsufficiency index (in red if <10%)
Shaded row: Protein coding gene located within the same hESC topologically associated domain (TAD)[25] with the breakpoints

Table S17. Convergent Genomic Analysis of DGAP259 18p11.31 breakpoints

DGAP259: 18p11.31 breakpoints on Rearrangement_D: 6,375,05{1}, Rearrangement_G: 6,559,611 and Rearrangement_H: 6,375,0{52-48} and 6,559,{598-602}							
Genes	**Nucleotides (GRCh37/hg19)**	**Description**	**OMIM[26]**	**OMIM Morbid[26]**	**DDG2P[27]**	**%HI[8]**	**Notes**
DLGAP1	3496030-4455335	Discs, Large (Drosophila) Homolog-Associated Protein 1	+	-	-	7.58	Candidate gene for schizophrenia[72]
C18orf42	5145284-5197502	Chromosome 18 Open Reading Frame 42	-	-	-	64.35	
ZBTB14	5289018-5297052	Zinc Finger And Btb Domain Containing 14	+	-	-	28.98	
EPB41L3	5392383-5630699	Erythrocyte Membrane Protein Band 4.1-Like 3	+	-	-	35.28	
TMEM200C	5882071-5895954	Transmembrane Protein 200c	-	-	-	77.42	
L3MBTL4 (Disrupted)	5954705-6415236	L(3)Mbt-Like 4 (Drosophila)	-	-	-	59.07	No reported phenotype association
ARHGAP28	6729717-6915715	Rho Gtpase Activating Protein 28	+	-	-	60.37	
LAMA1	6941743-7117813	Laminin, Alpha 1	+	-	+	60.73	Biallelic loss of function (autosomal recessive) associated with Poretti-Boltshauser syndrome (cerebellar dysplasia)[73]
LRRC30	7231123-7232045	Leucine Rich Repeat Containing 30	-	-	-	59.77	
PTPRM	7566780-8406859	Protein Tyrosine Phosphatase, Receptor Type, M	+	-	-	7.19	No reported phenotype association (Loss of *PTPRM* associated with pathogenic development of colorectal adenoma-carcinoma sequence)[74]
RAB12	8609443-8639379	RAB12, member RAS oncogene family	-	-	-	37.44	

DDG2P: Developmental Disorders Genotype-to-Phenotype Database, +: Confirmed DDG2P gene, HI: Haploinsufficiency index (in red if <10%)
Shaded rows: Protein coding genes located within the same hESC topologically associated domain (TAD)[25] with the breakpoints (blue: 5' breakpoints, red: 3' breakpoints)

Table S18. Convergent Genomic Analysis of DGAP259 18q21.3 breakpoints

DGAP259: 18q21.3 breakpoints on Rearrangement_F: 54,660,13{8} and Rearrangement_I: 54,660,136							
Genes	**Nucleotides (GRCh37/hg19)**	**Description**	**OMIM[2] 6**	**OMIM Morbid[2] 6**	**DDG2P[27]**	**%HI[8]**	**Notes**
CCDC68	52568740-52626739	Coiled-Coil Domain Containing 68	-	-	-	59.77	
TCF4	52889562-53332018	Transcription Factor 4	+	+	+	0.38	Haploinsufficiency (autosomal dominant, monoalle associated with Pitt-Hopkins Syndrome (severe epilep encephalopathy with mental retardation)[75] (relevant to cereb malformation phenotype of DGAP259) (7q35 breakpoints of DGAP259 disrupt *CNTNAP2*, a ge related with Pitt-Hopkins like Syndrome)[64]
TXNL1	54264439-54318831	Thioredoxin-Like 1	+	-	-	5.48	No reported phenotype association
WDR7 (Disrupted)	54318574-54698828	Wd Repeat Domain 7	+	-	-	14.85	No reported phenotype association Localized to synaptic vesicles in rat and mouse brain[76]
BOD1L2	54814293-54817531	Biorientation of Chromosomes In Cell Division 1-Like 2	-	-	-	87.92	
ST8SIA3	55018044-55038962	ST8 Alpha-N-Acetyl-Neuraminide Alpha-2,8-Sialyltransferase 3	+	-	-	11.2	
ONECUT2	55102917-55158529	One Cut Homeobox 2	+	-	-	12.99	
FECH	55215515-55254004	Ferrochelatase	+		-	28.28	
NARS	55267888-55289445	Asparaginyl-tRna Synthetase	+	-	-	21.6	
ATP8B1	55313658-55470333	ATPase, Aminophospholipid Transporter, Class I, Type 8B, Member 1	+	+	+	41.4	Biallelic loss of function (autosomal recessive) is associat with *ATP8B1*-related intrahepatic cholestasis[77]
NEDD4L	55711599-56068772	Neural Precursor Cell Expressed, Developmentally Down-Regulated 4-Like, E3 Ubiquitin Protein Ligase	+	-	-	8.66	Regulator of renal sodium channels and involved in t induction of mesoendodermal fates in mouse embryonic st cells[78] (renal agenesis and multicystic kidney in DGAP259)
ALPK2	56148479-56296189	Alpha-Kinase 2	-	-	-	88.74	

DDG2P: Developmental Disorders Genotype-to-Phenotype Database, +: Confirmed DDG2P gene, HI: Haploinsufficiency index (in red if <10%)
Shaded rows: Protein coding genes located within the same hESC topologically associated domain (TAD)[25] with the breakpoints

Table S19. Convergent Genomic Analysis of DGAP268 10p12.31 breakpoints

DGAP268: 10p12.31 breakpoints on Rearrangement_B: 21,606,655 and Rearrangement_C: 21,606,63{4-2}							
Genes	**Nucleotides (GRCh37/hg19)**	**Description**	**OMIM[26]**	**OMIM Morbid[26]**	**DDG2P[27]**	**%HI[8]**	**Notes**
NEBL	21068902-21463116	Nebulette	+	-	-	21.79	
C10orf113	21414692-21435488	Chromosome 10 Open Reading Frame 113	-	-	-	86.51	
CASC10	21781587-21786191	Cancer Susceptibility Candidate 10	-	-	-	83.87	
SKIDA1	21802407-21814611	SKI/DACH Domain Containing 1	-	-	-	18.69	
MLLT10	21823094-22032559	Myeloid/Lymphoid Or Mixed-Lineage Leukemia (Trithorax Homolog, Drosophila); Translocated To, 10	+	-	-	9.19	No reported phenotype association Fused with *AF10* in rare but recurrent chromosome rearrangement of acute monoblastic leukemia (inv ins(10;11)(p12;q23q12))[79]
DNAJC1	22045466-22292698	Dnaj (Hsp40) Homolog, Subfamily C, Member 1	+	-	-	38.97	
EBLN1	22497743-22498950	Endogenous Bornavirus-Like Nucleoprotein 1	+	-	-	90.27	
COMMD3	22604903-22609235	COMM Domain Containing 3	-	-	-	18.42	
BMI1	22610140-22620413	BMI1 Proto-Oncogene, Polycomb Ring Finger	+	-	-	1.63	No reported phenotype association, strongly expressed in proliferating cerebellar precursor cells in mice and humans[80] Important paralog of *PCGF5* (located in the vicinity of 10q23.32 breakpoints of DGAP268)
SPAG6	22634399-22743153	Sperm Associated Antigen 6	+	-	-	43.84	
PIP4K2A	22823778-23003484	Phosphatidylinositol-5-Phosphate 4-Kinase, Type II, Alpha	+	-	-	20.5	
ARMC3	23216953-23326518	Armadillo Repeat Containing 3	+	-	-	66.75	

DDG2P: Developmental Disorders Genotype-to-Phenotype Database, +: Confirmed DDG2P gene, HI: Haploinsufficiency index (in red if <10%)
Shaded rows: Protein coding genes located within the same hESC topologically associated domain (TAD)[25] with the breakpoints

Table S20. Convergent Genomic Analysis of DGAP268 10p12.2 breakpoints

DGAP268: 10p12.2 breakpoints on Rearrangement_A: 23,659,495~ and Rearrangement_C: 23,659,20{0-2}							
Genes	**Nucleotides (GRCh37/hg19)**	**Description**	**OMIM**[26]	**OMIM Morbid**[26]	**DDG2P**[27]	**%HI**[8]	**Notes**
MSRB2	23384435-23410942	Methionine Sulfoxide Reductase B2	+	-	-	79.51	
PTF1A	23481256-23483181	Pancreas Specific Transcription Factor, 1a	+	+	+	27.41	Biallelic loss of function (autosomal recessive) associated with Pancreatic and Cerebellar Agenesis[81]
C10orf67	23556124-23633774	Chromosome 10 Open Reading Frame 67	-	-	-	90.14	
OTUD1	23728198-23731308	OTU Deubiquitinase 1	+	-	-	75.7	
KIAA1217	23983675-24836772	Kiaa1217	-	-	-	41.11	
ARHGAP21	24872538-25012597	Rho Gtpase Activating Protein 21	+	-	-	56.74	

DDG2P: Developmental Disorders Genotype-to-Phenotype Database, +: Confirmed DDG2P gene, HI: Haploinsufficiency index (in red if <10%)
Shaded rows: Protein coding genes located within the same hESC topologically associated domain (TAD)[25] with the breakpoints

Table S21. Convergent Genomic Analysis of DGAP268 10q23.32 breakpoints

DGAP268: 10q23.32 breakpoints on Rearrangement_A: 93,983,897~ and Rearrangement_B: 93,982,408							
Genes	**Nucleotides (GRCh37/hg19)**	**Description**	**OMIM[26]**	**OMIM Morbid[26]**	**DDG2P[27]**	**%HI[8]**	**Notes**
RPP30	92631473-92668312	Ribonuclease P/MRP 30 kda Subunit	+	-	-	26.31	
ANKRD1	92671853-92681033	Ankyrin Repeat Domain 1 (Cardiac Muscle)	+	+	-	22.32	
PCGF5	92979908-93044088	Polycomb Group Ring Finger 5	-	-	-	8.55	No reported phenotype association Important paralog of *BMI1* (located in the vicinity of 10p12.31 breakpoints of DGAP268)
HECTD2	93170096-93274586	HECT Domain Containing E3 Ubiquitin Protein Ligase 2	-	-	-	16.83	
PPP1R3C	93388199-93392811	Protein Phosphatase 1, Regulatory Subunit 3C	+	-	-	39.43	
TNKS2	93558069-93625033	Tankyrase, TRF1-Interacting Ankyrin-Related ADP-Ribose Polymerase 2	+	-	-	11.01	
FGFBP3	93666346-93669240	Fibroblast Growth Factor Binding Protein 3	-	-	-	84.27	
BTAF1	93683526-93790082	BTAF1 RNA Polymerase II, B-TFIID Transcription Factor-Associated, 170 kda	+	-	-	5	No reported phenotype association
CPEB3 (Disrupted)	93806449-94050844	Cytoplasmic Polyadenylation Element Binding Protein 3	+	-	-	12.96	No reported phenotype association
MARCH5	94050920-94113721	Membrane-Associated Ring Finger (C3HC4) 5	+	-	-	7.01	No reported phenotype association
IDE	94211441-94333833	Insulin-Degrading Enzyme	+	-	-	1.37	No reported phenotype association
KIF11	94353043-94415150	Kinesin Family Member 11	+	+	+	9.02	Haploinsufficiency (autosomal dominant, monoallelic) associated with microcephaly with or without chorioretinopathy, lymphedema, or mental retardation[82]
HHEX	94447945-94455403	Hematopoietically Expressed Homeobox	+	-	-	7.77	No reported phenotype association
EXOC6	94590935-94819250	Exocyst Complex Component 6	+	-	-	7.76	No reported phenotype association
CYP26C1	94821021-94828454	Cytochrome P450, Family 26, Subfamily C, Polypeptide 1	+	+	-	38.94	Biallelic loss of function (autosomal recessive) associated with Focal facial dermal dysplasia, type IV[83]
CYP26A1	94833232-94837647	Cytochrome P450, Family 26, Subfamily A, Polypeptide 1	+	-	-	9.92	No reported phenotype association
MYOF	95066186-95242074	Myoferlin	+	-	-	23.07	
CEP55	95256389-95288849	Centrosomal Protein 55 kda	+	-	-	30.24	

DDG2P: Developmental Disorders Genotype-to-Phenotype Database, +: Confirmed DDG2P gene, HI: Haploinsufficiency index (in red if <10%)
Shaded rows: Protein coding genes located within the same hESC topologically associated domain (TAD)[25] with the breakpoints

Table S22. Convergent Genomic Analysis of DGAP285 Xp11.21 breakpoints

DGAP285: Xp11.21 breakpoints on Rearrangement_A: 55,174,723~ and Rearrangement_B: 55,174,381~							
Genes	**Nucleotides (GRCh37/hg19)**	**Description**	**OMIM[26]**	**OMIM Morbid[26]**	**DDG2P[27]**	**%HI[8]**	**Notes**
PAGE2B	55101496-55105342	P Antigen Family, Member 2B	-	-	-	96.76	
PAGE2	55115441-55119275	P Antigen Family, Member 2 (Prostate Associated)	+	-	-	96.53	
FAM104B (Disrupted)	55169535-55187743	Family With Sequence Similarity 104, Member B	-	-	-	93.08	No reported phenotype association
MTRNR2L10	55207824-55208944	MT-RNR2-Like 10	-	-	-	89.08	
PAGE5	55246788-55250541	P Antigen Family, Member 5 (Prostate Associated)	-	-	-	96.87	
PAGE3	55284848-55291279	P Antigen Family, Member 3 (Prostate Associated)	+	-	-	96.96	
MAGEH1	55478538-55479998	Melanoma Antigen Family H1	+	-	-	77.09	
USP51	55511049-55515635	Ubiquitin Specific Peptidase 51	-	-	-	73.85	
FOXR2	55649833-55652621	Forkhead Box R2	+	-	-	90.12	
RRAGB	55744172-55785207	Ras-Related GTP Binding B	+	-	-	34.1	
KLF8	56258854-56314322	Kruppel-Like Factor 8	+	-	-	60.52	

DDG2P: Developmental Disorders Genotype-to-Phenotype Database, +: Confirmed DDG2P gene, HI: Haploinsufficiency index (in red if <10%)
Shaded rows: Protein coding genes located within the same hESC topologically associated domain (TAD)[25] with the breakpoints

Table S23. Convergent Genomic Analysis of DGAP285 Xq28 breakpoints

DGAP285: Xq28 breakpoints on Rearrangement_A: 150,286,207~ and Rearrangement_B: 150,284,569~							
Genes	**Nucleotides (GRCh37/hg19)**	**Description**	**OMIM[26]**	**OMIM Morbid[26]**	**DDG2P[27]**	**%HI[8]**	**Notes**
IDS	148558521-148615470	Iduronate 2-Sulfatase	+	+	+	14.02	Hemizygous loss of function (X-linked recessive) associated with Mucopolysaccharidosis II[84]
CXorf40A	148621900-148632055	Chromosome X Open Reading Frame 40A	+	-	-	86.75	No reported phenotype association
MAGEA9B	148663308-148669116	Melanoma Antigen Family A9B	+	-	-	99.76	No reported phenotype association
MAGEA9	148663309-148669116	Melanoma Antigen Family A9	+	-	-	96.82	No reported phenotype association
TMEM185A	148678216-148713568	Transmembrane Protein 185A	+	-	-	38.34	No reported phenotype association
MAGEA11	148769894-148798926	Melanoma Antigen Family A11	+	-	-	95.69	No reported phenotype association
HSFX2	148855725-148858528	Heat Shock Transcription Factor Family, X Linked 2	-	-	-	99.69	
HSFX1	148855726-148858525	Heat Shock Transcription Factor Family, X Linked 1	-	-	-	99.26	
MAGEA8	149009941-149014609	Melanoma Antigen Family A8	+	-	-	96	No reported phenotype association
CXorf40B	149097745-149107029	Chromosome X Open Reading Frame 40B	-	-	-	86.08	
MAMLD1	149529689-149682448	Mastermind-Like Domain Containing 1	+	+	P	71.77	Hemizygous loss of function (X-linked recessive) associated with X-linked hypospadias, type II[85]
MTM1	149737069-149841795	Myotubularin 1	+	+	+	12.54	Hemizygous loss of function (X-linked recessive) associated with X-linked myotubular myopathy[86] (overlapping phenotype with DGAP285)
MTMR1	149861435-149933576	Myotubularin Related Protein 1	+	-	-	31.42	
CD99L2	149934810-150067289	CD99 Molecule-Like 2	+	-	-	82.42	No reported phenotype association
HMGB3	150148982-150159248	High Mobility Group Box 3	+	+	-	36.49	Hemizygous loss of function (X-linked recessive) associated with syndromic microphthalmia, 13[87]
GPR50	150345125-150349937	G Protein-Coupled Receptor 50	+	-	-	81.88	No reported phenotype association
VMA21	150564987-150577836	VMA21 Vacuolar H+-Atpase Homolog (*S. Cerevisiae*)	+	+	-	51.64	Hemizygous loss of function (X-linked recessive) associated with X-linked myopathy with excessive autophagy[88]
PASD1	150732094-150845211	PAS Domain Containing 1	-	-	-	99.84	
PRRG3	150863596-150874396	Proline Rich Gla (G-Carboxyglutamic Acid) 3 (Transmembrane)	+	-	-	58.49	No reported phenotype association
FATE1	150884507-150891666	Fetal And Adult Testis Expressed 1	+	-	-	95.68	No reported phenotype association

DDG2P: Developmental Disorders Genotype-to-Phenotype Database, +: Confirmed DDG2P gene, P: Probable DDG2P gene, HI: Haploinsufficiency index (in red if <10%)
Shaded rows: Protein coding genes located within the neighboring hESC topologically associated domains (TAD)[25] and the topological boundary regions (TBR) around the breakpoints

Table S24. Convergent Genomic Analysis of DGAP288 6q21 breakpoints

DGAP288: 6q21 breakpoints on Rearrangement_A: 112,976,04{2-4}and Rearrangement_B: 112,976,031							
Genes	**Nucleotides (GRCh37/hg19)**	**Description**	**OMIM[26]**	**OMIM Morbid[26]**	**DDG2P[27]**	**%HI[8]**	**Notes**
WISP3	112375275-112392171	WNT1 Inducible Signaling Pathway Protein 3	+	+	-	48.76	Biallelic loss of function (autosomal recessive) associated with progressive pseudorheumatoid arthropathy of childhood[89]
TUBE1	112391980-112408732	Tubulin, Epsilon 1	+	-	-	14.86	
FAM229B	112408802-112423993	Family With Sequence Similarity 229, Member B	-	-	-	19.09	
LAMA4	112429963-112576141	Laminin, Alpha 4	+	-	-	35.21	
RFPL4B	112668532-112672498	Ret Finger Protein-Like 4B	-	-	-	99.43	
MARCKS	114178541-114184648	Myristoylated Alanine-Rich Protein Kinase C Substrate	+	-	-	64.72	

DDG2P: Developmental Disorders Genotype-to-Phenotype Database, +: Confirmed DDG2P gene, HI: Haploinsufficiency index (in red if <10%)
Shaded rows: Protein coding genes located within the same hESC topologically associated domain (TAD)[25] with the breakpoints

Table S25. Convergent Genomic Analysis of DGAP288 17q24.3 breakpoints

DGAP288: 17q24.3 breakpoints on Rearrangement_A: 69,728,01{7-9} and Rearrangement_B: 69,728,006							
Gene	**Nucleotides (GRCh37/hg19)**	**Description**	**OMIM**[26]	**OMIM Morbid**[26]	**DDG2P**[27]	**%HI**[8]	**Notes**
SOX9	70117161-70122561	SRY (sex determining region Y)-box 9	+	+	+	0.56	Haploinsufficiency (autosomal dominant, monoallelic) associated with Campomelic dysplasia[90] Haploinsufficient (autosomal dominant, monoallelic) long-range cis-regulation associated with Pierre-Robin Sequence[22] (overlapping phenotype with DGAP288)

DDG2P: Developmental Disorders Genotype-to-Phenotype Database, +: Confirmed DDG2P gene, HI: Haploinsufficiency index (in red if <10%)
Shaded row: *SOX9* is the only protein coding gene located within the same hESC topologically associated domain (TAD)[25] with the breakpoints

Table S26. Convergent Genomic Analysis of DGAP290 2q32.3 breakpoints

DGAP290: 2q32.3 breakpoints on Rearrangement_A: 197,164,194 and Rearrangement_B: 197,164,206							
Genes	**Nucleotides (GRCh37/hg19)**	**Description**	**OMIM[26]**	**OMIM Morbid[26]**	**DDG2P[27]**	**%HI[8]**	**Notes**
SLC39A10	196440701-196602426	Solute Carrier Family 39 (Zinc Transporter), Member 10	+	-	-	36.25	
DNAH7	196602427-196933536	Dynein, Axonemal, Heavy Chain 7	+	-	-	48.83	
STK17B	196998290-197041227	Serine/Threonine Kinase 17b	+	-	-	37.72	
HECW2 (Disrupted)	197059094-197458416	HECT, C2 And WW Domain Containing E3 Ubiquitin Protein Ligase 2	-	-	-	18.5	No reported phenotype association
CCDC150	197504278-197628214	Coiled-Coil Domain Containing 150	-	-	-	62.11	
GTF3C3	197627756-197664449	General Transcription Factor IIIC, Polypeptide 3, 102 kda	+	-	-	30.03	
C2orf66	197669726-197675000	Chromosome 2 Open Reading Frame 66	-	-	-	77.88	
PGAP1	197697728-197792520	Post-GPI Attachment To Proteins 1	+	+	-	32.33	Biallelic loss of function (autosomal recessive) associated with mental retardation, type 42[91]
ANKRD44	197831741-198175897	Ankyrin Repeat Domain 44	-	-	-	28.93	
SF3B1	198254508-198299815	Splicing Factor 3b, Subunit 1, 155 kda	+	-	-	4.28	No reported phenotype association
COQ10B	198318147-198340032	Coenzyme Q10B	-	-	-	38.85	
HSPD1	198351305-198381461	Heat Shock 60 kda Protein 1 (Chaperonin)	+	+	+	2.85	Haploinsufficiency (autosomal dominant, monoallelic) associated with spastic paraplegia, type 13[92]
HSPE1	198364718-198368181	Heat Shock 10 kda Protein 1	+	-	-	9.58	
MOB4	198380295-198418423	MOB Family Member 4, Phocein	+	-	-	4.45	
RFTN2	198432948-198540769	Raftlin Family Member 2	-	-	-	66.28	
MARS2	198570087-198573113	Methionyl-Trna Synthetase 2, Mitochondrial	+	+	-	47.49	Biallelic loss of function (autosomal recessive) associated with Spastic ataxia, type 3[93]
BOLL	198591603-198651486	Boule-Like RNA-Binding Protein	+	-	-	18.25	

DDG2P: Developmental Disorders Genotype-to-Phenotype Database, +: Confirmed DDG2P gene, HI: Haploinsufficiency index (in red if <10%)
Shaded rows: Protein coding genes located within the same hESC topologically associated domain (TAD)[25] with the breakpoints

Table S27. Convergent Genomic Analysis of DGAP290 7q33 breakpoints

DGAP290: 7q33 breakpoints on Rearrangement_A: 135,905,923, Rearrangement_B: 135,299,810, and Rearrangement_C: 135,299,81{2} and 135,905,92{4}							
Genes	**Nucleotides (GRCh37/hg19)**	**Description**	**OMIM[26]**	**OMIM Morbid[26]**	**DDG2P[27]**	**%HI[8]**	**Notes**
BPGM	134331560-134364565	2,3-Bisphosphoglycerate Mutase	+	+	-	22.09	Biallelic loss of function (autosomal recessive) associated with erythrocytosis due to bisphosphoglycerate mutase deficiency[94]
CALD1	134429003-134655479	Caldesmon 1	+	-	-	20.29	
AGBL3	134671259-134832715	ATP/GTP Binding Protein-Like 3	-	-	-	64.12	
C7orf49	134777115-134855547	Chromosome 7 Open Reading Frame 49	-	-	-	80.37	
TMEM140	134832824-134850967	Transmembrane Protein 140	-	-	-	83.19	
WDR91	134868590-134896316	WD Repeat Domain 91	-	-	-	46.24	
STRA8	134916731-134943244	Stimulated By Retinoic Acid 8	+	-	-	56.99	
CNOT4	135046547-135194875	CCR4-NOT Transcription Complex, Subunit 4	+	-	-	6.19	No reported phenotype association
NUP205 (Disrupted)	135242667-135333505	Nucleoporin 205 kda	+	-	-	11.41	No reported phenotype association
C7orf73	135347244-135378166	Chromosome 7 Open Reading Frame 73	-	-	-	24.72	
SLC13A4	135365985-135414006	Solute Carrier Family 13 (Sodium/Sulfate Symporter), Member 4	+	-	-	40.17	
FAM180A	135413096-135433594	Family With Sequence Similarity 180, Member A	-	-	-	63.78	
MTPN	135611509-135662101	Myotrophin	+	-	-	15.72	
LUZP6	135612022-135612198	Leucine Zipper Protein 6	+	-	-	86.19	
CHRM2	136553416-136705002	Cholinergic Receptor, Muscarinic 2	+	+	-	11.59	A SNP variation may predispose to alcohol dependence, drug dependence, and affective disorders[95]
PTN	136912088-137028611	Pleiotrophin	+	-	-	5.33	No reported phenotype association
DGKI	137065783-137531838	Diacylglycerol Kinase, Iota	+	-	-	12.1	

DDG2P: Developmental Disorders Genotype-to-Phenotype Database, +: Confirmed DDG2P gene, HI: Haploinsufficiency index (in red if <10%)
Shaded rows: Protein coding genes located within the same hESC topologically associated domain (TAD)[25] with the breakpoints

Table S28. Convergent Genomic Analysis of DGAP295 2p13.3 breakpoints

DGAP295: 2p13.3 breakpoints on Rearrangement_D: 69,588,420~ and Rearrangement_E: 69,588,264~							
Genes	**Nucleotides (GRCh37/hg19)**	**Description**	**OMIM**[26]	**OMIM Morbid**[26]	**DDG2P**[27]	**%HI**[8]	**Notes**
GFPT1 (Disrupted)	69546905-69614382	Glutamine--Fructose-6-Phosphate Transaminase 1	+	+	-	22.36	Biallelic loss of function (autosomal recessive) associated with congenital myasthenia, type 12[96]
NFU1	69622882-69664760	NFU1 Iron-Sulfur Cluster Scaffold	+	+	+	7.52	Biallelic loss of function (autosomal recessive) associated with multiple mitochondrial dysfunctions syndrome, type 1 [97]
AAK1	69688532-69901481	AP2 Associated Kinase 1	+	-	-	27.81	
ANXA4	69871557-70053596	Annexin A4	+	-	-	36.41	
GMCL1	70056774-70108528	Germ Cell-Less, Spermatogenesis Associated 1	-	-	-	27.55	
SNRNP27	70120692-70132707	Small Nuclear Ribonucleoprotein 27 kda (U4/U6.U5)	-	-	-	21.9	
MXD1	70124820-70170077	MAX Dimerization Protein 1	+	-	-	19.62	
ASPRV1	70187226-70189397	Aspartic Peptidase, Retroviral-Like 1	+	-	-	44.23	
PCBP1	70314585-70316332	Poly(Rc) Binding Protein 1	+	-	-	22.38	
C2orf42	70377012-70475747	Chromosome 2 Open Reading Frame 42	-	-	-	28.59	
TIA1	70436576-70475792	TIA1 Cytotoxic Granule-Associated RNA Binding Protein	+	+	-	3.8	Haploinsufficiency (autosomal dominant, monoallelic mode) associated with Welander distal myopathy[98]
PCYOX1	70484518-70508323	Prenylcysteine Oxidase 1	+	-	-	55.49	

DDG2P: Developmental Disorders Genotype-to-Phenotype Database, +: Confirmed DDG2P gene, HI: Haploinsufficiency index (in red if <10%)
Shaded rows: Protein coding genes located within the same hESC topologically associated domain (TAD)[25] with the breakpoints

Table S29. Convergent Genomic Analysis of DGAP295 11p15.5 breakpoints

DGAP295: 11p15.5 Breakpoints on Rearrangement_A (1,915,057~ and 1,936,993~), Rearrangement_B (1,960,727~ and 1,936,668~), Rearrangement_C (1,915,843~ and 1,961,361~), Rearrangement_D (1,984,895~), and Rearrangement_E (1,985,019~)							
Gene	**Nucleotides (GRCh37/hg19)**	**Description**	**OMIM[26]**	**OMIM Morbid[26]**	**DDG2P[27]**	**%HI[8]**	**Notes**
TSPAN4	842808-867116	Tetraspanin 4	+	-	-	71.26	
CHID1	867357-915058	Chitinase Domain Containing 1	+	-	-	70.14	
AP2A2	924894-1012239	Adaptor-Related Protein Complex 2, Alpha 2 Subunit	+	-	-	72.44	
MUC6	1012821-1036706	Mucin 6, Oligomeric Mucus/Gel-Forming	+	-	-	92.04	
MUC2	1074875-1104419	Mucin 2, Oligomeric Mucus/Gel-Forming	+	-	-	78.34	
MUC5AC	1151580-1222364	Mucin 5AC, Oligomeric Mucus/Gel-Forming	+	-	-	82.42	
MUC5B	1244296-1283406	Mucin 5B, Oligomeric Mucus/Gel-Forming	+	+	-	94.15	
TOLLIP	1295601-1330884	Toll Interacting Protein	+	-	-	45.23	
BRSK2	1411129-1483919	BR Serine/Threonine Kinase 2	+	-	-	60.26	
MOB2	1490687-1522477	MOB Kinase Activator 2	+	-	-	62.66	
DUSP8	1575274-1593150	Dual Specificity Phosphatase 8	+	-	-	69.59	
KRTAP5-1	1605572-1606513	Keratin Associated Protein 5-1	+	-	-	82.35	
KRTAP5-2	1618409-1619524	Keratin Associated Protein 5-2	-	-	-	76.65	
KRTAP5-3	1628795-1629693	Keratin Associated Protein 5-3	-	-	-	84.7	
KRTAP5-4	1642188-1643368	Keratin Associated Protein 5-4	-	-	-	84.14	
KRTAP5-5	1651033-1652160	Keratin Associated Protein 5-5	-	-	-	76.4	
KRTAP5-6	1718425-1718985	Keratin Associated Protein 5-6	-	-	-	68.6	
IFITM10	1753640-1771821	Interferon Induced Transmembrane Protein 10	-	-	-	80.26	
CTSD	1773982-1785222	Cathepsin D	+	+	+	51.46	
SYT8	1848709-1858751	Synaptotagmin VIII	+	-	-	92.25	
TNNI2	1860219-1862910	Troponin I Type 2 (Skeletal, Fast)	+	+	-	67.71	
LSP1	1874200-1913497	Lymphocyte-Specific Protein 1	+	-	-	87.89	
PRR33	1910375-	Proline Rich 33	-	-	-	93.45	

	1912084						
TNNT3	1940792-1959936	Troponin T Type 3 (Skeletal, Fast)	+	+	-	54.88	
MRPL23	1968508-2005752	Mitochondrial Ribosomal Protein L23	+	-	-	79.39	
IGF2	2150342-2170833	Insulin-Like Growth Factor 2	+	+	+	79.01	Imprinted loss of function (epimutation) is associated with Silver-Russel Syndrome[24] (overlapping phenotype with DGAP295)
INS	2181009-2182571	Insulin	+	+	-	80.96	
TH	2185159-2193107	Tyrosine Hydroxylase	+	+	+	6.58	
ASCL2	2289725-2292182	Achaete-Scute Family Bhlh Transcription Factor 2	+	-	-	71.06	
C11orf21	2316875-2324279	Chromosome 11 Open Reading Frame 21	+	-	-	98.55	
TSPAN32	2323227-2339430	Tetraspanin 32	+	-	-	90.86	
CD81	2397407-2418649	CD81 Molecule	+	+	-	64.93	
TSSC4	2421718-2425106	Tumor Suppressing Subtransferable Candidate 4	+	-	-	88.63	
TRPM5	2425745-2444275	Transient Receptor Potential Cation Channel, Subfamily M, Member 5	+	-	-	76.97	

DDG2P: Developmental Disorders Genotype-to-Phenotype Database, +: Confirmed DDG2P gene, HI: Haploinsufficiency index (in red if <10%)
Shaded rows: Protein coding genes located within the same hESC topologically associated domain (TAD)[25] with the breakpoints

REFERENCES

1. Talkowski, M.E., Ordulu, Z., Pillalamarri, V., Benson, C.B., Blumenthal, I., Connolly, S., Hanscom, C., Hussain, N., Pereira, S., Picker, J., et al. (2012). Clinical diagnosis by whole-genome sequencing of a prenatal sample. N Engl J Med 367, 2226-2232.
2. Pagon, R.A., Graham, J.M., Jr., Zonana, J., and Yong, S.L. (1981). Coloboma, congenital heart disease, and choanal atresia with multiple anomalies: CHARGE association. J Pediatr 99, 223-227.
3. Blake, K.D., Davenport, S.L., Hall, B.D., Hefner, M.A., Pagon, R.A., Williams, M.S., Lin, A.E., and Graham, J.M., Jr. (1998). CHARGE association: an update and review for the primary pediatrician. Clin Pediatr (Phila) 37, 159-173.
4. Verloes, A. (2005). Updated diagnostic criteria for CHARGE syndrome: a proposal. Am J Med Genet A 133A, 306-308.
5. Brown, G.C. (1982). Optic nerve hypoplasia and colobomatous defects. J Pediatr Ophthalmol Strabismus 19, 90-93.
6. Maumenee, I.H., and Mitchell, T.N. (1990). Colobomatous malformations of the eye. Trans Am Ophthalmol Soc 88, 123-132; discussion 133-125.
7. Suzuki, Y., Kawase, E., Nishina, S., and Azuma, N. (2006). Two patients with different features of congenital optic disc anomalies in the two eyes. Graefes Arch Clin Exp Ophthalmol 244, 259-261.
8. Huang, N., Lee, I., Marcotte, E.M., and Hurles, M.E. (2010). Characterising and predicting haploinsufficiency in the human genome. PLoS Genet 6, e1001154.
9. Bowman, G.D., O'Donnell, M., and Kuriyan, J. (2004). Structural analysis of a eukaryotic sliding DNA clamp-clamp loader complex. Nature 429, 724-730.
10. Castermans, D., Wilquet, V., Parthoens, E., Huysmans, C., Steyaert, J., Swinnen, L., Fryns, J.P., Van de Ven, W., and Devriendt, K. (2003). The neurobeachin gene is disrupted by a translocation in a patient with idiopathic autism. J Med Genet 40, 352-356.
11. Wise, A., Tenezaca, L., Fernandez, R.W., Schatoff, E., Flores, J., Ueda, A., Zhong, X., Wu, C.F., Simon, A.F., and Venkatesh, T. (2015). Drosophila mutants of the autism candidate gene neurobeachin (rugose) exhibit neuro-developmental disorders, aberrant synaptic properties, altered locomotion, impaired adult social behavior and activity patterns. J Neurogenet, 1-34.
12. Nuytens, K., Gantois, I., Stijnen, P., Iscru, E., Laeremans, A., Serneels, L., Van Eylen, L., Liebhaber, S.A., Devriendt, K., Balschun, D., et al. (2013). Haploinsufficiency of the autism candidate gene Neurobeachin induces autism-like behaviors and affects cellular and molecular processes of synaptic plasticity in mice. Neurobiol Dis 51, 144-151.
13. Lauren, J., Airaksinen, M.S., Saarma, M., and Timmusk, T. (2003). A novel gene family encoding leucine-rich repeat transmembrane proteins differentially expressed in the nervous system. Genomics 81, 411-421.
14. Fernandez, B.A., Siegel-Bartelt, J., Herbrick, J.A., Teshima, I., and Scherer, S.W. (2005). Holoprosencephaly and cleidocranial dysplasia in a patient due to two position-effect mutations: case report and review of the literature. Clin Genet 68, 349-359.
15. Le Meur, N., Holder-Espinasse, M., Jaillard, S., Goldenberg, A., Joriot, S., Amati-Bonneau, P., Guichet, A., Barth, M., Charollais, A., Journel, H., et al. (2010). MEF2C haploinsufficiency caused by either microdeletion of the 5q14.3 region or mutation is responsible for severe mental retardation with stereotypic movements, epilepsy and/or cerebral malformations. J Med Genet 47, 22-29.
16. Alvarez, J.D., Yasui, D.H., Niida, H., Joh, T., Loh, D.Y., and Kohwi-Shigematsu, T. (2000). The MAR-binding protein SATB1 orchestrates temporal and spatial expression of multiple genes during T-cell development. Genes Dev 14, 521-535.
17. Kohwi-Shigematsu, T., Kohwi, Y., Takahashi, K., Richards, H.W., Ayers, S.D., Han, H.J., and Cai, S. (2012). SATB1-mediated functional packaging of chromatin into loops. Methods 58, 243-254.
18. Chen, H., Rossier, C., and Antonarakis, S.E. (1996). Cloning of a human homolog of the Drosophila enhancer of zeste gene (EZH2) that maps to chromosome 21q22.2. Genomics 38, 30-37.
19. Jungbluth, H., Wallgren-Pettersson, C., and Laporte, J. (2008). Centronuclear (myotubular) myopathy. Orphanet J Rare Dis 3, 26.
20. Joseph, M., Pai, G.S., Holden, K.R., and Herman, G. (1995). X-linked myotubular myopathy: clinical observations in ten additional cases. Am J Med Genet 59, 168-173.
21. Gordon, C.T., Tan, T.Y., Benko, S., Fitzpatrick, D., Lyonnet, S., and Farlie, P.G. (2009). Long-range regulation at the SOX9 locus in development and disease. J Med Genet 46, 649-656.

22. Benko, S., Fantes, J.A., Amiel, J., Kleinjan, D.J., Thomas, S., Ramsay, J., Jamshidi, N., Essafi, A., Heaney, S., Gordon, C.T., et al. (2009). Highly conserved non-coding elements on either side of SOX9 associated with Pierre Robin sequence. Nat Genet 41, 359-364.
23. Amarillo, I.E., Dipple, K.M., and Quintero-Rivera, F. (2013). Familial microdeletion of 17q24.3 upstream of SOX9 is associated with isolated Pierre Robin sequence due to position effect. Am J Med Genet A 161A, 1167-1172.
24. Gicquel, C., Rossignol, S., Cabrol, S., Houang, M., Steunou, V., Barbu, V., Danton, F., Thibaud, N., Le Merrer, M., Burglen, L., et al. (2005). Epimutation of the telomeric imprinting center region on chromosome 11p15 in Silver-Russell syndrome. Nat Genet 37, 1003-1007.
25. Dixon, J.R., Selvaraj, S., Yue, F., Kim, A., Li, Y., Shen, Y., Hu, M., Liu, J.S., and Ren, B. (2012). Topological domains in mammalian genomes identified by analysis of chromatin interactions. Nature 485, 376-380.
26. Amberger, J.S., Bocchini, C.A., Schiettecatte, F., Scott, A.F., and Hamosh, A. (2015). OMIM.org: Online Mendelian Inheritance in Man (OMIM(R)), an online catalog of human genes and genetic disorders. Nucleic Acids Res 43, D789-798.
27. Bragin, E., Chatzimichali, E.A., Wright, C.F., Hurles, M.E., Firth, H.V., Bevan, A.P., and Swaminathan, G.J. (2014). DECIPHER: database for the interpretation of phenotype-linked plausibly pathogenic sequence and copy-number variation. Nucleic Acids Res 42, D993-D1000.
28. Shiratsuchi, T., Nishimori, H., Ichise, H., Nakamura, Y., and Tokino, T. (1997). Cloning and characterization of BAI2 and BAI3, novel genes homologous to brain-specific angiogenesis inhibitor 1 (BAI1). Cytogenet Cell Genet 79, 103-108.
29. Rutsch, F., Gailus, S., Miousse, I.R., Suormala, T., Sagne, C., Toliat, M.R., Nurnberg, G., Wittkampf, T., Buers, I., Sharifi, A., et al. (2009). Identification of a putative lysosomal cobalamin exporter altered in the cblF defect of vitamin B12 metabolism. Nat Genet 41, 234-239.
30. Czarny-Ratajczak, M., Lohiniva, J., Rogala, P., Kozlowski, K., Perala, M., Carter, L., Spector, T.D., Kolodziej, L., Seppanen, U., Glazar, R., et al. (2001). A mutation in COL9A1 causes multiple epiphyseal dysplasia: further evidence for locus heterogeneity. Am J Hum Genet 69, 969-980.
31. Grant, A.V., El Baghdadi, J., Sabri, A., El Azbaoui, S., Alaoui-Tahiri, K., Abderrahmani Rhorfi, I., Gharbaoui, Y., Abid, A., Benkirane, M., Raharimanga, V., et al. (2013). Age-dependent association between pulmonary tuberculosis and common TOX variants in the 8q12-13 linkage region. Am J Hum Genet 92, 407-414.
32. Najmabadi, H., Hu, H., Garshasbi, M., Zemojtel, T., Abedini, S.S., Chen, W., Hosseini, M., Behjati, F., Haas, S., Jamali, P., et al. (2011). Deep sequencing reveals 50 novel genes for recessive cognitive disorders. Nature 478, 57-63.
33. Janssen, N., Bergman, J.E., Swertz, M.A., Tranebjaerg, L., Lodahl, M., Schoots, J., Hofstra, R.M., van Ravenswaaij-Arts, C.M., and Hoefsloot, L.H. (2012). Mutation update on the CHD7 gene involved in CHARGE syndrome. Hum Mutat 33, 1149-1160.
34. Haddad, R., Uwaydat, S., Dakroub, R., and Traboulsi, E.I. (2001). Confirmation of the autosomal recessive syndrome of ectopia lentis and distinctive craniofacial appearance. Am J Med Genet 99, 185-189.
35. Ouahchi, K., Arita, M., Kayden, H., Hentati, F., Ben Hamida, M., Sokol, R., Arai, H., Inoue, K., Mandel, J.L., and Koenig, M. (1995). Ataxia with isolated vitamin E deficiency is caused by mutations in the alpha-tocopherol transfer protein. Nat Genet 9, 141-145.
36. Gineau, L., Cognet, C., Kara, N., Lach, F.P., Dunne, J., Veturi, U., Picard, C., Trouillet, C., Eidenschenk, C., Aoufouchi, S., et al. (2012). Partial MCM4 deficiency in patients with growth retardation, adrenal insufficiency, and natural killer cell deficiency. J Clin Invest 122, 821-832.
37. Sanchez-Martin, M., Perez-Losada, J., Rodriguez-Garcia, A., Gonzalez-Sanchez, B., Korf, B.R., Kuster, W., Moss, C., Spritz, R.A., and Sanchez-Garcia, I. (2003). Deletion of the SLUG (SNAI2) gene results in human piebaldism. Am J Med Genet A 122A, 125-132.
38. Sanchez-Martin, M., Rodriguez-Garcia, A., Perez-Losada, J., Sagrera, A., Read, A.P., and Sanchez-Garcia, I. (2002). SLUG (SNAI2) deletions in patients with Waardenburg disease. Hum Mol Genet 11, 3231-3236.
39. Wooster, R., Bignell, G., Lancaster, J., Swift, S., Seal, S., Mangion, J., Collins, N., Gregory, S., Gumbs, C., and Micklem, G. (1995). Identification of the breast cancer susceptibility gene BRCA2. Nature 378, 789-792.
40. Alter, B.P., Rosenberg, P.S., and Brody, L.C. (2007). Clinical and molecular features associated with biallelic mutations in FANCD1/BRCA2. J Med Genet 44, 1-9.

41. Ichikawa, S., Imel, E.A., Kreiter, M.L., Yu, X., Mackenzie, D.S., Sorenson, A.H., Goetz, R., Mohammadi, M., White, K.E., and Econs, M.J. (2007). A homozygous missense mutation in human KLOTHO causes severe tumoral calcinosis. J Clin Invest 117, 2684-2691.
42. Collaborative Linkage Study of, A. (2001). An autosomal genomic screen for autism. Am J Med Genet 105, 609-615.
43. Lin, P.T., Gleeson, J.G., Corbo, J.C., Flanagan, L., and Walsh, C.A. (2000). DCAMKL1 encodes a protein kinase with homology to doublecortin that regulates microtubule polymerization. J Neurosci 20, 9152-9161.
44. Patel, H., Cross, H., Proukakis, C., Hershberger, R., Bork, P., Ciccarelli, F.D., Patton, M.A., McKusick, V.A., and Crosby, A.H. (2002). SPG20 is mutated in Troyer syndrome, an hereditary spastic paraplegia. Nat Genet 31, 347-348.
45. Villard, J., Lisowska-Grospierre, B., van den Elsen, P., Fischer, A., Reith, W., and Mach, B. (1997). Mutation of RFXAP, a regulator of MHC class II genes, in primary MHC class II deficiency. N Engl J Med 337, 748-753.
46. Shintani, M., Yagi, H., Nakayama, T., Saji, T., and Matsuoka, R. (2009). A new nonsense mutation of SMAD8 associated with pulmonary arterial hypertension. J Med Genet 46, 331-337.
47. Boczonadi, V., Muller, J.S., Pyle, A., Munkley, J., Dor, T., Quartararo, J., Ferrero, I., Karcagi, V., Giunta, M., Polvikoski, T., et al. (2014). EXOSC8 mutations alter mRNA metabolism and cause hypomyelination with spinal muscular atrophy and cerebellar hypoplasia. Nat Commun 5, 4287.
48. Berry, F.B., Lines, M.A., Oas, J.M., Footz, T., Underhill, D.A., Gage, P.J., and Walter, M.A. (2006). Functional interactions between FOXC1 and PITX2 underlie the sensitivity to FOXC1 gene dose in Axenfeld-Rieger syndrome and anterior segment dysgenesis. Hum Mol Genet 15, 905-919.
49. Nishimura, D.Y., Searby, C.C., Alward, W.L., Walton, D., Craig, J.E., Mackey, D.A., Kawase, K., Kanis, A.B., Patil, S.R., Stone, E.M., et al. (2001). A spectrum of FOXC1 mutations suggests gene dosage as a mechanism for developmental defects of the anterior chamber of the eye. Am J Hum Genet 68, 364-372.
50. Aldinger, K.A., Lehmann, O.J., Hudgins, L., Chizhikov, V.V., Bassuk, A.G., Ades, L.C., Krantz, I.D., Dobyns, W.B., and Millen, K.J. (2009). FOXC1 is required for normal cerebellar development and is a major contributor to chromosome 6p25.3 Dandy-Walker malformation. Nat Genet 41, 1037-1042.
51. Lee, S., Takeda, Y., Kawano, H., Hosoya, H., Nomoto, M., Fujimoto, D., Takahashi, N., and Watanabe, K. (2000). Expression and regulation of a gene encoding neural recognition molecule NB-3 of the contactin/F3 subgroup in mouse brain. Gene 245, 253-266.
52. Fernandez, T., Morgan, T., Davis, N., Klin, A., Morris, A., Farhi, A., Lifton, R.P., and State, M.W. (2004). Disruption of contactin 4 (CNTN4) results in developmental delay and other features of 3p deletion syndrome. Am J Hum Genet 74, 1286-1293.
53. Pomponio, R.J., Coskun, T., Demirkol, M., Tokatli, A., Ozalp, I., Huner, G., Baykal, T., and Wolf, B. (2000). Novel mutations cause biotinidase deficiency in Turkish children. J Inherit Metab Dis 23, 120-128.
54. Balamotis, M.A., Tamberg, N., Woo, Y.J., Li, J., Davy, B., Kohwi-Shigematsu, T., and Kohwi, Y. (2012). Satb1 ablation alters temporal expression of immediate early genes and reduces dendritic spine density during postnatal brain development. Mol Cell Biol 32, 333-347.
55. Close, J., Xu, H., De Marco Garcia, N., Batista-Brito, R., Rossignol, E., Rudy, B., and Fishell, G. (2012). Satb1 is an activity-modulated transcription factor required for the terminal differentiation and connectivity of medial ganglionic eminence-derived cortical interneurons. J Neurosci 32, 17690-17705.
56. Eerola, I., Boon, L.M., Mulliken, J.B., Burrows, P.E., Dompmartin, A., Watanabe, S., Vanwijck, R., and Vikkula, M. (2003). Capillary malformation-arteriovenous malformation, a new clinical and genetic disorder caused by RASA1 mutations. Am J Hum Genet 73, 1240-1249.
57. Saitsu, H., Igarashi, N., Kato, M., Okada, I., Kosho, T., Shimokawa, O., Sasaki, Y., Nishiyama, K., Tsurusaki, Y., Doi, H., et al. (2011). De novo 5q14.3 translocation 121.5-kb upstream of MEF2C in a patient with severe intellectual disability and early-onset epileptic encephalopathy. Am J Med Genet A 155A, 2879-2884.
58. Nowakowska, B.A., Obersztyn, E., Szymanska, K., Bekiesinska-Figatowska, M., Xia, Z., Ricks, C.B., Bocian, E., Stockton, D.W., Szczaluba, K., Nawara, M., et al. (2010). Severe mental retardation, seizures, and hypotonia due to deletions of MEF2C. Am J Med Genet B Neuropsychiatr Genet 153B, 1042-1051.
59. Barbosa, A.C., Kim, M.S., Ertunc, M., Adachi, M., Nelson, E.D., McAnally, J., Richardson, J.A., Kavalali, E.T., Monteggia, L.M., Bassel-Duby, R., et al. (2008). MEF2C, a transcription factor that facilitates learning and memory by negative regulation of synapse numbers and function. Proc Natl Acad Sci U S A 105, 9391-9396.

60. Middendorp, S., Paoletti, A., Schiebel, E., and Bornens, M. (1997). Identification of a new mammalian centrin gene, more closely related to Saccharomyces cerevisiae CDC31 gene. Proc Natl Acad Sci U S A 94, 9141-9146.
61. Abadie, C., Blanchet, C., Baux, D., Larrieu, L., Besnard, T., Ravel, P., Biboulet, R., Hamel, C., Malcolm, S., Mondain, M., et al. (2012). Audiological findings in 100 USH2 patients. Clin Genet 82, 433-438.
62. Arking, D.E., Cutler, D.J., Brune, C.W., Teslovich, T.M., West, K., Ikeda, M., Rea, A., Guy, M., Lin, S., Cook, E.H., et al. (2008). A common genetic variant in the neurexin superfamily member CNTNAP2 increases familial risk of autism. Am J Hum Genet 82, 160-164.
63. Strauss, K.A., Puffenberger, E.G., Huentelman, M.J., Gottlieb, S., Dobrin, S.E., Parod, J.M., Stephan, D.A., and Morton, D.H. (2006). Recessive symptomatic focal epilepsy and mutant contactin-associated protein-like 2. N Engl J Med 354, 1370-1377.
64. Zweier, C., de Jong, E.K., Zweier, M., Orrico, A., Ousager, L.B., Collins, A.L., Bijlsma, E.K., Oortveld, M.A., Ekici, A.B., Reis, A., et al. (2009). CNTNAP2 and NRXN1 are mutated in autosomal-recessive Pitt-Hopkins-like mental retardation and determine the level of a common synaptic protein in Drosophila. Am J Hum Genet 85, 655-666.
65. Yu, Z.K., Gervais, J.L., and Zhang, H. (1998). Human CUL-1 associates with the SKP1/SKP2 complex and regulates p21(CIP1/WAF1) and cyclin D proteins. Proc Natl Acad Sci U S A 95, 11324-11329.
66. Di Meglio, T., Kratochwil, C.F., Vilain, N., Loche, A., Vitobello, A., Yonehara, K., Hrycaj, S.M., Roska, B., Peters, A.H., Eichmann, A., et al. (2013). Ezh2 orchestrates topographic migration and connectivity of mouse precerebellar neurons. Science 339, 204-207.
67. Belloni, E., Muenke, M., Roessler, E., Traverso, G., Siegel-Bartelt, J., Frumkin, A., Mitchell, H.F., Donis-Keller, H., Helms, C., Hing, A.V., et al. (1996). Identification of Sonic hedgehog as a candidate gene responsible for holoprosencephaly. Nat Genet 14, 353-356.
68. Anderson, E., Devenney, P.S., Hill, R.E., and Lettice, L.A. (2014). Mapping the Shh long-range regulatory domain. Development 141, 3934-3943.
69. Ross, A.J., Ruiz-Perez, V., Wang, Y., Hagan, D.M., Scherer, S., Lynch, S.A., Lindsay, S., Custard, E., Belloni, E., Wilson, D.I., et al. (1998). A homeobox gene, HLXB9, is the major locus for dominantly inherited sacral agenesis. Nat Genet 20, 358-361.
70. Choucair, N., Mignon-Ravix, C., Cacciagli, P., Abou Ghoch, J., Fawaz, A., Megarbane, A., Villard, L., and Chouery, E. (2015). Evidence that homozygous PTPRD gene microdeletion causes trigonocephaly, hearing loss, and intellectual disability. Mol Cytogenet 8, 39.
71. Uetani, N., Kato, K., Ogura, H., Mizuno, K., Kawano, K., Mikoshiba, K., Yakura, H., Asano, M., and Iwakura, Y. (2000). Impaired learning with enhanced hippocampal long-term potentiation in PTPdelta-deficient mice. EMBO J 19, 2775-2785.
72. Li, J.M., Lu, C.L., Cheng, M.C., Luu, S.U., Hsu, S.H., and Chen, C.H. (2013). Genetic analysis of the DLGAP1 gene as a candidate gene for schizophrenia. Psychiatry Res 205, 13-17.
73. Aldinger, K.A., Mosca, S.J., Tetreault, M., Dempsey, J.C., Ishak, G.E., Hartley, T., Phelps, I.G., Lamont, R.E., O'Day, D.R., Basel, D., et al. (2014). Mutations in LAMA1 cause cerebellar dysplasia and cysts with and without retinal dystrophy. Am J Hum Genet 95, 227-234.
74. Sudhir, P.R., Lin, S.T., Chia-Wen, C., Yang, S.H., Li, A.F., Lai, R.H., Wang, M.J., Chen, Y.T., Chen, C.F., Jou, Y.S., et al. (2015). Loss of PTPRM associates with the pathogenic development of colorectal adenoma-carcinoma sequence. Sci Rep 5, 9633.
75. Zweier, C., Peippo, M.M., Hoyer, J., Sousa, S., Bottani, A., Clayton-Smith, J., Reardon, W., Saraiva, J., Cabral, A., Gohring, I., et al. (2007). Haploinsufficiency of TCF4 causes syndromal mental retardation with intermittent hyperventilation (Pitt-Hopkins syndrome). Am J Hum Genet 80, 994-1001.
76. Kawabe, H., Sakisaka, T., Yasumi, M., Shingai, T., Izumi, G., Nagano, F., Deguchi-Tawarada, M., Takeuchi, M., Nakanishi, H., and Takai, Y. (2003). A novel rabconnectin-3-binding protein that directly binds a GDP/GTP exchange protein for Rab3A small G protein implicated in Ca(2+)-dependent exocytosis of neurotransmitter. Genes Cells 8, 537-546.
77. Bull, L.N., van Eijk, M.J., Pawlikowska, L., DeYoung, J.A., Juijn, J.A., Liao, M., Klomp, L.W., Lomri, N., Berger, R., Scharschmidt, B.F., et al. (1998). A gene encoding a P-type ATPase mutated in two forms of hereditary cholestasis. Nat Genet 18, 219-224.

78. Gao, S., Alarcon, C., Sapkota, G., Rahman, S., Chen, P.Y., Goerner, N., Macias, M.J., Erdjument-Bromage, H., Tempst, P., and Massague, J. (2009). Ubiquitin ligase Nedd4L targets activated Smad2/3 to limit TGF-beta signaling. Mol Cell 36, 457-468.
79. Tanabe, S., Bohlander, S.K., Vignon, C.V., Espinosa, R., 3rd, Zhao, N., Strissel, P.L., Zeleznik-Le, N.J., and Rowley, J.D. (1996). AF10 is split by MLL and HEAB, a human homolog to a putative Caenorhabditis elegans ATP/GTP-binding protein in an invins(10;11)(p12;q23q12). Blood 88, 3535-3545.
80. Leung, C., Lingbeek, M., Shakhova, O., Liu, J., Tanger, E., Saremaslani, P., Van Lohuizen, M., and Marino, S. (2004). Bmi1 is essential for cerebellar development and is overexpressed in human medulloblastomas. Nature 428, 337-341.
81. Sellick, G.S., Barker, K.T., Stolte-Dijkstra, I., Fleischmann, C., Coleman, R.J., Garrett, C., Gloyn, A.L., Edghill, E.L., Hattersley, A.T., Wellauer, P.K., et al. (2004). Mutations in PTF1A cause pancreatic and cerebellar agenesis. Nat Genet 36, 1301-1305.
82. Ostergaard, P., Simpson, M.A., Mendola, A., Vasudevan, P., Connell, F.C., van Impel, A., Moore, A.T., Loeys, B.L., Ghalamkarpour, A., Onoufriadis, A., et al. (2012). Mutations in KIF11 cause autosomal-dominant microcephaly variably associated with congenital lymphedema and chorioretinopathy. Am J Hum Genet 90, 356-362.
83. Slavotinek, A.M., Mehrotra, P., Nazarenko, I., Tang, P.L., Lao, R., Cameron, D., Li, B., Chu, C., Chou, C., Marqueling, A.L., et al. (2013). Focal facial dermal dysplasia, type IV, is caused by mutations in CYP26C1. Hum Mol Genet 22, 696-703.
84. Young, I.D., and Harper, P.S. (1982). Incidence of Hunter's syndrome. Hum Genet 60, 391-392.
85. Fukami, M., Wada, Y., Miyabayashi, K., Nishino, I., Hasegawa, T., Nordenskjold, A., Camerino, G., Kretz, C., Buj-Bello, A., Laporte, J., et al. (2006). CXorf6 is a causative gene for hypospadias. Nat Genet 38, 1369-1371.
86. Buj-Bello, A., Biancalana, V., Moutou, C., Laporte, J., and Mandel, J.L. (1999). Identification of novel mutations in the MTM1 gene causing severe and mild forms of X-linked myotubular myopathy. Hum Mutat 14, 320-325.
87. Scott, A.F., Mohr, D.W., Kasch, L.M., Barton, J.A., Pittiglio, R., Ingersoll, R., Craig, B., Marosy, B.A., Doheny, K.F., Bromley, W.C., et al. (2014). Identification of an HMGB3 frameshift mutation in a family with an X-linked colobomatous microphthalmia syndrome using whole-genome and X-exome sequencing. JAMA Ophthalmol 132, 1215-1220.
88. Ramachandran, N., Munteanu, I., Wang, P., Aubourg, P., Rilstone, J.J., Israelian, N., Naranian, T., Paroutis, P., Guo, R., Ren, Z.P., et al. (2009). VMA21 deficiency causes an autophagic myopathy by compromising V-ATPase activity and lysosomal acidification. Cell 137, 235-246.
89. Hurvitz, J.R., Suwairi, W.M., Van Hul, W., El-Shanti, H., Superti-Furga, A., Roudier, J., Holderbaum, D., Pauli, R.M., Herd, J.K., Van Hul, E.V., et al. (1999). Mutations in the CCN gene family member WISP3 cause progressive pseudorheumatoid dysplasia. Nat Genet 23, 94-98.
90. Kwok, C., Weller, P.A., Guioli, S., Foster, J.W., Mansour, S., Zuffardi, O., Punnett, H.H., Dominguez-Steglich, M.A., Brook, J.D., Young, I.D., et al. (1995). Mutations in SOX9, the gene responsible for Campomelic dysplasia and autosomal sex reversal. Am J Hum Genet 57, 1028-1036.
91. Murakami, Y., Tawamie, H., Maeda, Y., Buttner, C., Buchert, R., Radwan, F., Schaffer, S., Sticht, H., Aigner, M., Reis, A., et al. (2014). Null mutation in PGAP1 impairing Gpi-anchor maturation in patients with intellectual disability and encephalopathy. PLoS Genet 10, e1004320.
92. Hansen, J.J., Durr, A., Cournu-Rebeix, I., Georgopoulos, C., Ang, D., Nielsen, M.N., Davoine, C.S., Brice, A., Fontaine, B., Gregersen, N., et al. (2002). Hereditary spastic paraplegia SPG13 is associated with a mutation in the gene encoding the mitochondrial chaperonin Hsp60. Am J Hum Genet 70, 1328-1332.
93. Thiffault, I., Rioux, M.F., Tetreault, M., Jarry, J., Loiselle, L., Poirier, J., Gros-Louis, F., Mathieu, J., Vanasse, M., Rouleau, G.A., et al. (2006). A new autosomal recessive spastic ataxia associated with frequent white matter changes maps to 2q33-34. Brain 129, 2332-2340.
94. Lemarchandel, V., Joulin, V., Valentin, C., Rosa, R., Galacteros, F., Rosa, J., and Cohen-Solal, M. (1992). Compound heterozygosity in a complete erythrocyte bisphosphoglycerate mutase deficiency. Blood 80, 2643-2649.
95. Luo, X., Kranzler, H.R., Zuo, L., Wang, S., Blumberg, H.P., and Gelernter, J. (2005). CHRM2 gene predisposes to alcohol dependence, drug dependence and affective disorders: results from an extended case-control structured association study. Hum Mol Genet 14, 2421-2434.

96. Senderek, J., Muller, J.S., Dusl, M., Strom, T.M., Guergueltcheva, V., Diepolder, I., Laval, S.H., Maxwell, S., Cossins, J., Krause, S., et al. (2011). Hexosamine biosynthetic pathway mutations cause neuromuscular transmission defect. Am J Hum Genet 88, 162-172.
97. Navarro-Sastre, A., Tort, F., Stehling, O., Uzarska, M.A., Arranz, J.A., Del Toro, M., Labayru, M.T., Landa, J., Font, A., Garcia-Villoria, J., et al. (2011). A fatal mitochondrial disease is associated with defective NFU1 function in the maturation of a subset of mitochondrial Fe-S proteins. Am J Hum Genet 89, 656-667.
98. Hackman, P., Sarparanta, J., Lehtinen, S., Vihola, A., Evila, A., Jonson, P.H., Luque, H., Kere, J., Screen, M., Chinnery, P.F., et al. (2013). Welander distal myopathy is caused by a mutation in the RNA-binding protein TIA1. Ann Neurol 73, 500-509.